DOT/FAA/TC-17/5

Federal Aviation Administration
William J. Hughes Technical Center
Aviation Research Division
Atlantic City International Airport
New Jersey 08405

A Test Protocol for Collecting Thermal Data From Aviation Fuel Fires Involving Large Aircraft Mockups

January 2017

Final Report

U.S. Department of Transportation
Federal Aviation Administration

NOTICE

Technical Report Documentation Page

1. Report No.	2. Government Accession No.	3. Recipient's Catalog No.
DOT/FAA/TC-17/5		

4. Title and Subtitle	5. Report Date
A TEST PROTOCOL FOR COLLECTING THERMAL DATA FROM AVIATION FUEL FIRES INVOLVING LARGE AIRCRAFT MOCKUPS	January 2017
	6. Performing Organization Code Air Force Civil Engineer Center (AFCEC/CXAE)

7. Author(s)	8. Performing Organization Report No.
Cozart, Kristofor; Hawk, John; Wells, Steven; and Enlow, Mark	

9. Performing Organization Name and Address	10. Work Unit No. (TRAIS)
Applied Research Associates, Inc. 430 West 5th Street, Suite 700 Panama City, FL 32401	
	11. Contract or Grant No. FA4819-09-C-0030

12. Sponsoring Agency Name and Address	13. Type of Report and Period Covered
U.S. Department of Transportation Federal Aviation Administration Airport Safety and Operations Division (AAS-300) 800 Independence Avenue SW Washington, DC 20591	Final report October 2012—June 2014
	14. Sponsoring Agency Code AAS-300

15. Supplementary Notes

The FAA Airport Technology Research & Development Branch COR was Mr. Stephen Murphy.

16. Abstract

Wind conditions present a specific challenge when fighting fuel fires. To address this issue and to determine effective measurement techniques for firefighting strategies in various wind conditions, researchers conducted a study to devise and employ a test protocol for mockup pool fires exposed to various wind velocity conditions. The study was intended to record a series of reference thermal profiles on unsuppressed 1:10-scale and full-scale New Large Aircraft (NLA) mockup pool fires exposed to a range of wind velocity conditions. Temperature and heat flux measurements from carefully controlled, 1:10-scale NLA mockup fires were analyzed to determine a wind velocity envelope for which the test data was repeatable. Tests with the 1:10-scale NLA mockup revealed very stable and repeatable data conducted with the same initial conditions. However, even small differences in initial wind speed and/or direction significantly changed results of the tests and sensor group repeatability. Both 1:10-scale and full-scale NLA mockup tests demonstrated a linear relationship between the integrated perimeter heat flux and wind speed from any direction. This relationship was such that at a quasi-constant wind speed and direction, the cumulative integrated perimeter heat flux for an unsuppressed, fully involved fire could be predicted. The cumulative integrated perimeter heat flux profiles recorded in the present study can be used as a baseline reference to determine the surface cooling and suppression effectiveness firefighting agents, delivery apparatus, and firefighting techniques have on the full-scale NLA mockup.

17. Key Words	18. Distribution Statement
Pool fires, Heat flux, Kinematic similitude, New Large Aircraft mockup, Crosswinds, Fuel coverage, Aircraft rescue and fire fighting	This document is available to the U.S. public through the National Technical Information Service (NTIS), Springfield, Virginia 22161. This document is also available from the Federal Aviation Administration William J. Hughes Technical Center at actlibrary.tc.faa.gov.

19. Security Classif. (of this report)	20. Security Classif. (of this page)	21. No. of Pages	22. Price
Unclassified	Unclassified	91	

TABLE OF CONTENTS

		Page
EXECUTIVE SUMMARY		xi
1.	INTRODUCTION	1
1.1	Purpose	1
1.2	Background	1
2.	DISCUSSION	2
3.	EVALUATION APPROACH	2
3.1	Evaluation Method	4
3.1.1	The 1:10-Scale NLA Mockup Trials in Windless Conditions	4
3.1.2	The 1:10-Scale NLA Mockup Trials in Controlled Wind Conditions	7
3.1.3	The 1:10-Scale NLA Mockup Fuel Coverage Measurements	11
3.1.4	Full-Scale NLA Mockup Trials	12
3.2	Initial Conditions	15
3.2.1	Initial Conditions for 1:10-Scale NLA Mockup Trials in Windless Conditions	15
3.2.2	Initial Conditions for 1:10-Scale NLA Mockup Trials in Controlled Wind Conditions	15
3.2.3	Initial Conditions for 1:10-Scale NLA Mockup Fuel Coverage Trials	16
3.2.4	Initial Conditions for Full-Scale NLA Mockup Trials	16
3.3	Procedures	16
3.3.1	Procedures for 1:10-Scale NLA Mockup Trials in Windless Conditions	16
3.3.2	Procedures for the 1:10-Scale NLA Mockup Trials in Controlled Wind Conditions	16
3.3.3	Procedures for Full-Scale NLA Mockup Trials	17

4. RESULTS AND DISCUSSION 17

4.1 The 1:10-Scale NLA Mockup Trials in Windless Conditions 17
4.2 The 1:10-Scale NLA Mockup Trials in Controlled Wind Conditions 22

4.2.1 Trials in 0.7-mph Wind Conditions 23
4.2.2 Trials in 1.4-mph Wind Conditions 33
4.2.3 Trials in 5.5-mph Wind Conditions 44

4.3 The 1:10-Scale NLA Mockup Perimeter Heat Flux 54
4.4 The 1:10-Scale NLA Mockup Fuel Coverage Trials 55
4.5 Full-Scale NLA Mockup Trials 57

5. CONCLUSIONS 58

6. REFERENCES 59

APPENDICES

A—Windless Data
B—Data From the 0.7-mph, 90° Crosswind Trials
C—Data From the 0.7-mph, 45° Crosswind Trials
D—Data From the 1.4-mph, 90° Crosswind Trials
E—Data From the 1.4-mph, 45° Crosswind Trials
F—Data From the 5.5-mph, 90° Crosswind Trials
G—Data From the 5.5-mph, 45° Crosswind Trials

LIST OF FIGURES

Figure		Page
1	New Large Aircraft Mockup at Tyndall Air Force Base	2
2	The 1:10-Scale NLA Mockup Test Fixture	5
3	Diagram of 1:10-Scale NLA Mockup Test Fixture	5
4	End View of the 1:10-Scale NLA Mockup Test Fixture Sensors	6
5	Section View of the 1:10-Scale NLA Mockup Test Fixture Sensors	6
6	Air Entrance Into Hangar Through Flow Straightener	8
7	Airflow Exiting Hangar Through Fans	9
8	The CFD Hangar Airflow Velocity Calculations	9
9	Diagram of Full-Scale NLA Mockup Test Fixture	13
10	Thermocouple Locations on the Left Side of the Full-Scale NLA Mockup	13
11	Surface-Mounted TC Locations on the Right Side of the Full-Scale NLA Mockup	13
12	Full-Scale NLA Mockup Test Fixture Perimeter Sensor Locations	14
13	Full-Scale NLA Mockup Spray Nozzle Layout	15
14	Typical Perimeter Heat Flux, Windless Condition	18
15	Typical Perimeter Temperature, Windless Condition	19
16	Typical Wing Underside Temperature, Windless Condition	19
17	Typical Fuselage Underside Temperature, Windless Condition	20
18	Typical Side Fuselage Temperature, Windless Condition	21
19	Typical 1.4-mph Wind Speed Progression	23
20	Typical Perimeter Heat Flux—0.7-mph, 90° Crosswinds	24
21	Typical Perimeter Temperature—0.7-mph, 90° Crosswinds	24
22	Typical Wing Underside Temperature—0.7-mph, 90° Crosswinds	25
23	Typical Fuselage Underside Temperature—0.7-mph, 90° Crosswinds	26

24	Typical Side Fuselage Temperature—0.7-mph, 90° Crosswinds	27
25	Typical Perimeter Heat Flux—0.7-mph, 45° Crosswinds	29
26	Typical Perimeter Temperature—0.7-mph, 45° Crosswinds	29
27	Typical Wing Underside Temperature—0.7-mph, 45° Crosswinds	30
28	Typical Fuselage Underside Temperature—0.7-mph, 45° Crosswinds	31
29	Typical Side Fuselage Temperature—0.7-mph, 45° Crosswinds	32
30	Typical Perimeter Heat Flux—1.4-mph, 90° Crosswinds	34
31	Typical Perimeter Temperature—1.4-mph, 90° Crosswinds	35
32	Typical Wing Underside Temperature—1.4-mph, 90° Crosswinds	36
33	Typical Fuselage Underside Temperature—1.4-mph, 90° Crosswinds	36
34	Typical Side Fuselage Temperature—1.4-mph, 90° Crosswinds	37
35	Typical Perimeter Heat Flux—1.4-mph, 45° Crosswinds	39
36	Typical Perimeter Temperature—1.4-mph, 45° Crosswinds	40
37	Typical Wing Underside Temperature—1.4-mph, 45° Crosswinds	41
38	Typical Fuselage Underside Temperature—1.4-mph, 45° Crosswinds	41
39	Typical Side Fuselage Temperature—1.4-mph, 45° Crosswinds	42
40	Typical Perimeter Heat Flux—5.5-mph, 90° Crosswinds	44
41	Typical Perimeter Temperature—5.5-mph, 90° Crosswinds	45
42	Typical Wing Underside Temperature—5.5-mph, 90° Crosswinds	46
43	Typical Fuselage Underside Temperature—5.5-mph, 90° Crosswinds	46
44	Typical Side Fuselage Temperature—5.5-mph, 90° Crosswinds	47
45	Typical Perimeter Heat Flux—5.5-mph, 45° Crosswinds	49
46	Typical Perimeter Temperature—5.5-mph, 45° Crosswinds	50
47	Typical Wing Underside Temperature—5.5-mph, 45° Crosswinds	51

48	Typical Fuselage Underside Temperature—5.5-mph, 45° Crosswinds	51
49	Typical Side Fuselage Temperature—5.5-mph, 45° Crosswinds	52
50	Cumulative Integrated Perimeter Heat Flux vs During-Test Wind Speed	55
51	Wind Speed vs Observed Fuel Coverage	56
52	Trends Observed During Fuel Spread Estimations for 1 gal Under 3.2-mph Wind Conditions, 5 gal Under 3.7-mph Wind Conditions, 7.5 gal Under 4.3-mph Wind Conditions, and 10 gal Under 4.3-mph Wind Conditions	57
53	The NLA Cumulative Integrated Perimeter Heat Flux vs During-Test Wind Speed	58

LIST OF TABLES

Table		Page
1	Controlled Wind Test Matrix	9
2	The RSE Values From Windless Trials	21
3	The RSE Values From 0.7-mph, 90° Crosswind Trials	27
4	The *t*-Test Comparison—0.7-mph, 90° Crosswind to Windless Conditions	28
5	The RSE Values From 0.7-mph, 45° Crosswind Trials	32
6	The *t*-Test Comparison—0.7-mph, 45° Crosswind to Windless Conditions	33
7	The RSE Values From 1.4-mph, 90° Crosswind Trials	38
8	The *t*-Test Comparison—1.4-mph, 90° Crosswind to Windless Conditions	38
9	The RSE Values From the 1.4-mph, 45° Crosswind Trials	43
10	The *t*-Test Comparison—1.4-mph, 45° Crosswind to Windless Conditions	43
11	The RSE Values From the 5.5-mph, 90° Crosswind Trials	48
12	The *t*-Test Comparison—5.5-mph, 90° Crosswind to Windless Conditions	48
13	The RSE Values From the 5.5-mph, 45° Crosswind Trials	53
14	The *t*-Test Comparison—5.5-mph, 45° Crosswind to Windless Conditions	53

LIST OF ABBREVIATIONS AND ACRONYMS

cfm	Cubic feet per minute
D	Diameter of the fire pool
gal	Gallon
hp	Horsepower
kJ	Kilojoules
kW	kilowatt
L	Liter
m	Meter
mg	Milligram
min	Minute
mph	Miles per hour
s	Second
AFCEC	Air Force Civil Engineer Center
AFB	Air Force Base
CFD	Computational fluid dynamics
DAQ	Data acquisition system
FLIR	Forward looking infrared
HFS	Heat flux sensor
HT	Heat flux detector-thermocouple pairs
IR	Infrared
JP-8	Jet propellant 8 aviation fuel
NLA	New Large Aircraft
RSE	Relative standard error
TC	Thermocouple
VFD	Variable frequency drive

EXECUTIVE SUMMARY

Wind conditions present a specific challenge when fighting fuel fires and cannot be controlled in an outdoor environment. To address this issue and to determine effective measurement techniques for evaluating firefighting strategies in various wind conditions, researchers conducted a study to instrument in and around mockup pool fires exposed to various wind conditions. The study was intended to devise and employ a test protocol to record a series of reference thermal profiles on unsuppressed 1:10-scale and full-scale New Large Aircraft (NLA) mockup pool fires exposed to a range of wind velocity conditions. The multiscale NLA mockups were located at Tyndall Air Force Base, Florida. Temperature and heat flux measurements from carefully controlled, 1:10-scale NLA mockup fires were analyzed to determine a wind velocity envelope for which the test data was repeatable. Tests with the 1:10-scale NLA mockup revealed very stable and repeatable data conducted with the same initial conditions. However, even small differences in initial wind speed and/or direction significantly changed results of the tests and sensor group repeatability. Both 1:10-scale and full-scale NLA mockup tests demonstrated a linear relationship between the integrated perimeter heat flux and wind speed from any direction. This relationship was such that at a quasi-constant wind speed and direction, the cumulative integrated perimeter heat flux for an unsuppressed, fully involved fire could be predicted. The cumulative integrated perimeter heat flux profiles recorded in the present study can be used as a baseline reference to determine the surface cooling and suppression effectiveness firefighting agents, delivery apparatus, and firefighting techniques have on the full-scale NLA mockup.

1. INTRODUCTION.

In 2008, a series of fire experiments were conducted in the New Large Aircraft (NLA) test facility in an attempt to establish baseline or reference temperature data on and in the surrounding area of the mockup from large-scale aviation fuel pool fires. However, because temperature data varied widely from fire test to fire test, a reference temperature profile for the mockup could not be determined. The most obvious source of variation was the difference in initial conditions for the fires, particularly the difference in wind speed and direction. As a result, the current research effort was undertaken to quantify the variation in mockup surface temperature caused by changing wind speed and direction. The research effort was also conducted to determine if it was possible to establish a practical and repeatable test protocol for comparing the effects of different vehicles, equipment, tactics, and extinguishing agents.

1.1 PURPOSE.

This research effort was intended to devise and employ a test protocol to establish a reference thermal profile for a 1:10-scale and full-scale NLA mockup. The goal was to use the reference thermal profile to eventually determine the surface cooling and suppression effectiveness of firefighting agents, agent delivery apparatus, and firefighting techniques have on the full-scale NLA mockup. Any decrease in cumulative integrated perimeter heat flux measured, compared to this baseline reference, should be a measure of implemented firefighting strategies; with greater differences indicating more effective strategies.

1.2 BACKGROUND.

Figure 1 shows the NLA outdoor test facility located at Tyndall Air Force Base (AFB) near Panama City, Florida. It was designed and built in cooperation with the Airbase Technologies Division of the Air Force Research Laboratory, now the Requirements and Acquisitions Division of the Air Force Civil Engineer Center (AFCEC/CXA). The mockup is a full-scale replica based on a 60-ft mid-section of the Airbus A380 aircraft. The replica's steel escape slides, similar to the rest of the mockup, provide realistic obstructions to firefighting. The mockup sits in a 100-ft-diameter depression, or pit, in which aviation fuel, floating on water, is burned to create a ground fire under the suspended structure. The mockup was built for the purpose of evaluating vehicles, equipment, tactics, and extinguishing agents used for Aircraft Rescue and Fire Fighting. It also provides a test bed to gather data for verification and validation of computer models designed to simulate aircraft fires.

Figure 1. New Large Aircraft Mockup at Tyndall Air Force Base

2. DISCUSSION.

Because of the large number of experimental trials, fuel quantities, and repeatable wind velocities necessary to complete this research effort using the full-scale NLA mockup, a 1:10-scale model of the full-scale test environment was fabricated and installed inside a large hangar. The first series of experimental trials was designed to determine the repeatability of temperature and heat flux data from carefully controlled, 1:10-scale NLA mockup fires under windless conditions. Thermal data from multiple trials executed under identical conditions were compared. The second series of experiments was designed to determine the repeatability of data from multiple trials on the 1:10-scale NLA mockup in controlled wind conditions of various speeds and directions. Sensors were arranged into groups for analysis, and any data group that was repeatable under a set of initial wind velocity conditions became part of the reference thermal profile. By using the results from the 1:10-scale NLA mockup fires, a wind speed and direction envelope for which there were repeatable thermal data was determined. Ultimately, a series of full-scale NLA mockup fire trials were conducted within the appropriately scaled established wind velocity envelope to verify the consistency of the reference thermal profile. In addition, non-fire tests were conducted on the 1:10-scale NLA mockup to evaluate wind speed effects on the fuel spill coverage area.

3. EVALUATION APPROACH.

For the 1:10-scale NLA mockup test approach, several fire trials were conducted in identical wind conditions; then measured temperature and heat flux data were compared to determine if the procedure yielded repeatable results. It was unlikely that each pan fire would spread identically and that temperatures and heat fluxes in each fire would reach the same magnitude in exactly the same period of time after first igniting the Jet Propellant 8 aviation fuel (JP-8).

Therefore, data were taken at 1-second (s) intervals so that data from individual tests could be shifted and aligned in time to a common point of reference. By this method, temperatures and heat fluxes for each sensor and for multiple fires could be compared as a function of time starting from the same reference point.

For the 1:10-scale NLA mockup trials, the thermal data recorded included numerous individual sensors that were combined into the following sensor groups for analysis purposes.

- Eight plate-style heat flux sensors arranged around the perimeter of the pool fire.
- Eight exposed, bead-welded thermocouples (TC) arranged around the perimeter of the pool fire.
- Three surface-mounted TCs located on the underside of the wing.
- Four surface-mounted TCs located on the underside of the fuselage.
- Four surface-mounted TCs located on the right side of the fuselage.
- Four surface-mounted TCs located on the left side of the fuselage.

Four to nine trials were run at seven different combinations of wind speed and direction, as described in section 3.1. First, data were analyzed within each set of trials done at a specific wind speed and direction to determine whether the results were repeatable. Once it was determined that the results were repeatable at each of the seven different initial conditions, data sets from tests at different conditions of wind speed and direction were compared to determine whether the results were repeatable across different initial conditions. Data were compared within sets of trials with the same initial conditions and across sets with different initial conditions by comparing data at 15-s intervals over the initial 240 s of each fire. Assuming a *t*-distribution of the data, any data point that fell outside a 95% confidence interval was rejected as anomalous.

Defined in equation 1, relative standard error (RSE) was used as the measure of repeatability for data collected from all trials conducted under the same initial conditions:

$$RSE = \frac{sample\ standard\ deviation}{(number\ of\ samples)^{\frac{1}{2}}(sample\ mean)} \quad (1)$$

Data with an RSE of 10% or less are generally accepted as a very reliable indicator of repeatability and data with an RSE up to about 30% are generally considered a reliable indicator. Sample data with an RSE above 30% are usually not considered a good estimator of the state of the statistical population or a good estimator of future results. Therefore, for the 1:10-scale trials, the success criterion established that at least 80% of the RSE values at 15-s intervals was 30% or less for the recorded sensor group. If this condition was met, the sensor group data were deemed repeatable for that combination of wind speed and direction.

To determine whether wind speed and direction had a significant effect on temperature and heat flux, thermal data sets from trials conducted at different initial conditions were compared by

using *t*-tests. Significant differences in the data were determined by *t*-tests that were analyzed at the 1% level (high significant difference) and the 5% level (probable significant difference). The *t*-test function built into Microsoft® Excel® was used to do the analysis assuming a two-tailed test with unequal variance. For each individual sensor at each of the 15-s intervals, Microsoft® Excel® generated a *p*-value. The *p*-value is the probability of obtaining the observed data assuming all results were from the same population. If the *p*-value is less than or equal to the previously mentioned significance levels, it suggests that the observed data are inconsistent with the assumption that the results from the two test conditions were the same. Individual *p*-values for each trial are presented in the appendices. The success criterion established that at least 80% of the *t*-test *p*-values had to exceed the 1% level of significance criterion to show that there was no highly significant difference between the two sensor group data sets. If at least 80% of the *p*-values exceeded the 5% level of significance criteria, then it was assumed there was no probable significant difference between the two sensor group data sets. Otherwise, the assumption was that wind speed or direction caused a significant change in the results; and therefore, the results from one set of initial conditions could not be used to accurately predict the results from a different set of initial conditions.

For the full-scale mockup trials, data recorded and analyzed included just eight plate-style heat flux sensors (HFS) arranged along the perimeter of the pool fire. Heat flux data exceeding a threshold value was integrated over time and summed for all eight sensors to establish a relative measure of the total heat released from each fire. This cumulative integrated perimeter heat flux was plotted versus the wind speed during each test for comparison to the results of the 1:10-scale trials.

3.1 EVALUATION METHOD.

3.1.1 The 1:10-Scale NLA Mockup Trials in Windless Conditions.

All 1:10-scale NLA mockup fire trials were conducted inside the Sky X hangar at Tyndall AFB, Florida. As shown in figure 2, the 1:10-scale NLA mockup was supported over a steel pan to simulate full-scale NLA mockup conditions. The pan was 10 ft. in diameter with 4-in.-tall sides and made from 0.25-in.-thick carbon steel. The fuselage of the 1:10-scale NLA mockup was 6 ft. long and mostly made from 0.135-in.thick steel. Twenty gallons of JP-8 were used for all 1:10-scale NLA mockup trials. Figures 3 through 5 show OMEGA® model XCIB-K-4-7-10 surface-mounted TCs used to measure the interior bottom and side fuselage temperatures, as well as the underside of the wing. To measure air temperature and heat flux around the periphery of the fire, SANDIA-style HFS-thermocouple pairs (HT) were placed around the pan, as shown in figure 3, at a height level with the bottom of the fuselage and at a distance of 32 in. from the edge of the steel pan. The TCs used in the HT pairs were K-type, 24-gauge, bead-welded TCs. The HFSs in the HT pairs were flat-plate sensors, which are described in reference 1. HFSs were roughly calibrated with a known heat source to determine correction factors for each sensor and to ensure consistency in the measurements. However, the measurements were only taken for comparison among trials and not to determine the actual heat flux from the fires. Schmidt–Boelter-type, water-cooled heat flux transducers were installed at the HT4 and HT8 positions, as shown in figure 3.

Figure 2. The 1:10-Scale NLA Mockup Test Fixture

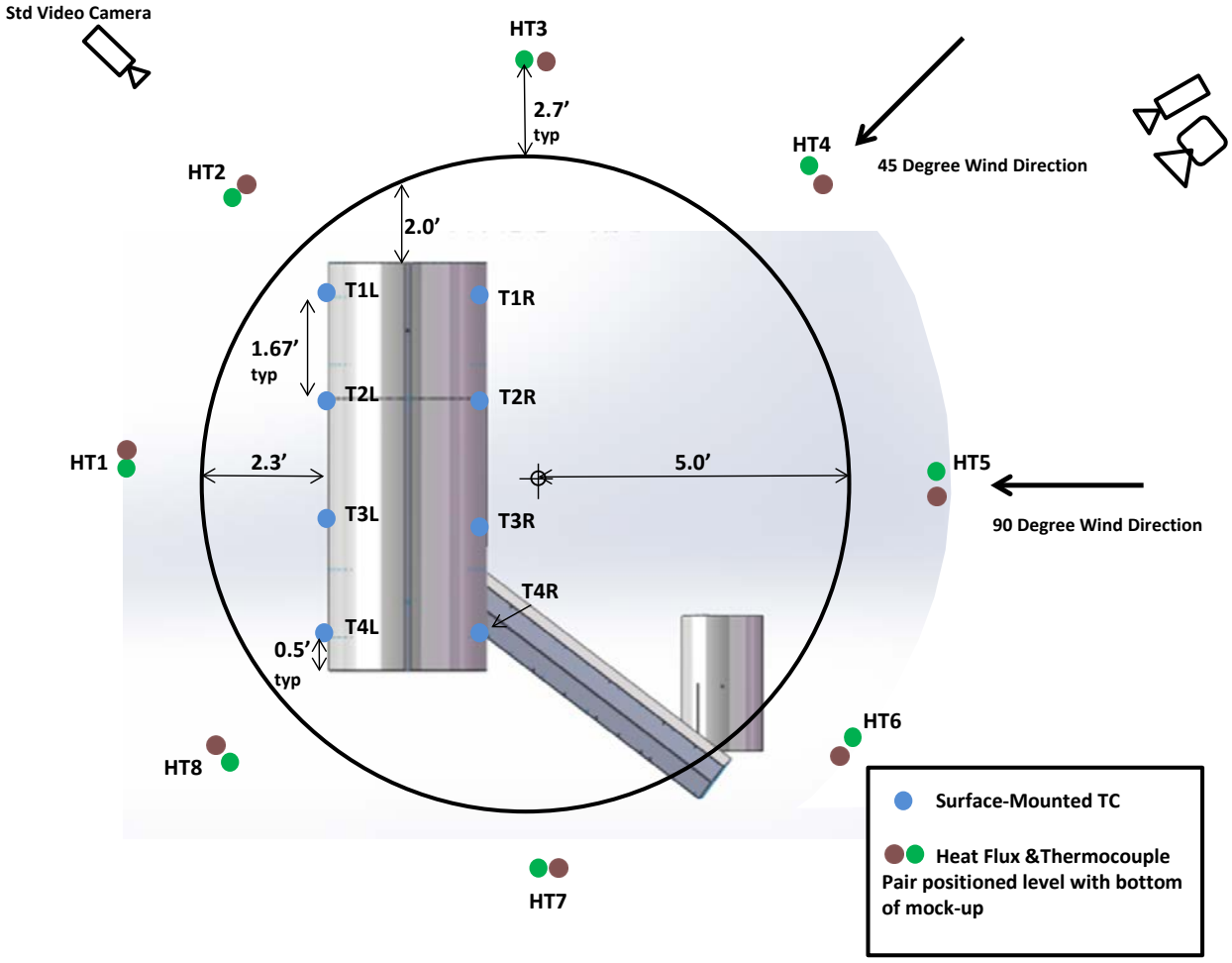

Figure 3. Diagram of 1:10-Scale NLA Mockup Test Fixture

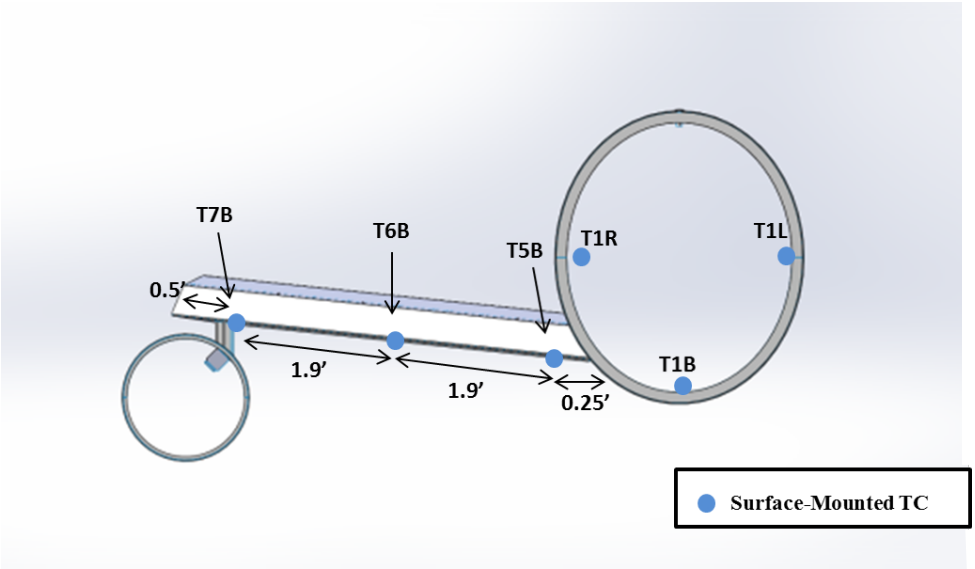

Figure 4. End View of the 1:10-Scale NLA Mockup Test Fixture Sensors

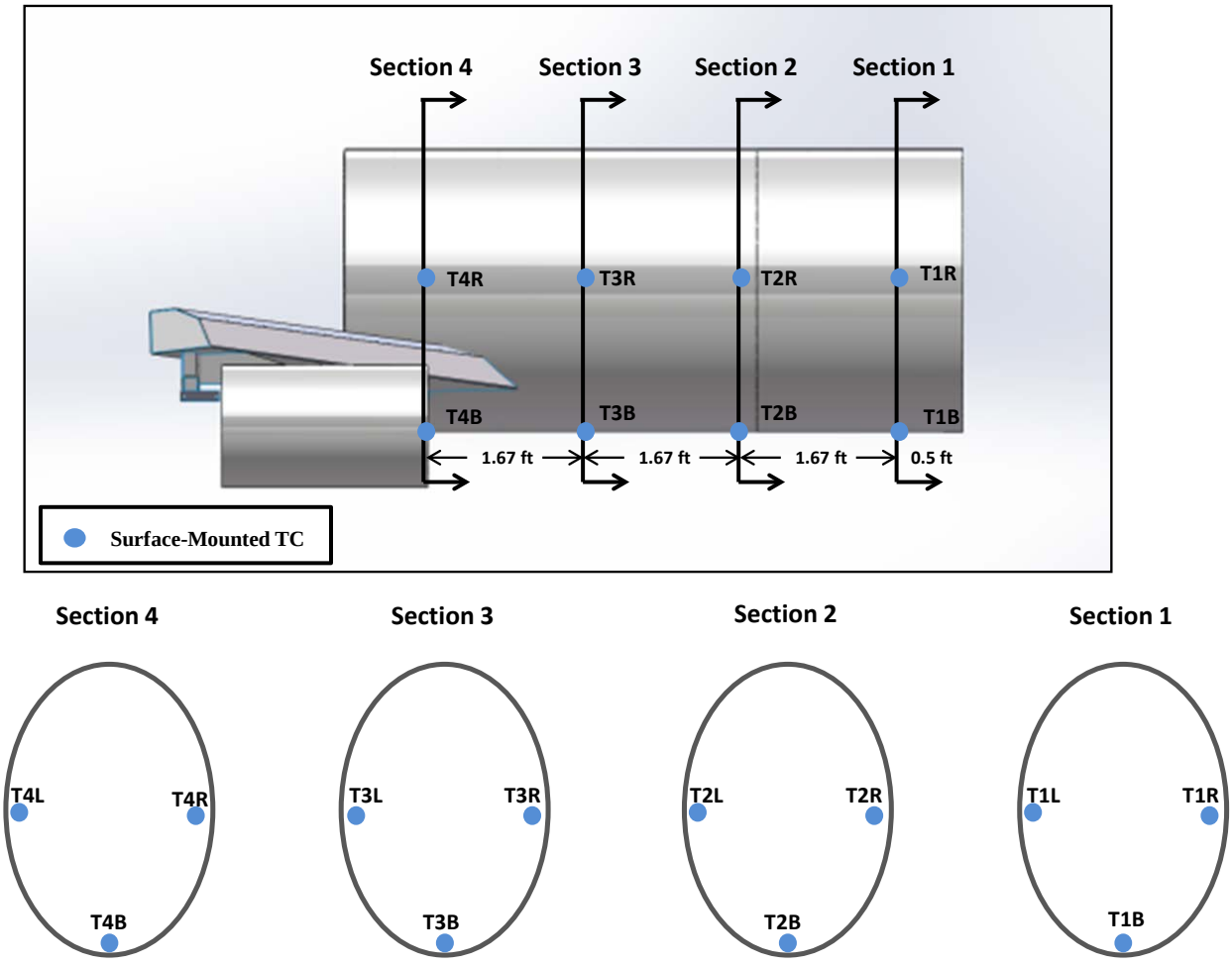

Figure 5. Section View of the 1:10-Scale NLA Mockup Test Fixture Sensors

An Extech 42520 infrared (IR) thermometer was used to measure the initial temperatures of the JP-8, steel pan, and the mockup. A Kestrel® 4000 Pocket Weather Tracker was used to measure ambient air temperature and humidity in the test facility. A data acquisition system (DAQ) utilizing LabVIEW software and National Instruments™ hardware was used to record data from the various sensors at 1-s intervals. A California Analytical Instruments model 602P gas analyzer was used to measure the oxygen concentration at the base of the flames to verify the fires were not self-extinguishing due to lack of oxygen. The samples were drawn through a 0.375-in. tube and transported 85 ft. away to protect the instrument from the fire. For safety reasons, a handheld MultiRAE Lite gas monitoring unit was used inside the test facility to measure oxygen (O_2), carbon dioxide (CO_2), carbon monoxide (CO), hydrogen cyanide (HCN), and hydrogen sulfide (H_2S) concentrations to ensure personnel could safely re-enter the test area without respiratory protection after the fire self-extinguished.

Standard video cameras were used to make photographic records of the trials and to monitor the descent of the smoke layer during each windless experiment. Reflective tape was used to mark a structural column in the test facility at 2.5-ft intervals starting from a level equal to that of the base of the steel pan, and then the descent of the smoke layer was captured on video during each fire test. A forward looking infrared (FLIR) camera model SC620 was used to record a visual image of temperature on the mockup during each fire test.

3.1.2 The 1:10-Scale NLA Mockup Trials in Controlled Wind Conditions.

Controlled wind trials used the same 1:10-scale NLA mockup test environment and were conducted similarly to windless trials. An additional Schmidt–Boelter-type, water-cooled heat flux transducer was included at the HT1 position. Two RM Young Model 81000 ultrasonic anemometers were added to measure the wind speed and direction entering the test facility and the exterior ambient wind speed and direction. A differential pressure transducer was added to the test pan to measure fuel recession.

The hangar facility had two large doors: a 20- by 17-ft doorway on the south-facing wall and a 12- by 12-ft doorway on the north-facing wall. A 12.3- by 11.3- by 9.1-ft flow straightener was fabricated from Royal Building Systems extruded polymer concrete forms and positioned along the center of the south doorway, as shown in figure 6. The remainder of the open doorway space was filled with a fire-resistant cloth tarp. Ambient air entered the hangar through the flow straightener to remove any lateral air stream components, ensuring that the air flowed smoothly over the mockup located in the center of the hangar.

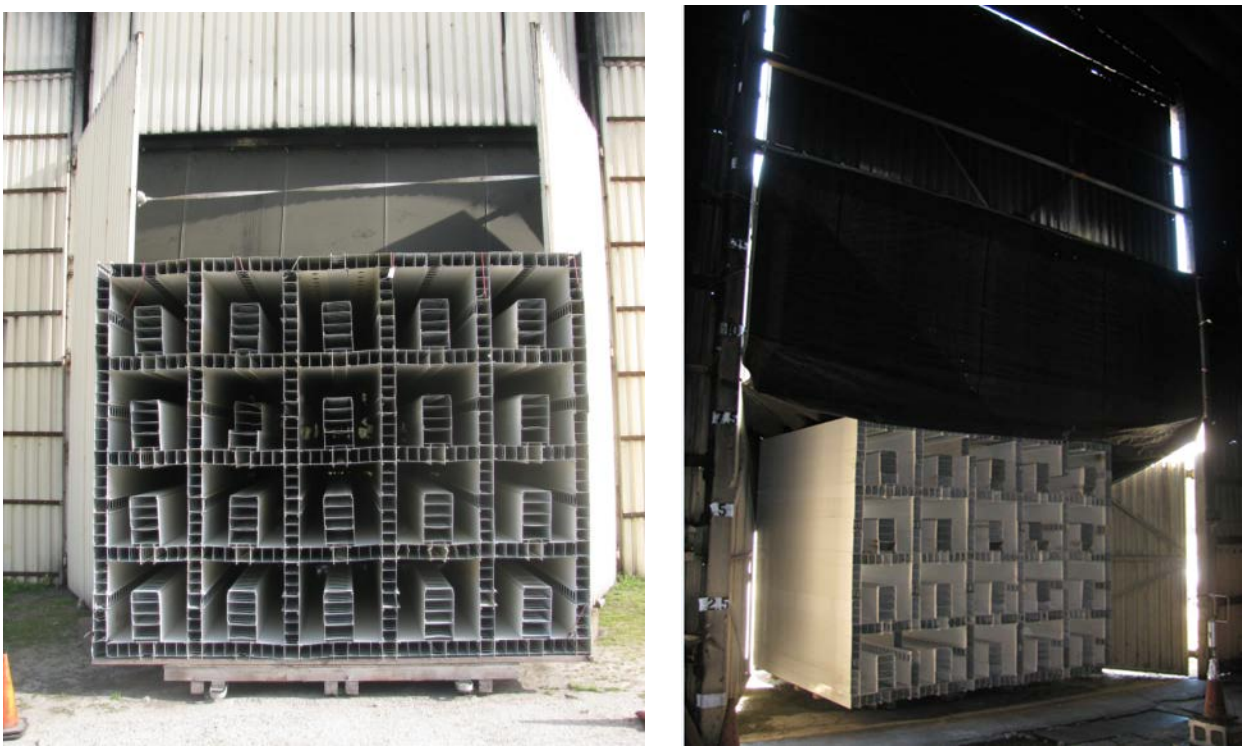

Figure 6. Air Entrance Into Hangar Through Flow Straightener

Air flow through the hangar and around the mockup was provided by eight fans mounted in the north doorway, as shown in figure 7. Six of the fans were 36-in., 3-horsepower (hp), 20,500-cubic feet per minute (cfm) units, and two were 42-in., 5-hp, 27,000-cfm units. A 30-hp variable-frequency drive (VFD) was wired into separate manual motor starters for each fan. In this manner, the VFD allowed for the rotational velocity of all fans to be adjusted to achieve different wind speeds. The separate manual motor starters allowed for individual fans to be switched off. The fans exhausted out of the test facility and drew in ambient air through the flow straightener located on the opposite side of the hangar.

When designing the wind speed control system, a computational fluid dynamics (CFD) model of the facility was created and airflow through the facility was simulated. CFD simulations were conducted on the internal flow environment of the facility when exposed to wind gusts at the main entry doors and using the smaller doors near the exhaust exit as the outflow (and conversely, using the small doors for inflow and the main doors for outflow), to determine optimum parameters and requirements to achieve uniform flow in the vicinity of the mockup. The CFD results assisted in determining the number and placement of fans and the required amount of air the fans must be able to move. The overhead view of one set of CFD results is shown in figure 8, oriented with the inflow at the top of the figure and the exhaust fans at the bottom.

Figure 7. Airflow Exiting Hangar Through Fans

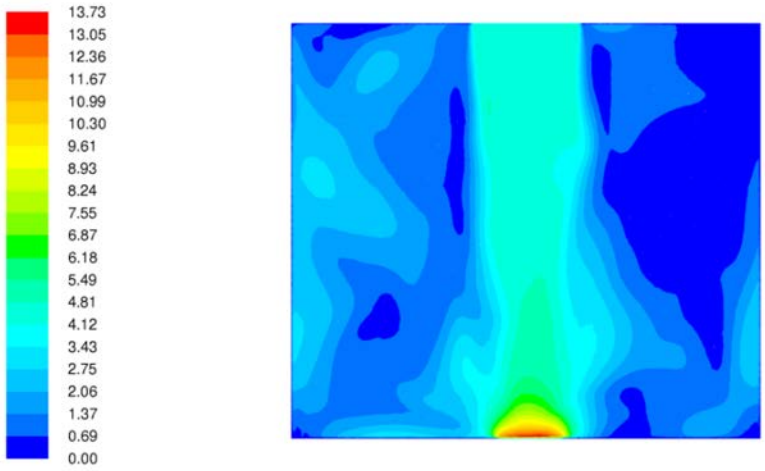

Figure 8. The CFD Hangar Airflow Velocity Calculations (m/s)

Three different wind speeds were tested from two different wind directions. Table 1 outlines the controlled wind test matrix.

Table 1. Controlled Wind Test Matrix

Wind Speed (mph)	90° Relative Angle (Number of trials)	45° Relative Angle (Number of trials)
0.7	6	6
1.4	9	6
5.5	6	4

Wind speeds inside the hangar were measured with one of the aforementioned anemometers positioned 25 ft from the edge of the pan, between the pan and the flow straightener. Only the

north/south velocity component was reported because the east/west and up/down components were negligible. Wind speeds outside of the test facility were measured by a similar anemometer positioned on the top of the hangar. Only the north/south and east/west velocity components were reported because the up/down component was negligible. Outside data from all but one controlled wind test (Trial 2 of the 5.5-mph, 90° crosswind) was recorded.

The rotational speed of the fans was set by adjusting the VFD to a preset frequency. Minor pretest adjustments were made to compensate for dominant ambient wind conditions of the day. Once set, the fan speed was kept constant for the duration of the test. No attempt was made to actively control the speed of the fans to compensate for small changes caused by variations in ambient wind conditions. This meant the wind speed was somewhat influenced by the ambient wind conditions, particularly at lower wind speeds when the fans were turning slowly.

Because the winds generated by the fans were fixed in position through the doors of the hangar, any attempt to change the relative wind direction had to be realized by rotating the mockup. Initially, the mockup was oriented with the fuselage along an east/west axis. The south-to-north-generated winds were at a 90° relative angle to the fuselage. The mockup and all perimeter sensors were rotated 45° clockwise when viewed from above to generate the 45° crosswind condition.

3.1.2.1 Scale Model Similitude.

Relatively low (0.7 and 1.4 mph) wind speeds over the 1:10-scale NLA mockup were chosen partially based on model similitude. A scale flow model is considered similar to its full-scale counterpart if they share a combination of geometric, kinematic, and dynamic similarities [2]. Geometric similarity was met as all mockup dimensions in each of the three coordinate directions maintained the same length scale ratio. However, the full-scale NLA mockup was equipped with evacuation slides, to ensure structural stability when exposed to potentially strong outdoor crosswind forces, whereas the 1:10-scale NLA mockup was not. The NLA mockup scale model and accompanying fire pan was one tenth of the size of the NLA mockup and respective fire pit. Dynamic similarity was not considered since forces or mass was not measured or addressed.

Kinematic similarity requires fluid flow of both the model and full-scale application to undergo similar time rates of change of motion where fluid streamlines are similar. This condition is also met if both the model and application have the same degree of flame lean. Flame lean is the resultant of the upward buoyantly driven flow and the horizontal wind velocity.

The nondimensional Froude number (*Fr*), often used in hydraulics when describing liquid flows, is also applicable to the high-temperature gas in the combustion zone flames [3] and can be defined as:

$$Fr = \frac{v}{\sqrt{gD}} \tag{2}$$

where v is the wind velocity, g is the acceleration due to gravity, and D is the diameter of the fire pan. Similar past trials have shown that a strong, quasi-linear relationship exists between flame lean and Froude number. Furthermore, if two pool fires have the same flame lean, then they

must also have the same Froude number [4]. Equating the Froude number for both the 1:10-scale model (m) and full-scale (fs) mockup results in the relationship shown in equations 3 and 4.

$$\frac{v_{\mathrm{m}}}{\sqrt{gD_{\mathrm{m}}}} = \frac{v_{\mathrm{fs}}}{\sqrt{gD_{\mathrm{fs}}}} \tag{3}$$

$$\frac{v_{\mathrm{m}}}{v_{\mathrm{fs}}} = \sqrt{\frac{gD_{\mathrm{m}}}{gD_{\mathrm{fs}}}} = \sqrt{\frac{1}{10}} = 0.316 \tag{4}$$

Employing equation 4, a 0.7-mph wind speed over the 1:10-scale test fixture would be similar in flame lean to a 2.2-mph wind condition over the NLA full-scale mockup. A 1.4-mph 1:10-scale generated wind would produce flame lean similar to a 4.4-mph, full-scale ambient wind, and the 5.5-mph 1:10-scale wind would equate to a 17.4-mph, full-scale ambient wind speed.

3.1.3 The 1:10-Scale NLA Mockup Fuel Coverage Measurements.

Wind is known to affect the fuel distribution in pool fire tests by pushing the fuel toward the leeward side of the pool. As a result, the fuel surface area coverage is decreased, which affects the fire heat release duration and mockup temperature profile. Adding fuel to the test facility can offset some wind effects by increasing the fuel surface area, but this action adds cost to the experiment. Measuring the fuel distribution aids in understanding how the NLA mockup temperature profile may be influenced due to the combined effects of fuel quantity and wind conditions.

Upon the completion of the 1:10-scale NLA mockup fire tests, additional nonfire tests were conducted using the same procedures with the exception of fuel quantity and ignition. Fuel was incrementally added to the test pan and the wind speed was varied to determine the fuel quantity required to overcome the effects of wind on the fuel's coverage of the surface area of the test article.

Since it can be difficult to visualize fuel coverage over the water, dye was added to the fuel to improve the contrast between the fuel and water layers. The JP-8 fuel was dyed red using Sudan IV, a compound used internationally to dye diesel fuel and heating oil. Enough Sudan IV was added to the JP-8 fuel to bring the concentration to 42 mg/gal (11 mg/L) of Sudan IV. This concentration was selected based on the Internal Revenue Service guidelines for the use of a chemically similar dye (Solvent Red 26) used to dye tax-exempt diesel fuel [5]. At this concentration, the JP-8 fuel had a noticeable red-orange coloration. In good lighting conditions, it was easy to distinguish the dyed fuel as it was poured over a water surface.

Because the bottom of the test pan had a dark grey to rust-red color, it was decided to also dye the water to enhance the visibility of the water-fuel interface. Water in the test pan was dyed blue using methylene blue. Methylene blue has a wide variety of industrial and medicinal uses. However, no concentration standard relevant to this application was available; a concentration of 3.3 mg/gal (0.88 mg/L) of methylene blue was chosen based on best judgment. At this concentration, the water had a dark blue coloration, which significantly improved the contrast between the fuel and the water in the test pan.

3.1.4 Full-Scale NLA Mockup Trials.

Full-scale NLA mockup fire tests were conducted in a 100-ft-diameter fire pit at Tyndall AFB, Florida (see figure 1). The fuselage of the NLA mockup was 60 ft in length and made up of mostly 0.25-in.-thick steel. Full-scale trials burned 750 gal of JP-8. Similar instrumentation and placement guidelines were used for both the 1:10-scale and full-scale NLA mockup tests where practical. Although the fuel recession rate was not measured for the present test, it was expected to average approximately 0.173 in./min based on similar trials conducted by Gritzo and Suo-Antilla [6]. Surface-mounted TCs measured interior temperatures on the bottom and sides of the fuselage as well as the bottom of the wing. To measure heat flux around the periphery of the fire, plate-style HFSs were placed around the fire pit at eight different locations at a height level with the bottom of the fuselage. The same two anemometers used for the 1:10-scale tests were also used for the full-scale tests to measure wind speed before and during each trial. Standard video cameras were used to make photographic records of the trials. A FLIR model SC620 camera was used to record a temperature image of the mockup during each fire test.

Figures 9 through 11 depict the full-scale NLA mockup instrumentation layout. Side fuselage TCs were installed 2 ft below the centerline of the fuselage due to a centerline expansion gap that existed on the full-scale NLA mockup. The TCs were installed at least 1 ft away from any doors or structural gussets. As a result, the sensor spacing was not symmetrical. On the fuselage's right side where escape slides were present, surface-mounted TCs were installed below fuselage–slide intersections at a 45° location with respect to the fuselage vertical centerline (or halfway between the side and the bottom TCs). Three TCs were installed to measure flame temperature below the bottom middle of the mockup at heights of 1, 4, and 8 ft above the fuel surface, as shown in figure 10. A TC was also installed below the bottom center of the mockup just above the pool water substrate to measure fuel temperature. Measurements were recorded with a LabVIEW DAQ program and two National Instruments™ NI-9213 USB modules on a laptop computer. The DAQ was installed in an insulated box inside of the aircraft fuselage.

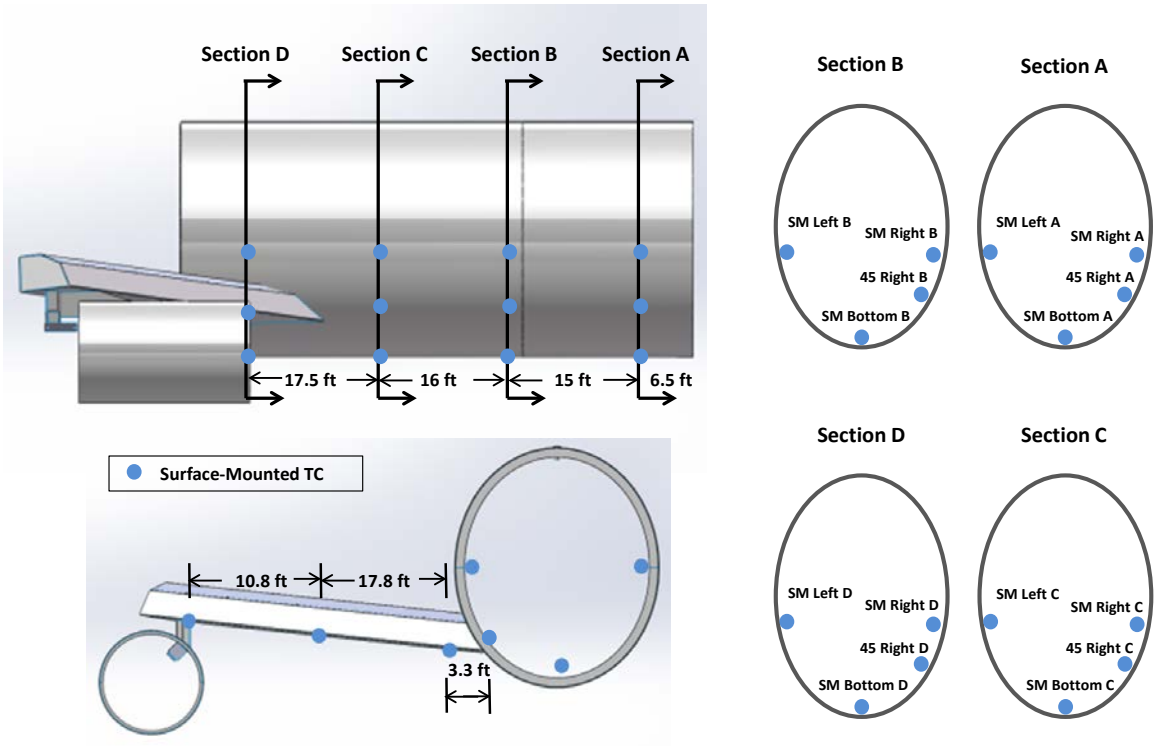

Figure 9. Diagram of Full-Scale NLA Mockup Test Fixture

Figure 10. Thermocouple Locations on the Left Side of the Full-Scale NLA Mockup

Figure 11. Surface-Mounted TC Locations on the Right Side of the Full-Scale NLA Mockup

SANDIA plate-style HFSs were mounted on poles at the same height as the bottom of the full-scale NLA mockup fuselage, 27 ft from the edge of the fire pit. The number of HFSs used was the same as was used in the 1:10-scale tests (eight). HFSs were checked with a known heat source to verify proper operation and to determine consistency among detectors. Four Medtherm model 96-30T-30 RP (Znse)-120-21746 Schmidt–Boelter-type, water-cooled heat flux transducers were also installed on opposite sides of the fire pit. Figure 12 shows the locations of these sensors. The anemometers were installed, also shown in figure 12, toward the southwest and southeast corner of the fire pit for recording wind speed during the fire trials. The southwest anemometer was installed above the fire pit observation tower at a 25-ft elevation, and the other was on a tall stand at an 8.5-ft elevation. A LabVIEW DAQ program and a National Instruments™ PXI/SCXI DAQ were installed adjacent to the fire pit in a portable building. Data were recorded from the HFSs and anemometers at 1-s intervals. IR and standard video cameras were located as close as possible to the same positions as the 1:10-scale tests. An additional camera was installed on the fire pit observation tower located southwest of the fire pit.

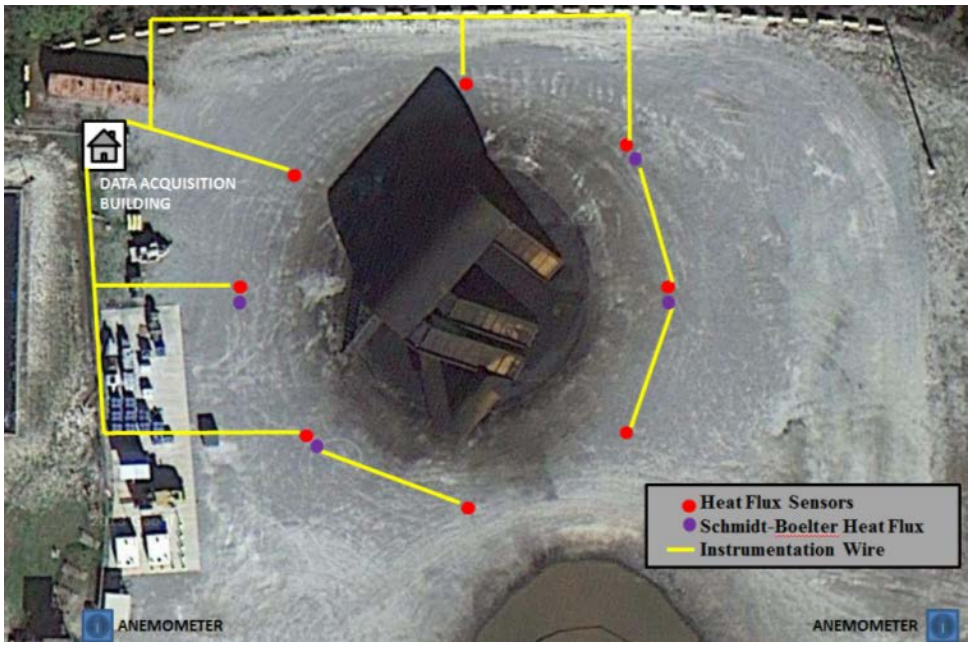

Figure 12. Full-Scale NLA Mockup Test Fixture Perimeter Sensor Locations

To ensure rapid and reliable ignition of the fuel, a gasoline distribution system and an ignition system were installed in the fire pit. In past experiments, a firefighter would walk around the pit and ignite the JP-8 using a propane torch. However, to expedite ignition of fuel over the surface of the pit and to ensure a repeatable ignition sequence, a spray system was installed in the fire pit to create a gasoline spray over a large surface area. A drawing of the spray system coverage area is shown in figure 13.

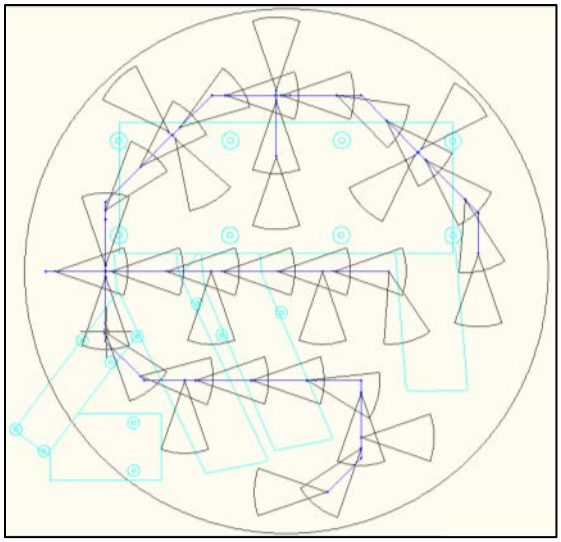

Figure 13. Full-Scale NLA Mockup Spray Nozzle Layout

Ignition methods were different in the first three trials, they did not vary. In the initial test, after approximately 30 gal of gasoline was discharged into the fire pit, the fuel was ignited from outside of the pit by a firefighter with a propane torch. In the second test, gasoline was not used to allow for a comparison of ignition times. Instead, two propane torches were used to ignite the JP-8 at multiple locations. Even though the initial conditions for these first two tests were different, they were included in the data analysis to follow. In subsequent tests, after approximately 30 gal of gasoline were discharged into the fire pit, the fuel spray was temporarily stopped while an electric ignition system was used to ignite the gasoline. The fuel spray was then reinitiated, continued running until the fire propagated across the fire pit, and was then shut down. The electrical ignition system consisted of a rheostat to produce 20 volts alternating current, which was used to heat coils of nichrome wire installed in four locations in the fire pit. The nichrome wires were in contact with small bundles of excelsior (wood wool) material that ignited from contact with the hot wires. These four small fires then, in turn, ignited the gasoline.

3.2 INITIAL CONDITIONS.

3.2.1 Initial Conditions for 1:10-Scale NLA Mockup Trials in Windless Conditions.

The test facility doors were closed, and the ventilation system was deactivated for all windless trials. The 1:10-scale NLA mockup surface and JP-8 fuel temperature were both within 5°F of ambient temperature inside the test facility. The initial water depth in the fire pan was 2±0.125 in., and 20±0.50 gal of JP-8 was used in each trial.

3.2.2 Initial Conditions for 1:10-Scale NLA Mockup Trials in Controlled Wind Conditions.

The flow straightener was placed at the south end of the hangar, and eight fans were installed at the north end. Ambient winds were less than 5.0 mph for the 5.5-mph tests, less than 2.0 mph for the 1.4-mph tests, and less than 1.5 mph for the 0.7-mph tests. Similar to the windless condition trials, both the 1:10-scale NLA mockup surface and the JP-8 fuel temperature were within 5°F of ambient temperature inside the test facility. The initial water depth in the fire pan was 2±0.125 in. and 20±0.50 gal of JP-8 was used in each trial.

3.2.3 Initial Conditions for 1:10-Scale NLA Mockup Fuel Coverage Trials.

The flow straightener was placed at the south end of the hangar, and fans were installed at the north end. Ambient winds were less than 5.0 mph for all tests. The combined JP-8 fuel and water depth in the fire pan was 3.875 in. for all trials.

3.2.4 Initial Conditions for Full-Scale NLA Mockup Trials.

Ambient winds were less than 10 mph and quasi-steady. Water depth in the fire pit was 4±0.125 in. and 750 gal of JP-8 was used in each trial.

3.3 PROCEDURES.

3.3.1 Procedures for 1:10-Scale NLA Mockup Trials in Windless Conditions.

The procedures for trials done in windless conditions are summarized in the following steps:

- Verify the steel fire pan and NLA mockup temperatures are no more than 5°F above ambient air temperature in the hangar.
- Pour water into the fire pan to a depth of 2±0.125 in., and then add 20±0.50 gal of JP-8.
- Verify the JP-8 fuel temperature in the fire pan is no more than 5°F above ambient air temperature in the hangar.
- Start the video cameras and the DAQ system.
- Ignite the fire.
- Allow the fire to burn until self-extinguished.
- During the fire, note whether the fire leans in a particular direction during the test.
- Record data and video for at least 1 min after flames are no longer visible and no heat flux was detected.
- Open the test facility doors and de-smoke.

3.3.2 Procedures for the 1:10-Scale NLA Mockup Trials in Controlled Wind Conditions.

- Verify that ambient wind conditions are within limits.
- Verify the steel fire pan and NLA mockup temperatures are no more than 5°F above ambient air temperature in the hangar.
- Pour water into the fire pan to a depth of 2±0.125 in., and then add 20±0.50 gal of JP-8.
- Verify the JP-8 fuel temperature in the fire pan is no more than 5 °F above ambient air temperature in the hangar.

- Start the fans preset to correct wind speed.
- Close the personnel doors to the indoor test facility.
- Start the video cameras and the DAQ system.
- Ignite the fire.
- Allow the fire to burn until self-extinguished.
- During the fire, note whether the fire leans in a particular direction during the test.
- Record data and video for at least 1 min after the fire goes out.
- Turn on the overhead exhaust fan and de-smoke.

3.3.3 Procedures for Full-Scale NLA Mockup Trials.

- Verify that ambient wind conditions are within limits.
- Verify water level in the fire pit is at correct height.
- Verify the four nichrome wires are installed with excelsior material.
- Begin flowing JP-8 fuel into the fire pit.
- When 700 gal of JP-8 have been flowed into the pit, spray 30 gal of gasoline into the fire pit.
- Stop the flow of JP-8 at 750 gal.
- Turn on ignition system.
- Spray an additional 10 gal of gasoline into the fire pit.
- Allow the fire to burn until self-extinguished.
- Record data and video for at least 1 min after the fire goes out.

4. RESULTS AND DISCUSSION.

4.1 THE 1:10-SCALE NLA MOCKUP TRIALS IN WINDLESS CONDITIONS.

The data recorded for a typical windless trial at 1-s intervals are shown in figures 14 through 18. The data for these graphs came from Trial 6 and are typical of all nine trials done in windless conditions. The vertical scales of the graphs are the same for all wind conditions, for easy comparison among test conditions. The horizontal axis ends at 360 s, with the fire usually diminishing (or self-extinguishing) after about 240 s, as shown in figure 14. Time zero is when the JP-8 was ignited with a propane torch.

Figure 14 shows a plot of the perimeter heat flux data measured with the flat-plate HFSs in Trial 6 and is typical of all trials. As explained in section 3.1.1, the flat-plate sensors were not accurately calibrated because they were intended only to show differences in relative heat flux from trial to trial and not to measure precise heat flux values at each location. Because there was no wind, the flames and hot gases rose straight up, resulting in nearly equal heat flux values around the perimeter.

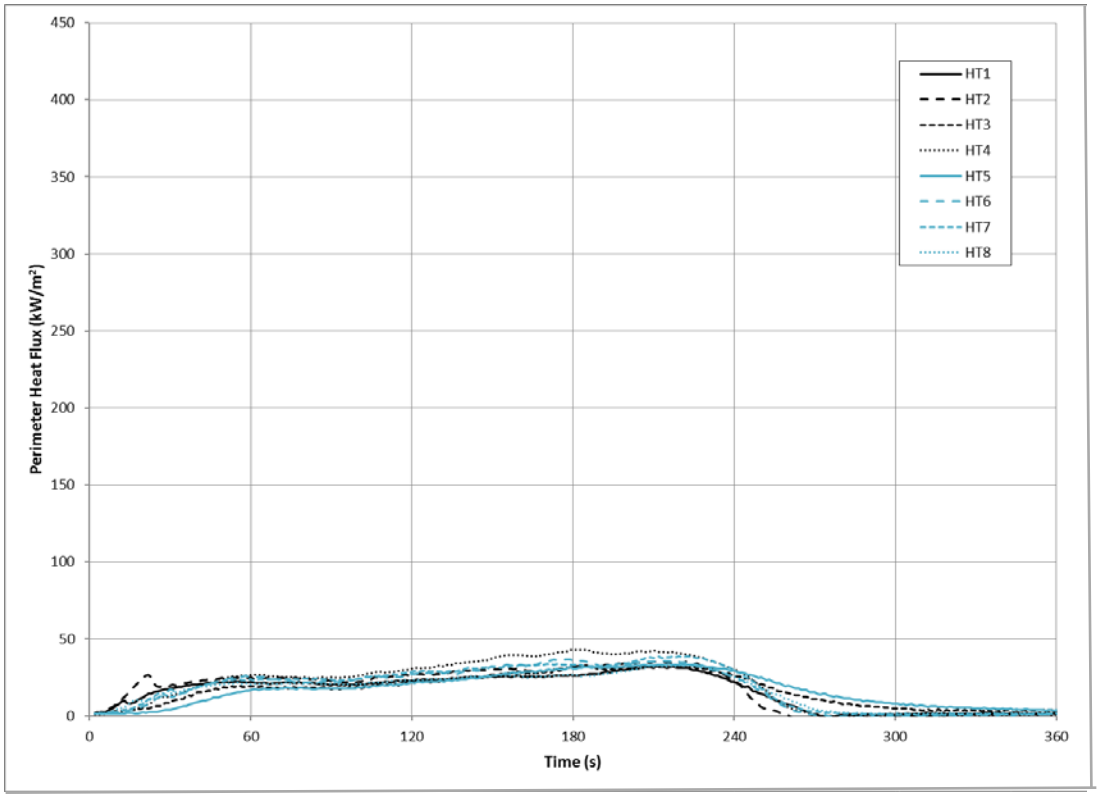

Figure 14. Typical Perimeter Heat Flux, Windless Condition

Figure 15 shows a graph of the data for Trial 6 from the eight TCs collocated with the flat-plate HFSs around the perimeter of the 1:10-scale NLA mockup. Again, the fire rising straight up resulted in a nearly even distribution of air temperatures around the perimeter of the pan.

Figure 16 shows a plot of the data from the three wing TCs in Trial 6. The thermal mass of the 0.135-in.-thick steel caused the wing to heat up and cool down slowly, resulting in a steady curve. The TCs closer to the center of the fire pan reached higher temperatures than the TC near the edge.

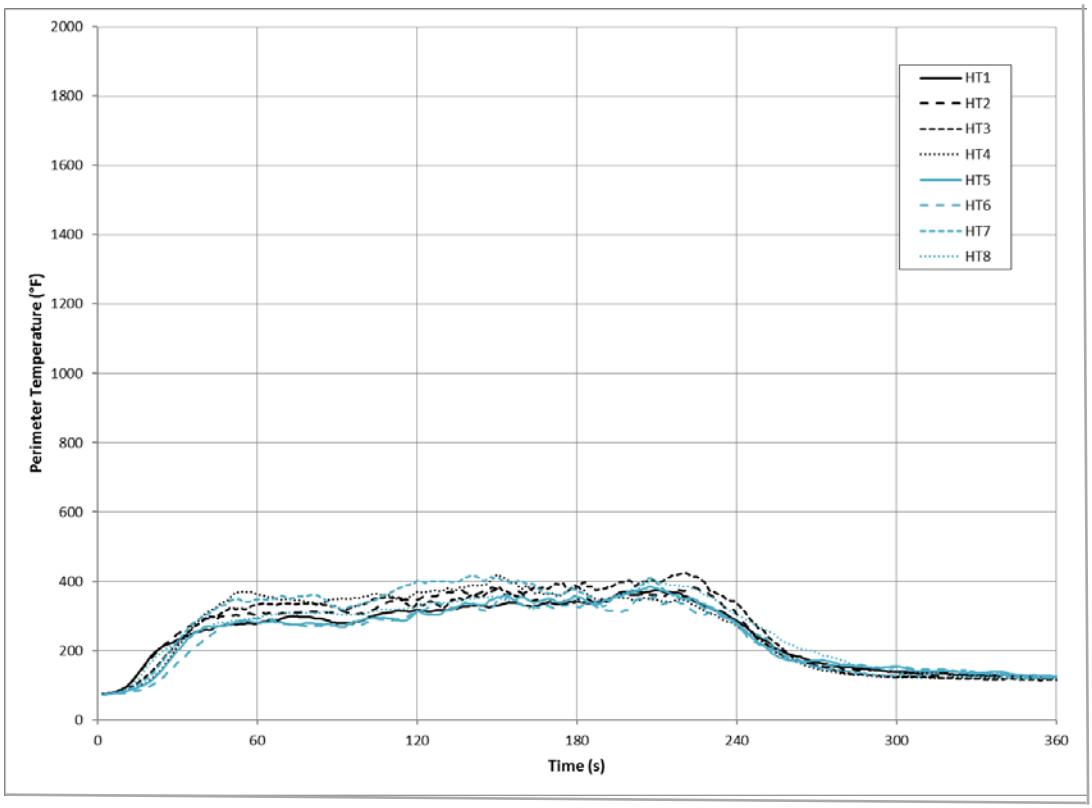

Figure 15. Typical Perimeter Temperature, Windless Condition

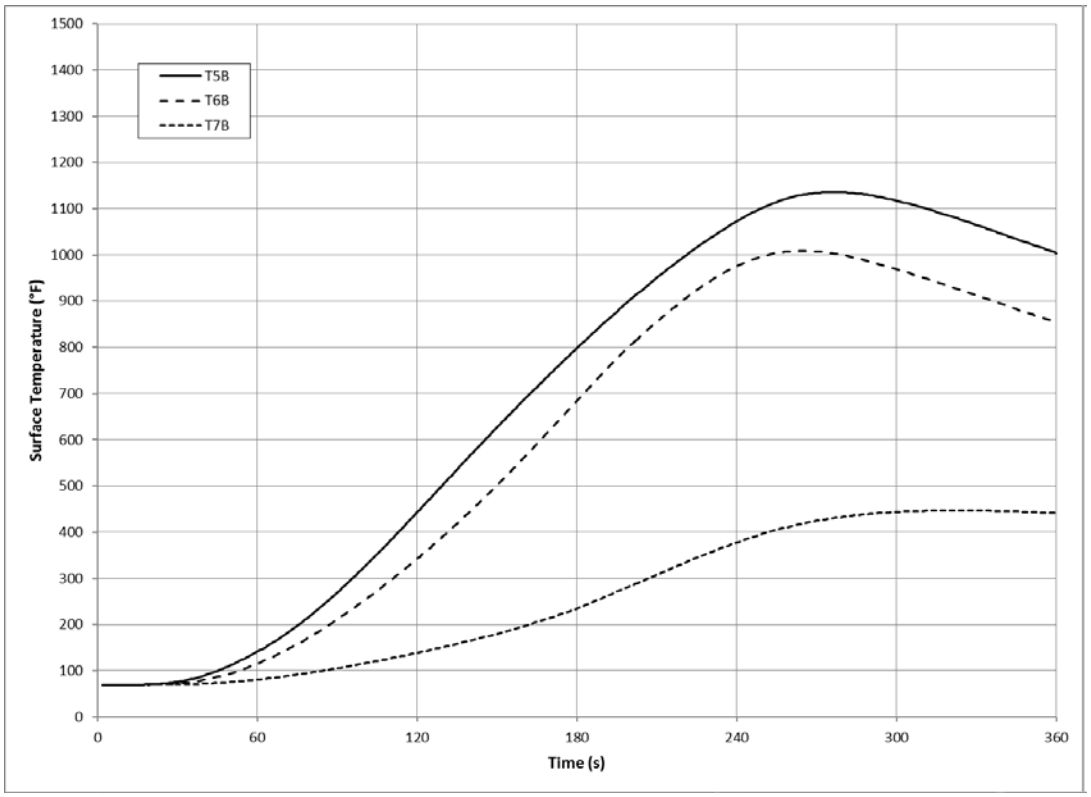

Figure 16. Typical Wing Underside Temperature, Windless Condition

Figure 17 shows a graph of the data from the four fuselage underside TCs in Trial 6, which is typical of all trials. Like the wing TCs, the 0.135-in. steel mass connected to the TCs made them slow to change, with the middle getting hotter than the ends.

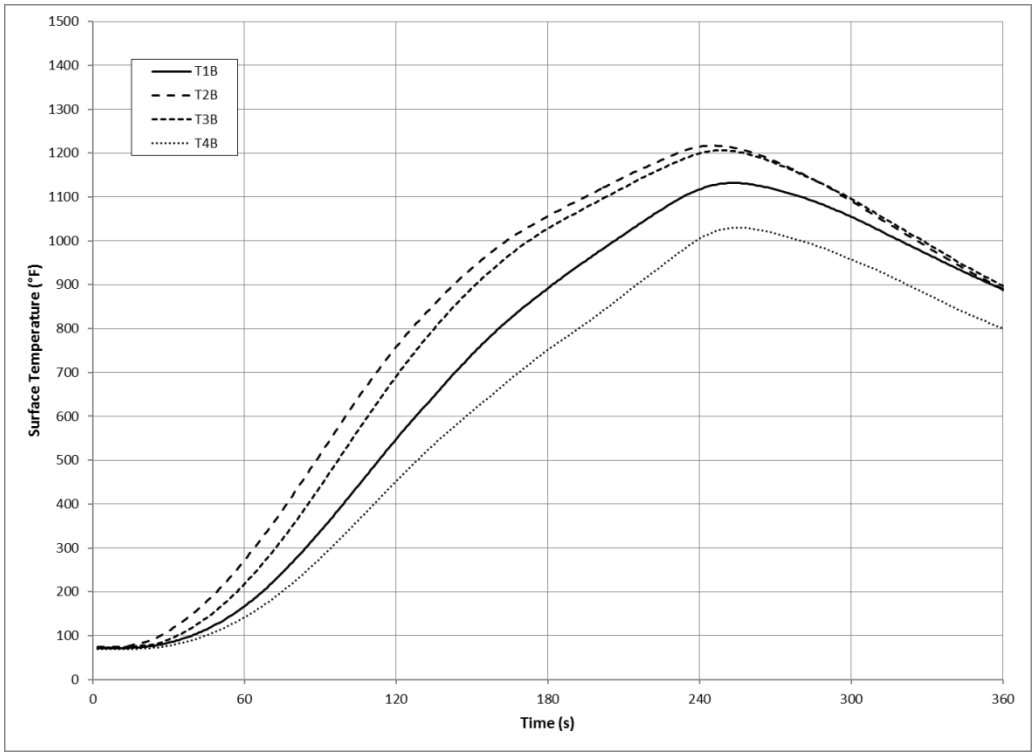

Figure 17. Typical Fuselage Underside Temperature, Windless Condition

Figure 18 shows the data from the right and left sides of the fuselage in Trial 6. The fire plume predominantly rose to the right side of the fuselage; therefore, the left side of the fuselage, which was closer to the edge of the fire pan, stayed much cooler. Again, the middle TCs reached higher temperatures than the TCs near the ends.

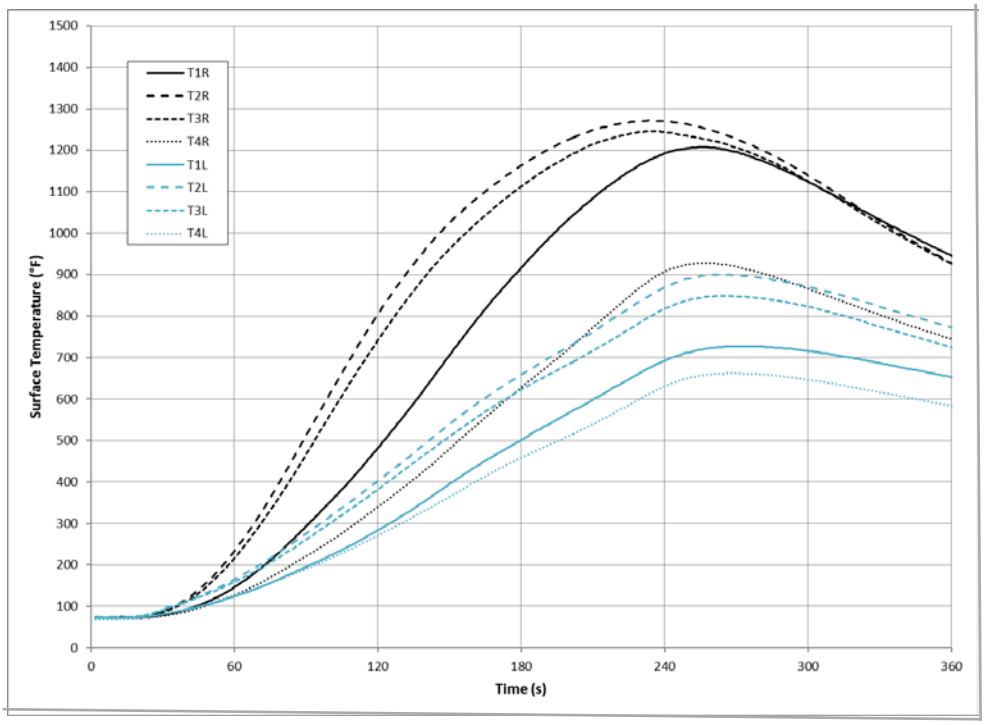

Figure 18. Typical Side Fuselage Temperature, Windless Condition

Appendix A shows the average and standard deviation data at 15-s intervals for the series of nine trials conducted in windless conditions. The data for the nine trials were so consistent from trial to trial that shifting to better align the temperature curves in time, as explained in section 3, was not necessary. Thirty-one separate temperatures and heat fluxes were measured for each trial, and the data were compared at 15-s intervals for the first 4 min of each trial for a total of 527 separate RSE values to compare. The percentage of data that fell below the 10% and 30% criteria for each sensor group is summarized in table 2. Sensor groups with at least 80% of their RSE values below 10% were considered a very reliable indicator of repeatability from test to test; those below 30% were considered a good indicator of repeatability.

Table 2. The RSE Values From Windless Trials

Nine Trials in Windless Conditions			
Sensor Group	Percent of Data With RSE ≤10%	Percent of Data With RSE ≤30%	Result
Eight perimeter plate-style HFSs	99.3	100.0	Very reliable indicator
Eight perimeter-exposed TCs	100.0	100.0	Very reliable indicator
Three wing underside surface TCs	100.0	100.0	Very reliable indicator
Four fuselage underside surface TCs	100.0	100.0	Very reliable indicator
Four fuselage right-side surface TCs	100.0	100.0	Very reliable indicator
Four fuselage left-side surface TCs	100.0	100.0	Very reliable indicator

In all 527 cases, the RSE values were less than 10%, except for a single RSE value from perimeter heat flux (annotated in appendix A). A total of 136 RSE values were calculated from the data taken at 15-s intervals over the first 4 min of each fire for the flat-plate sensors. Only

one exceeded 10%. The RSE value that exceeded 10% occurred near the finish, as the fire was beginning to diminish from a lack of sufficient fuel to cover the entire surface of the pool. A large majority of the RSE values for sensors during the middle part of the fires were well below 10%. Again, this was consistent with the criterion generally accepted as indication of a very reliable statistical indicator.

The success criterion established for a repeatable test procedure was that at least 80% of the calculated RSE values for the data had to be 30% or less. All the sensor groups easily met this requirement. A thorough review of the data indicated that the test procedure was very repeatable, and that the results were very predictable under windless conditions.

4.2 THE 1:10-SCALE NLA MOCKUP TRIALS IN CONTROLLED WIND CONDITIONS.

During the 1:10-scale NLA mockup controlled wind tests inside the hangar, it was observed that the indicated wind speed would change once the fire was ignited. Figure 19 shows a plot of the north–south velocity component (the other components are negligible) from the interior anemometer over the entire sequence of events during a typical 1.4-mph experiment. The far left of the graph shows where ambient wind was blowing through the hangar. A negative value means that the wind direction was from the north. At -390 s, the fans were turned on at the preset speed to generate approximately 1.4-mph wind speeds through the center of the hangar. It took roughly 30 s for the fans to ramp up in speed and for steady winds to move through the hangar. The crosswind stayed relatively constant at 1.4 mph until the fire was ignited (consistently time zero in this report). After the fire was ignited, the measured wind speed initially dropped to 0.3 mph and then steadily increased to nearly 4.0 mph by the time the fire started to self-extinguish. The portion of the data from ignition to 240 s after ignition is referred to as during-test wind speed. Wind speeds slowly returned to pretest conditions as the fire completely self-extinguished and the fixture cooled down.

This initial decrease in measured wind speed, followed by a steady increase and then slow return, was typical of all 1:10-scale NLA mockup trials, regardless of initial (pretest) setting or orientation. For this reason, two quantitative measurements for wind speed were recorded: pretest and during-test. Average pretest wind speeds were taken directly from the north–south component velocity data recorded at 1-s intervals from 40 s after the fans were turned on until the fire was ignited. Average during-test wind speeds were taken from the same recorded north–south data from the time the fire was ignited until 240 s later.

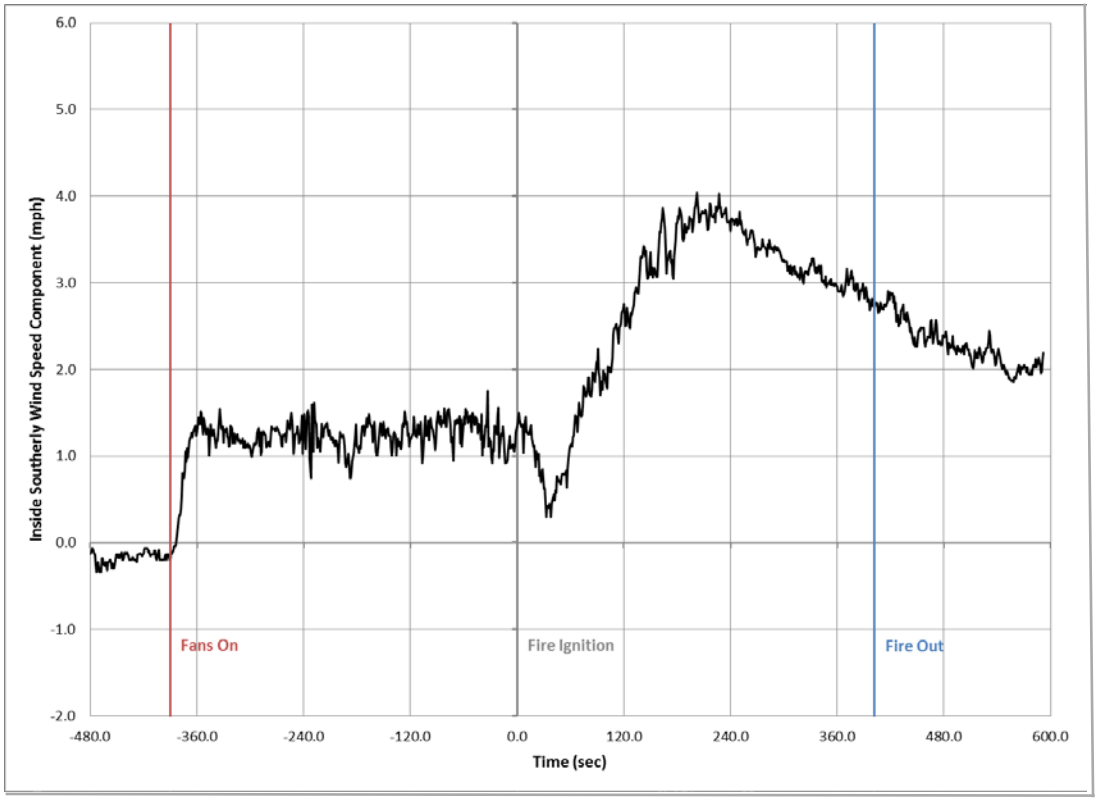

Figure 19. Typical 1.4-mph Wind Speed Progression

4.2.1 Trials in 0.7-mph Wind Conditions.

To generate very low wind speeds inside the hangar, three fans were blocked. Thus, five fans in an X-shaped pattern were used at low rotational speeds. Furthermore, the five original fan blades were changed out for lower pitch blades to consistently achieve 0.7-mph interior wind speeds. A consequence of conducting the 0.7-mph tests in extremely low ambient wind conditions was a 0.1-mph standard deviation in data among all tests.

4.2.1.1 Trials With 90° Crosswinds.

The data from a typical 0.7-mph, 90° crosswind test, are shown in figures 20 through 24. The data for these graphs are from Trial 4, which are typical for all six trials done at 0.7-mph, 90° crosswind (see figure 3 for a description of 90° crosswind). The vertical scales of the graphs are the same for all wind conditions for easy comparison among test conditions. The horizontal axis ends at 360 s with the fire usually diminishing after 240 s. Time zero is when JP-8 was ignited with a propane torch.

Figure 20 shows a plot of the perimeter heat flux data measured with the flat-plate HFSs. The sensors were not accurately calibrated because they were intended only to show differences in relative heat flux from trial to trial and not to measure precise heat flux values at each location. At the very low wind speed, the fire plume leaned slightly in the leeward direction (see figure 3) and caused higher heat flux values at HT1, HT2, and HT8. The same was evident for the perimeter temperature, as shown in figure 21.

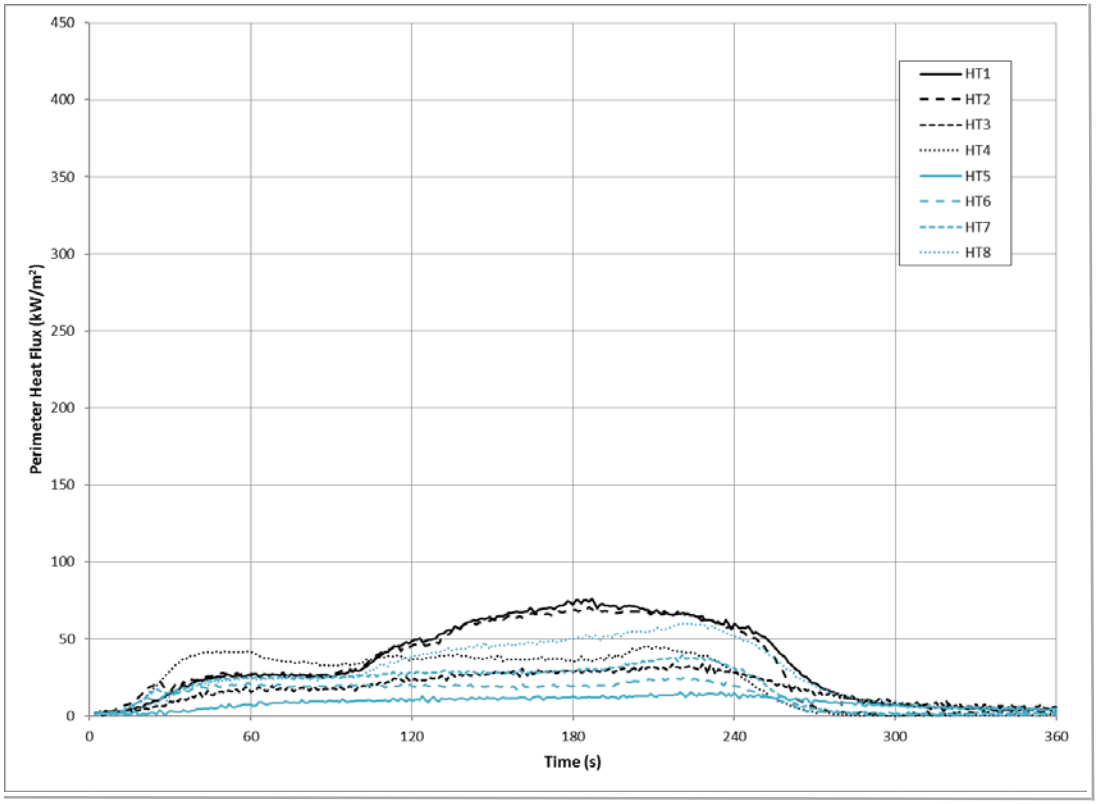

Figure 20. Typical Perimeter Heat Flux—0.7-mph, 90° Crosswinds

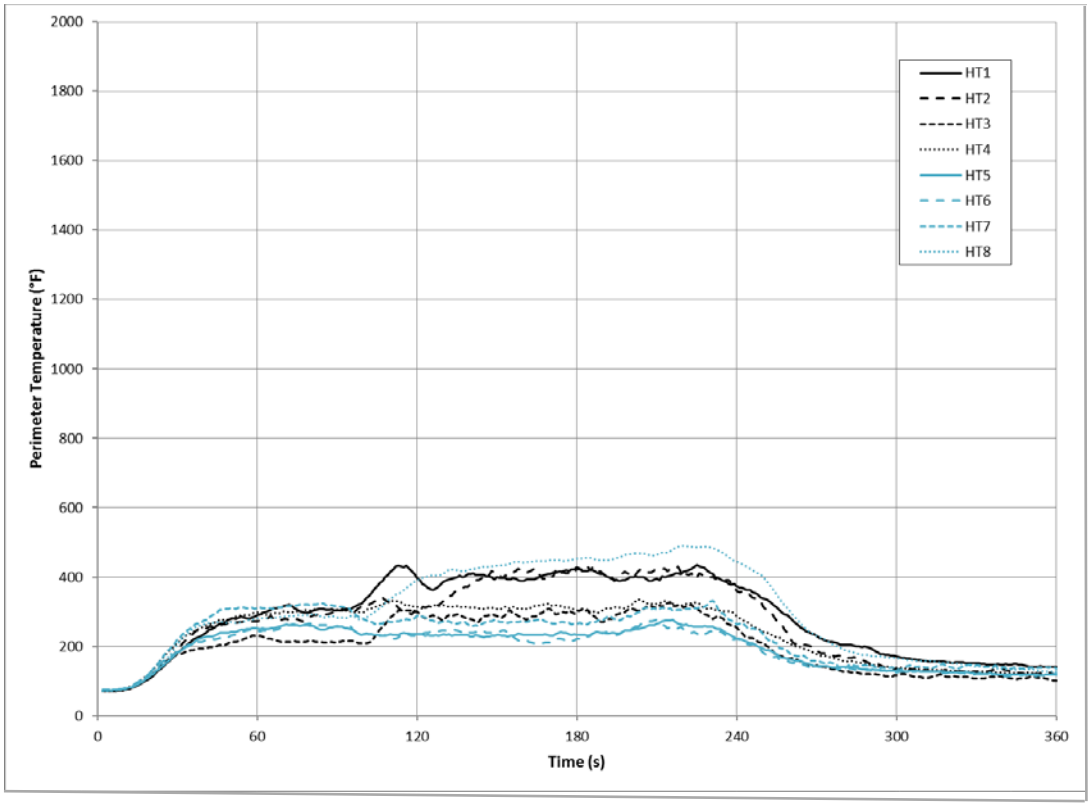

Figure 21. Typical Perimeter Temperature—0.7-mph, 90° Crosswinds

Figure 22 shows a plot of the data from the three wing TCs. The heat capacity of the 0.135-in.-thick steel caused the wing to heat up and cool down slowly, resulting in steady curves. The TCs closer to the fire center reached higher temperatures than the TC near the wing tip. Note that temperatures at TC locations T6B and T7B decreased compared to the windless tests, but the temperature at location T5B was nearly unchanged.

A graph of the data from the four underside fuselage TCs is shown in figure 23. As observed for the wing TCs, the 0.135-in.-thick steel made them slow to change. In contrast to the windless condition trials, the TCs near the middle of the fuselage were not hotter than either end. The slightly leaning fire plume wrapped around the fuselage and up the left side more compared to the windless tests. All temperatures were greater than for the windless tests.

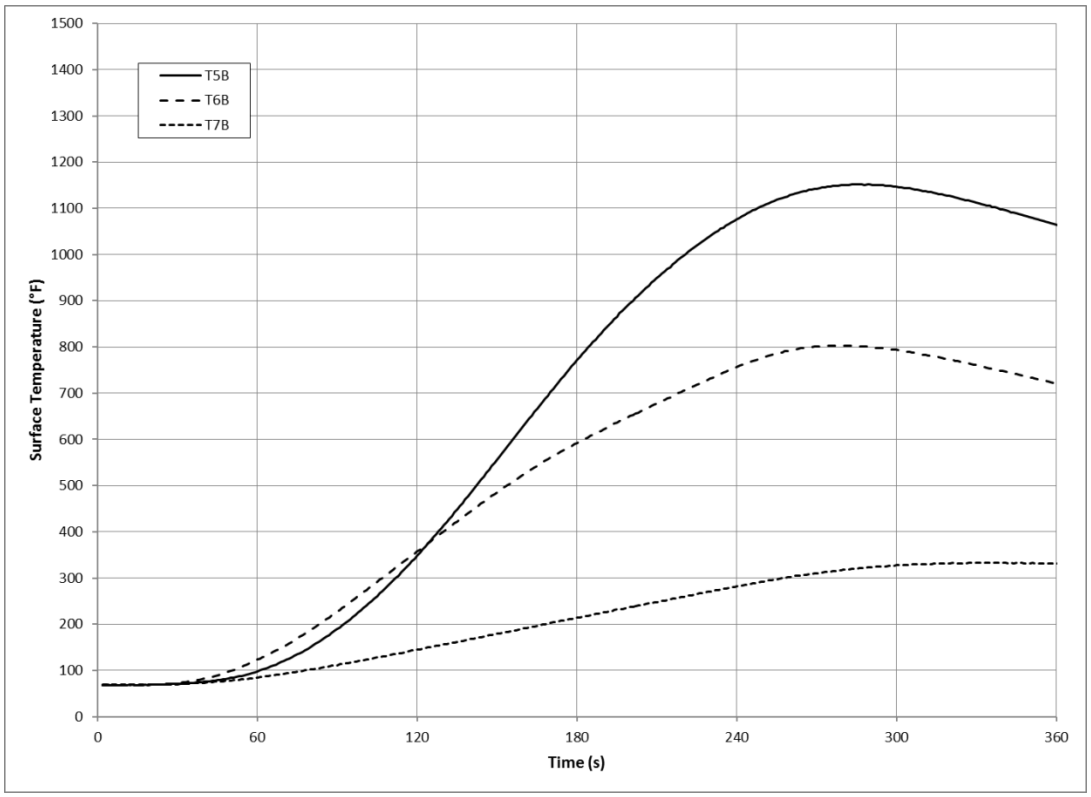

Figure 22. Typical Wing Underside Temperature—0.7-mph, 90° Crosswinds

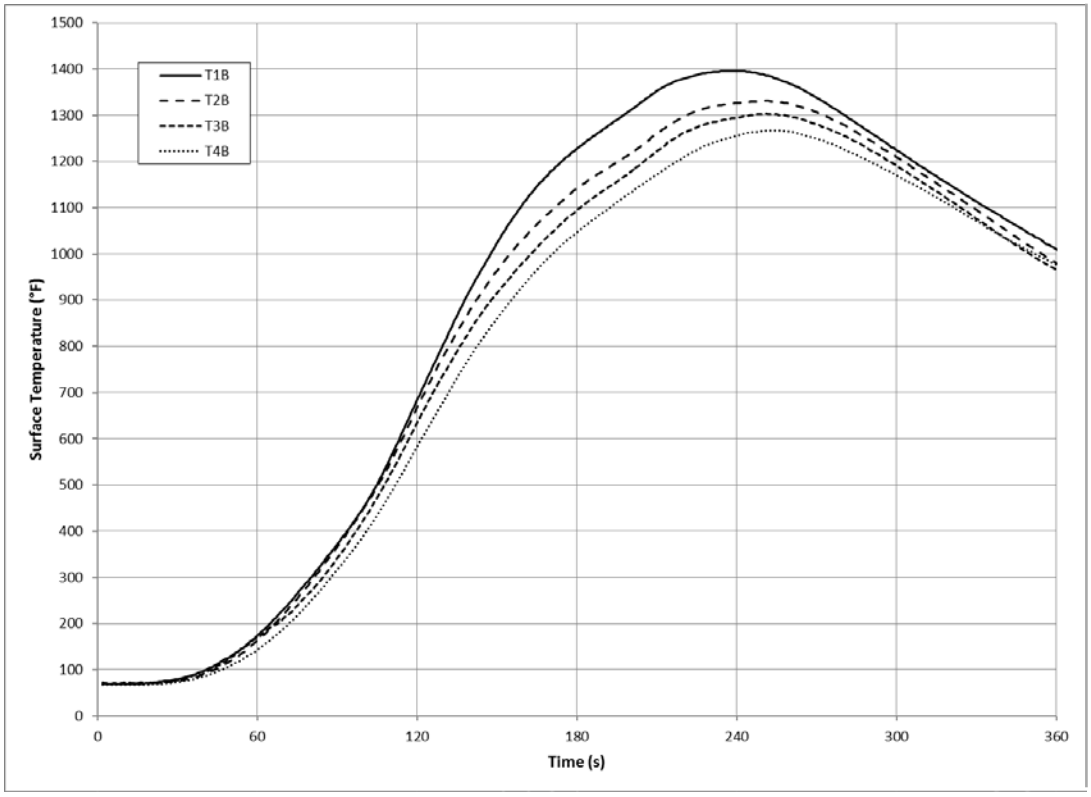

Figure 23. Typical Fuselage Underside Temperature—0.7-mph, 90° Crosswinds

Figure 24 shows a graph of the data from the right and left sides of the fuselage. The left and right sides of the fuselage were about equally heated, contrasted to the windless conditions, for which the right side got much hotter than the left side. Temperatures at both the left and right sides increased compared to the windless tests. The right-side middle TCs reached higher temperatures than those near the ends, but this was not true on the left side.

Appendix B shows the average and standard deviation data at 15-s intervals for the series of six trials conducted in the 0.7-mph, 90°crosswind condition. The data for the six trials were so consistent from trial to trial that time shifting to better align the temperature curves in time, as explained in section 3, was not necessary. Thirty-one separate temperatures and heat fluxes were measured for each trial. The data were compared at 15-s intervals for the first 4 min of each trial, for a total of 527 separate RSE values to compare. The percentage of data that fell below the 10% and 30% criteria for each sensor group is summarized in table 3. Sensor groups with at least 80% of their RSE values below 10% were considered a very reliable indicator of repeatability from trial to trial; those below 30% were considered a good indicator of repeatability.

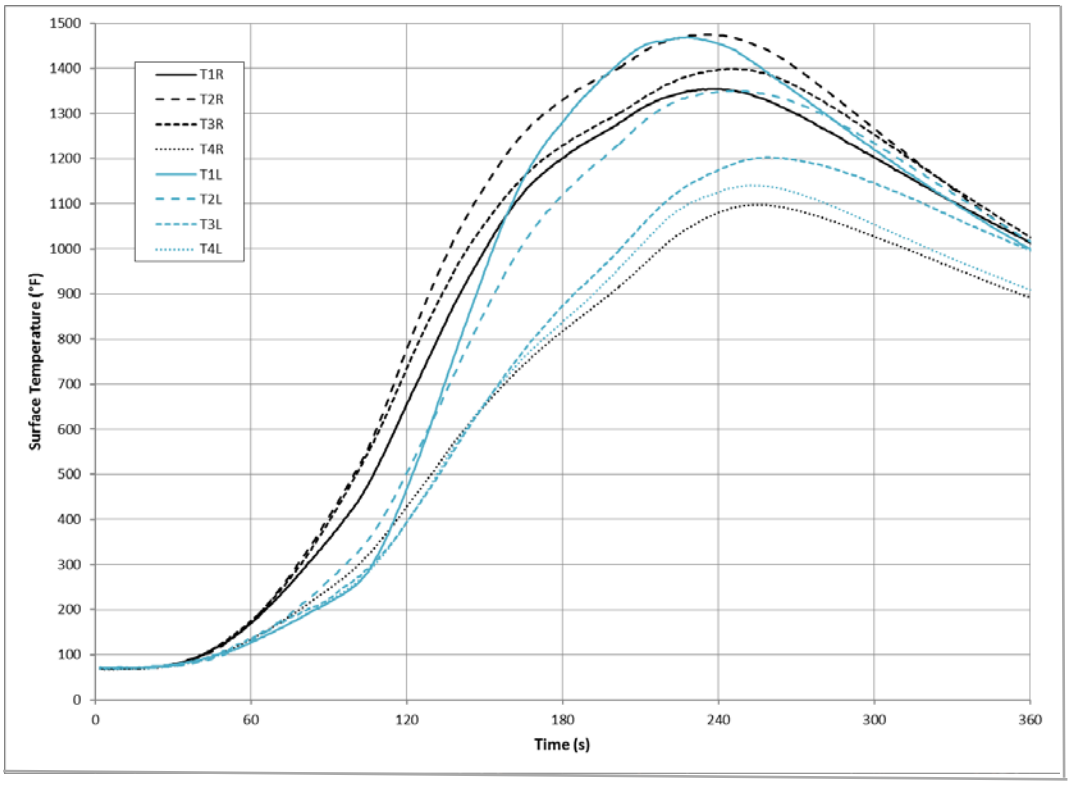

Figure 24. Typical Side Fuselage Temperature—0.7-mph, 90° Crosswinds

Table 3. The RSE Values From 0.7-mph, 90° Crosswind Trials

Six Trials With 0.7-mph, 90° Crosswinds			
Sensor Group	Percent of Data With RSE ≤10%	Percent of Data With RSE ≤30%	Result
Eight perimeter plate-style HFSs	92.6	99.3	Very reliable indicator
Eight perimeter-exposed TCs	100.0	100.0	Very reliable indicator
Three wing underside surface TCs	100.0	100.0	Very reliable indicator
Four fuselage underside surface TCs	100.0	100.0	Very reliable indicator
Four fuselage right-side surface TCs	100.0	100.0	Very reliable indicator
Four fuselage left-side surface TCs	100.0	100.0	Very reliable indicator

The criterion established to determine that the test procedure was repeatable was that at least 80% of the calculated RSE values for the data had to be 30% or less. All sensor groups easily met this requirement. A thorough review of the data indicated that the test procedure was very repeatable and that all results were predictable under the 0.7-mph, 90° crosswind condition.

Statistical analyses were conducted to compare the results from the 0.7-mph, 90° crosswind trials to the trials done in windless conditions. For each individual temperature and HFS, the data from trials at the two different wind conditions were compared by *t*-test at each 15-s interval over a period of 240 s starting when the fires were ignited. Appendix B shows the calculated *p*-value tables for the different sensors. The percentage of data that fell above the 1% (0.01) and 5% (0.05) criteria for each sensor group is summarized in table 4. Data sets with at least 80% of

their *p*-values greater than 0.05 were considered to have no probable significant difference between the two trial conditions. Data sets with at least 80% of their *p*-values greater than 0.01 were considered to have no highly significant difference between them.

Table 4. The *t*-Test Comparison—0.7-mph, 90° Crosswind to Windless Conditions

0 and 0.7-mph, 90° Crosswind *t*-Test		
Sensor Group	Percent of Data With *p*-Values >0.05	Percent of Data With *p*-Values >0.01
Eight perimeter plate-style HFSs	27	39
Eight perimeter-exposed TCs	18	29
Three wing underside surface TCs	8	20
Four fuselage underside surface TCs	16	24
Four fuselage right-side surface TCs	9	15
Four fuselage left-side surface TCs	12	15

Since no sensor groups exceeded the 80% threshold percentage of *p*-values above 0.01 or 0.05, there was enough evidence to conclude that there was a significant difference between the two trial conditions. The 0.7-mph, 90° crosswind trials produced different results than those under windless conditions. Even a relatively small difference in wind speed had a significant effect on the results of these trials.

4.2.1.2 Trials With 45° Crosswinds.

The data recorded from a typical 0.7-mph, 45° crosswind test are shown in figures 25 through 29. The data for these graphs are from Trial 3, which are typical for all six trials done at 0.7-mph, 45° crosswind (see figure 3 for a description of 45° crosswind). The vertical scales of each graph are the same for all wind conditions for easy comparison among test conditions. The horizontal axis ends at 360 s with the fire usually diminishing after 240 s. Time zero is when JP-8 was ignited with a propane torch.

Figure 25 shows a plot of the perimeter heat flux data measured with the flat-plate HFSs. The sensors were not accurately calibrated because they were intended only to show differences in relative heat flux from trial to trial and not to measure precise heat flux values at each location. Because there was very little wind, the fire plume leaned slightly in the downwind direction resulting in slightly higher heat flux values at HT1, HT7, and HT8. The same trend was evident with the perimeter temperature, as shown in figure 26.

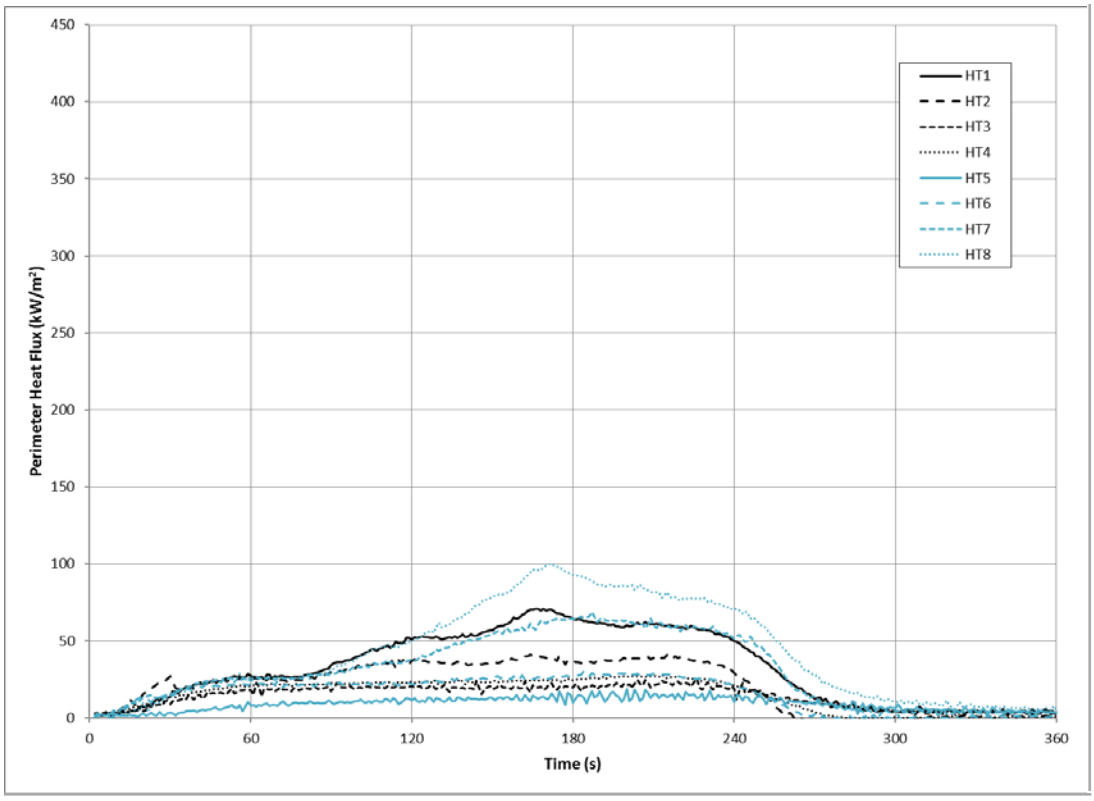

Figure 25. Typical Perimeter Heat Flux—0.7-mph, 45° Crosswinds

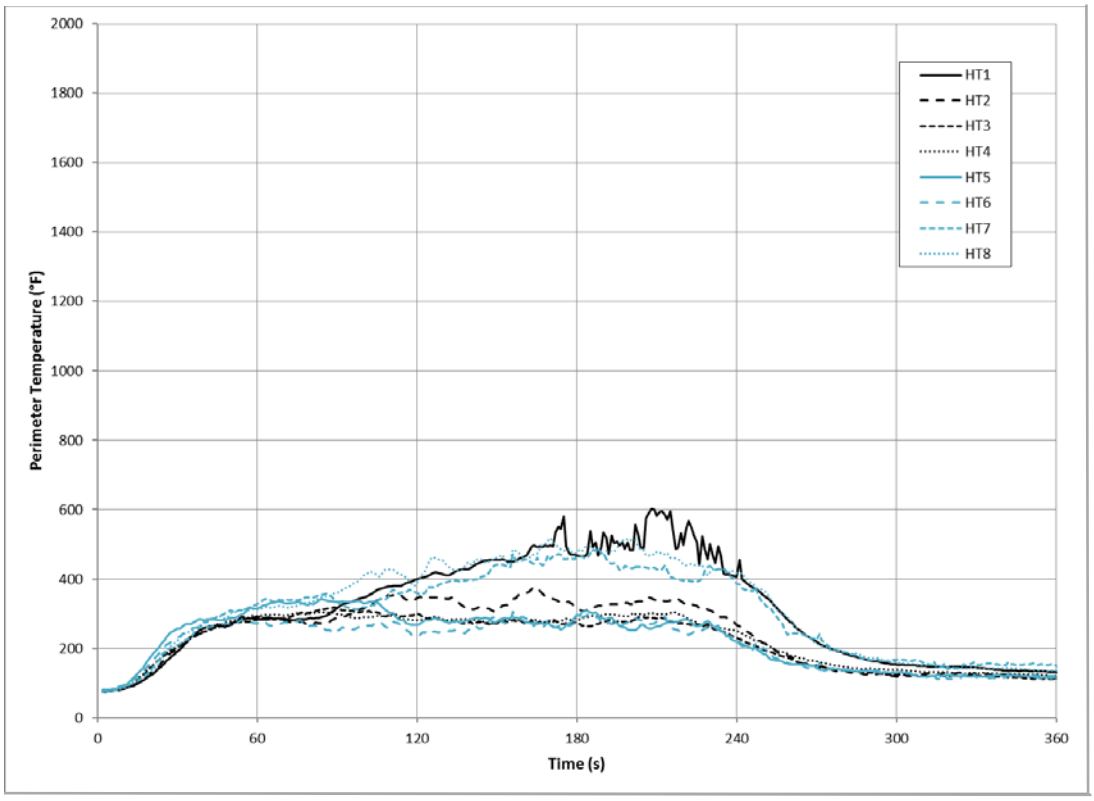

Figure 26. Typical Perimeter Temperature—0.7-mph, 45° Crosswinds

Figure 27 shows a plot of the data from the three wing TCs. The heat capacity of the 0.135-in.-thick steel caused the wing to heat up and cool down slowly, which resulted in steady curves. Location T6B reached the highest temperature of the three and showed an increase from the windless condition trials. The temperature at location T7B also increased compared to the windless trials, while the temperature at T5B decreased.

A graph of the data from the four underside fuselage TCs is shown in figure 28. As with the wing TCs, the 0.25-in. steel mass slows the TC's temperature change. T4B, the location of the TC farthest downwind, reached the highest temperature, with very little temperature spread among all four. The slightly leaning fire plume enveloped the fuselage and rose up the left side more than during the windless trials.

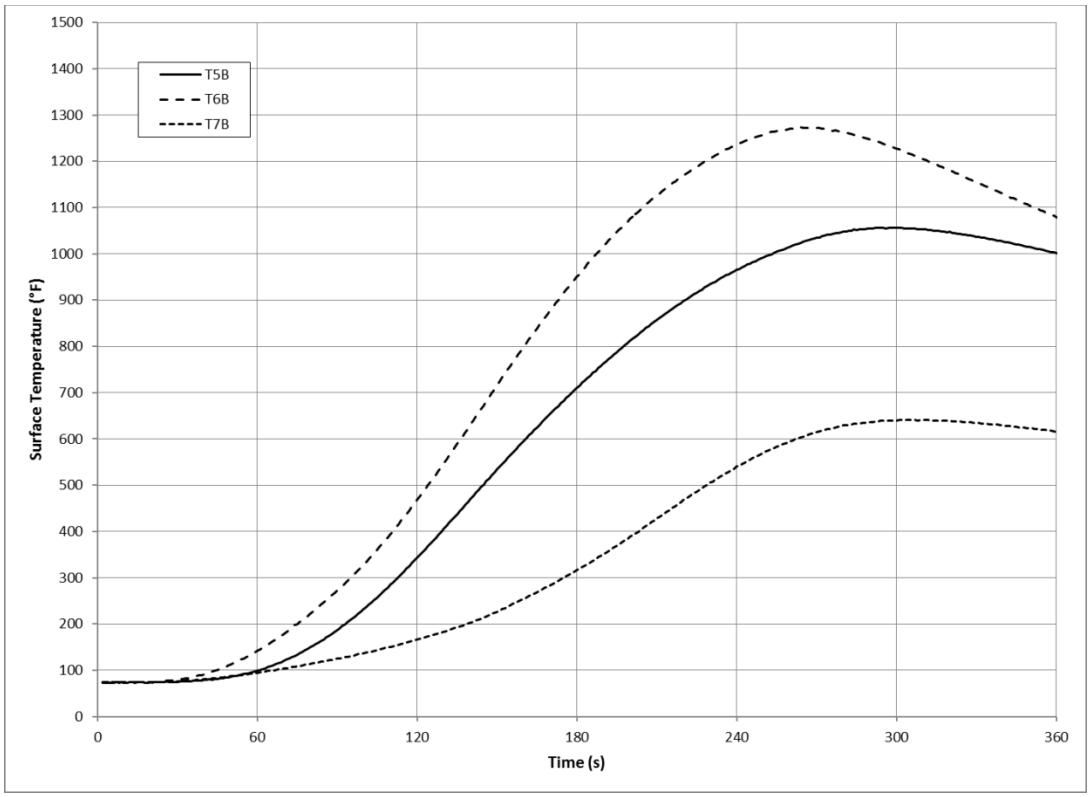

Figure 27. Typical Wing Underside Temperature—0.7-mph, 45° Crosswinds

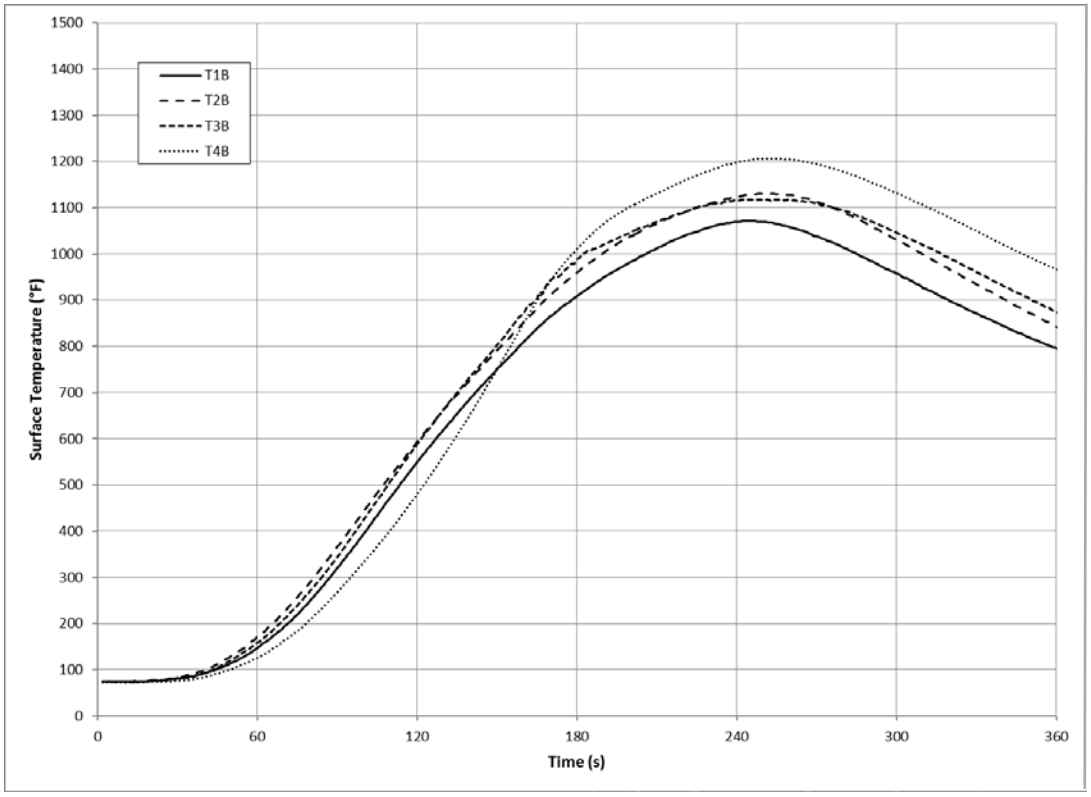

Figure 28. Typical Fuselage Underside Temperature—0.7-mph, 45° Crosswinds

Figure 29 shows the data from the right and left sides of the fuselage. The temperature for the left and right sides of the fuselage was approximately the same. Temperatures increased from upwind T1, in order, to downwind T4 on both the right and left sides.

Appendix C shows the average and standard deviation data at 15-s intervals for the series of six trials conducted in the 0.7-mph, 45° crosswind condition. The data for the six trials were so consistent from trial to trial that time shifting to better align the temperature curves in time, as explained in section 3, was not necessary. Thirty-one separate temperatures and heat fluxes were measured for each trial. The data were compared at 15-s intervals for the first 4 min of each trial for a total of 527 separate RSE values to compare. The percentage of data that fell below the 10% and 30% criteria for each sensor group is summarized in table 5. Sensor groups with at least 80% of their RSE values below 10% were considered a very reliable indicator of repeatability from trial to trial; those below 30% were considered a good indicator of repeatability.

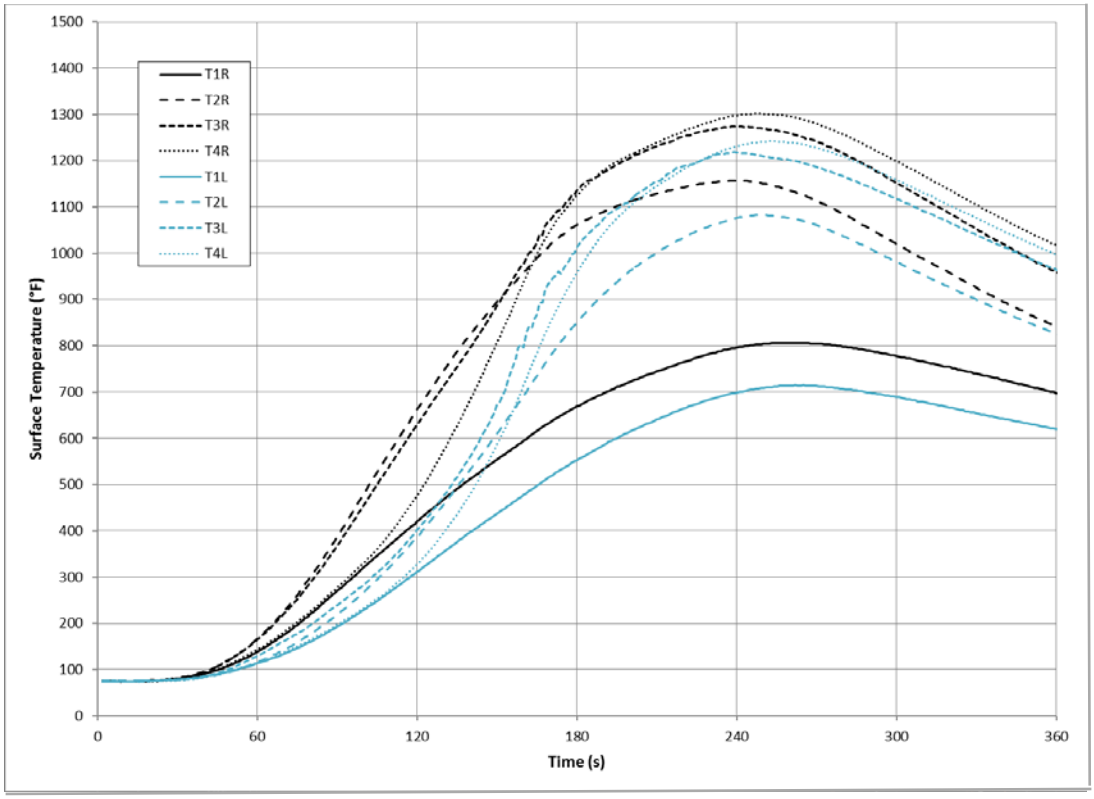

Figure 29. Typical Side Fuselage Temperature—0.7-mph, 45° Crosswinds

Table 5. The RSE Values From 0.7-mph, 45° Crosswind Trials

Six Trials With 0.7-mph, 45° Crosswinds			
Sensor Group	Percent of Data With RSE ≤10%	Percent of Data With RSE ≤30%	Result
Eight perimeter plate-style HFSs	92.6	100.0	Very reliable indicator
Eight perimeter-exposed TCs	100.0	100.0	Very reliable indicator
Three wing underside surface TCs	100.0	100.0	Very reliable indicator
Four fuselage underside surface TCs	100.0	100.0	Very reliable indicator
Four fuselage right-side surface TCs	100.0	100.0	Very reliable indicator
Four fuselage left-side surface TCs	100.0	100.0	Very reliable indicator

The criterion established to determine that the test procedure was repeatable was that at least 80% of the calculated RSE values for the data had to be 30% or less. All sensor groups easily met this requirement. A thorough review of the data indicated that the test procedure was very repeatable and that all results were predictable under the 0.7-mph, 45° crosswind condition.

Statistical analyses were conducted to compare the results from the 0.7-mph, 45° crosswind trials to the trials done in windless conditions. For each individual temperature and HFS, the data from trials at the two different wind conditions were compared by *t*-test at each 15-s interval over a period of 240 s, starting when the fires were ignited. Appendix C shows the calculated *p*-value tables for the different sensors. The percentage of data that fell above the 1% (0.01) and 5%

(0.05) criteria for each sensor group is summarized in table 6. Data sets with at least 80% of their *p*-values greater than 0.05 were considered to have no probable significant difference between the two trial conditions. Data sets with at least 80% of their *p*-values greater than 0.01 were considered to have no highly significant difference between them.

Table 6. The *t*-Test Comparison—0.7-mph, 45° Crosswind to Windless Conditions

0- and 0.7-mph, 45° Crosswind *t*-Test		
Sensor Group	Percent of Data With *p*-Values >0.05	Percent of Data With *p*-Values >0.01
Eight perimeter plate-style HFSs	16	21
Eight perimeter-exposed TCs	27	36
Three wing underside surface TCs	35	41
Four fuselage underside surface TCs	21	29
Four fuselage right-side surface TCs	7	21
Four fuselage left-side surface TCs	22	32

Since no sensor groups exceeded the 80% threshold percentage of *p*-values above 0.01 or 0.05, there is enough evidence to conclude that there was a significant difference between the two test conditions. The 0.7-mph, 45° crosswind trials produced different results than those under windless conditions. Even a relatively small difference in wind speed had a significant effect on the results of these trials.

For comparison, a similar *t*-test was also conducted for the 0.7-mph, 90° crosswind and the 0.7-mph, 45° crosswind conditions. Again, none of the sensor groups exceeded the 80% threshold. It was concluded that the two test conditions were different, and that even a 45° wind direction change produced different temperature and heat flux distributions.

4.2.2 Trials in 1.4-mph Wind Conditions.

To generate these low wind speeds inside the hangar, three fans had to be blocked. Thus, five fans in an X pattern, with the original fan blades, were used at medium rotational speeds. A consequence of conducting the 1.4-mph tests in low ambient wind conditions was a 0.2-mph standard deviation among all tests.

4.2.2.1 Trials With 90° Crosswinds.

The data for a typical 1.4-mph, 90° crosswind test are shown in figures 30 through 34. The data for these graphs are from Trial 4, which are typical for all nine trials done at 1.4-mph, 90° crosswind (see figure 3 for a description of 90° crosswind). The vertical scales of the graphs are the same for all wind conditions for easy comparison among test conditions. The horizontal axis ends at 360 s, with the fire usually dying out after 240 s. Time zero is when the JP-8 was ignited with a propane torch.

Figure 30 shows a plot of the perimeter heat flux data measured with the flat-plate HFSs. The sensors were not accurately calibrated because they were intended only to show differences in relative heat flux from trial to trial and not necessarily to measure precise heat flux values at each location. At the low wind speed, the fire plume leaned in the leeward direction (refer to figure 3)

and caused higher heat flux values at HT1, HT2, and HT8. The same is evident for perimeter temperature, as shown in figure 31.

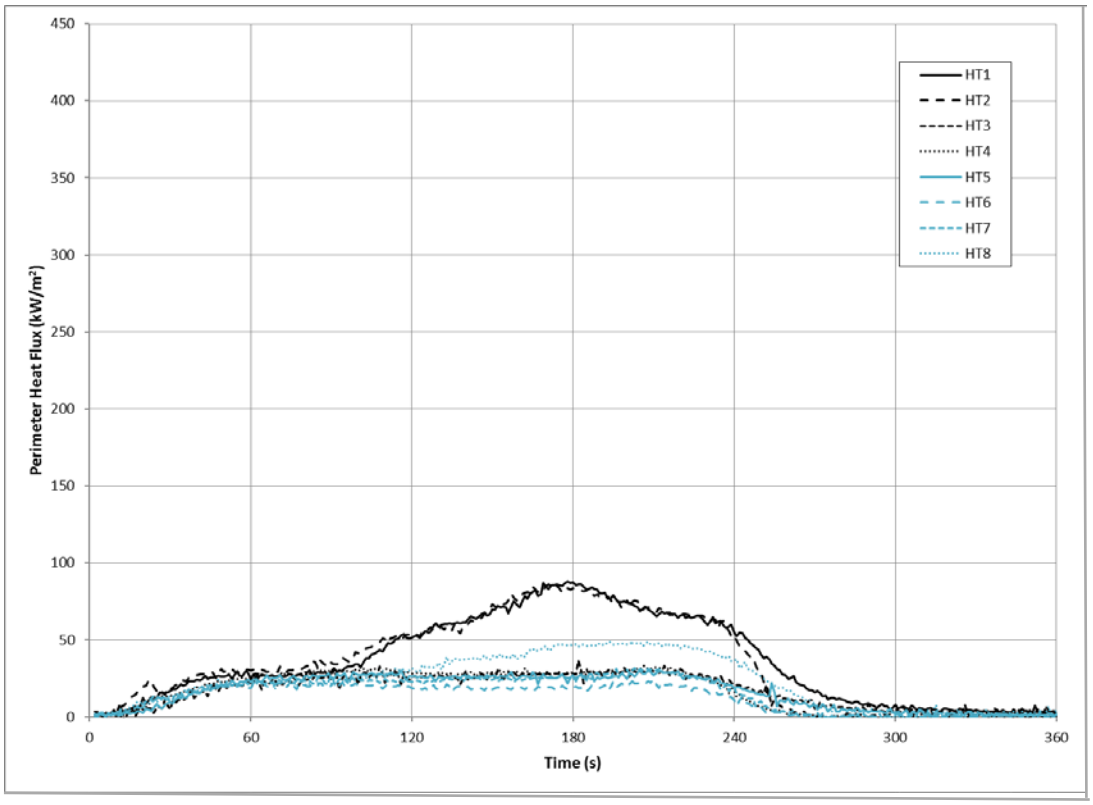

Figure 30. Typical Perimeter Heat Flux—1.4-mph, 90° Crosswinds

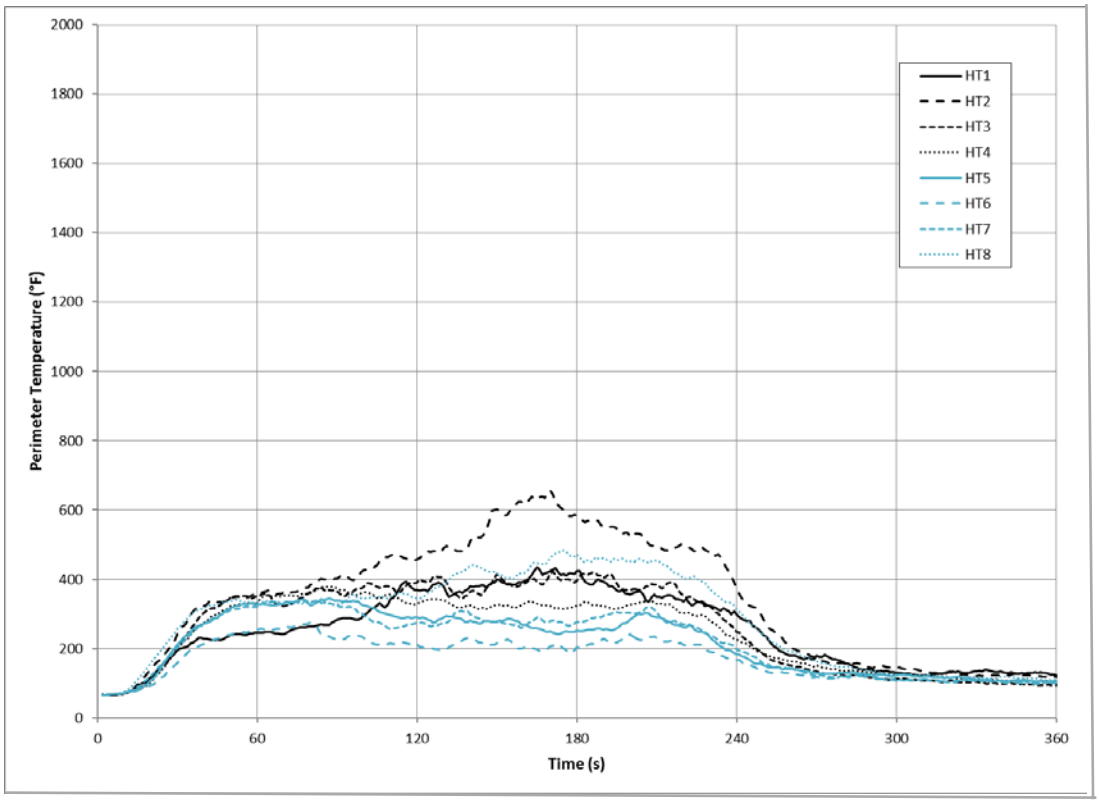

Figure 31. Typical Perimeter Temperature—1.4-mph, 90° Crosswinds

Figure 32 shows a plot of the data from the three wing TCs. The TCs closer to the center of the fire reached higher temperatures than the TC near the edge. Temperatures at T6B and T7B decreased compared to the windless tests, probably due to the leaning fire plume.

A graph of the data from the four underside fuselage TCs is shown in figure 33. Like the wing TCs, the 1/4-in. steel mass made them slow to change. As observed in the 0.7-mph trials, the temperature at location T1B was highest, and the temperatures were lower at each succeeding TC. The leaning fire plume enveloped the fuselage and rose up the left side more than it did in the windless trials. All temperatures were higher than for the windless trials.

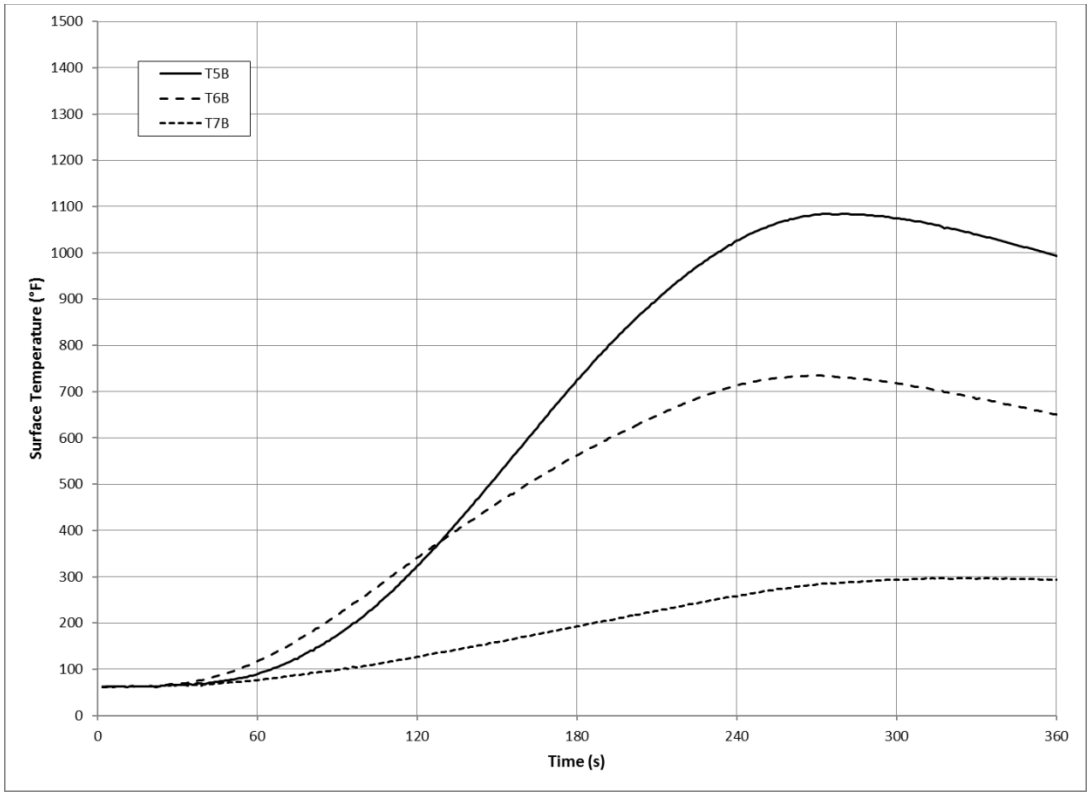

Figure 32. Typical Wing Underside Temperature—1.4-mph, 90° Crosswinds

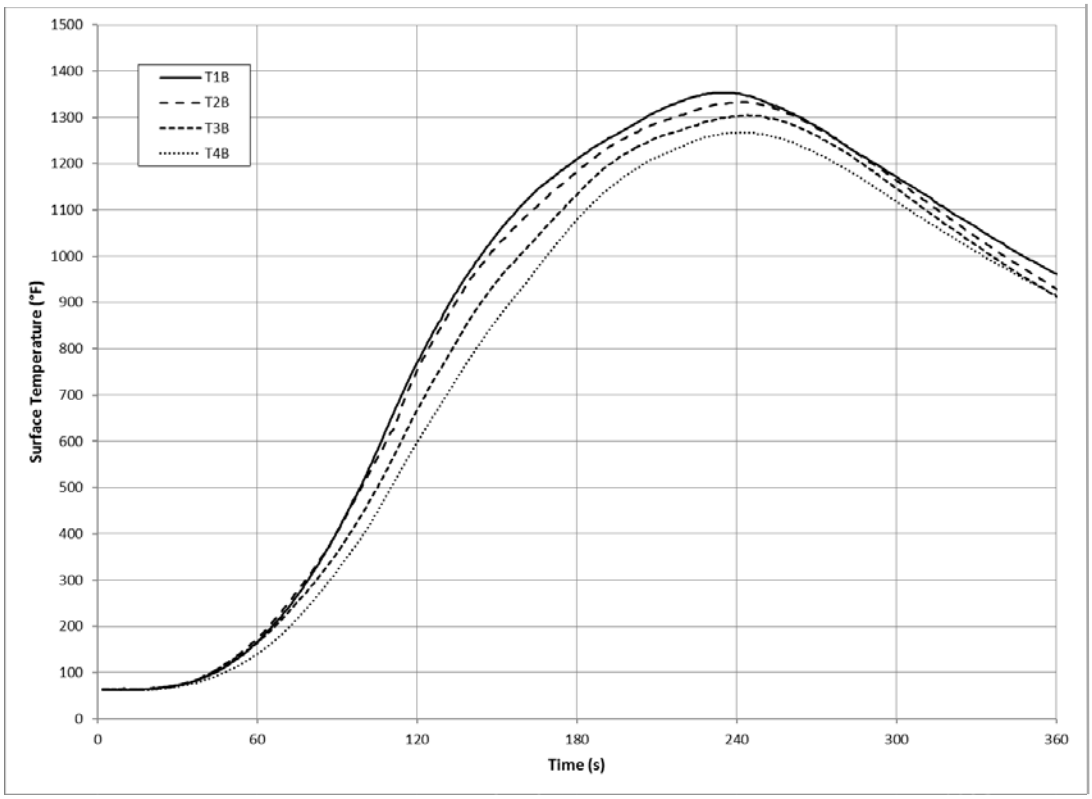

Figure 33. Typical Fuselage Underside Temperature—1.4-mph, 90° Crosswinds

Figure 34 shows the data from the right and left sides of the fuselage. Temperatures at the TCs near the middle were approximately the same on both sides of the fuselage, while temperatures near the ends were higher on the leeward side. Both the left- and right-side temperatures increased compared to the windless tests, with the left-side temperatures increasing to a great degree.

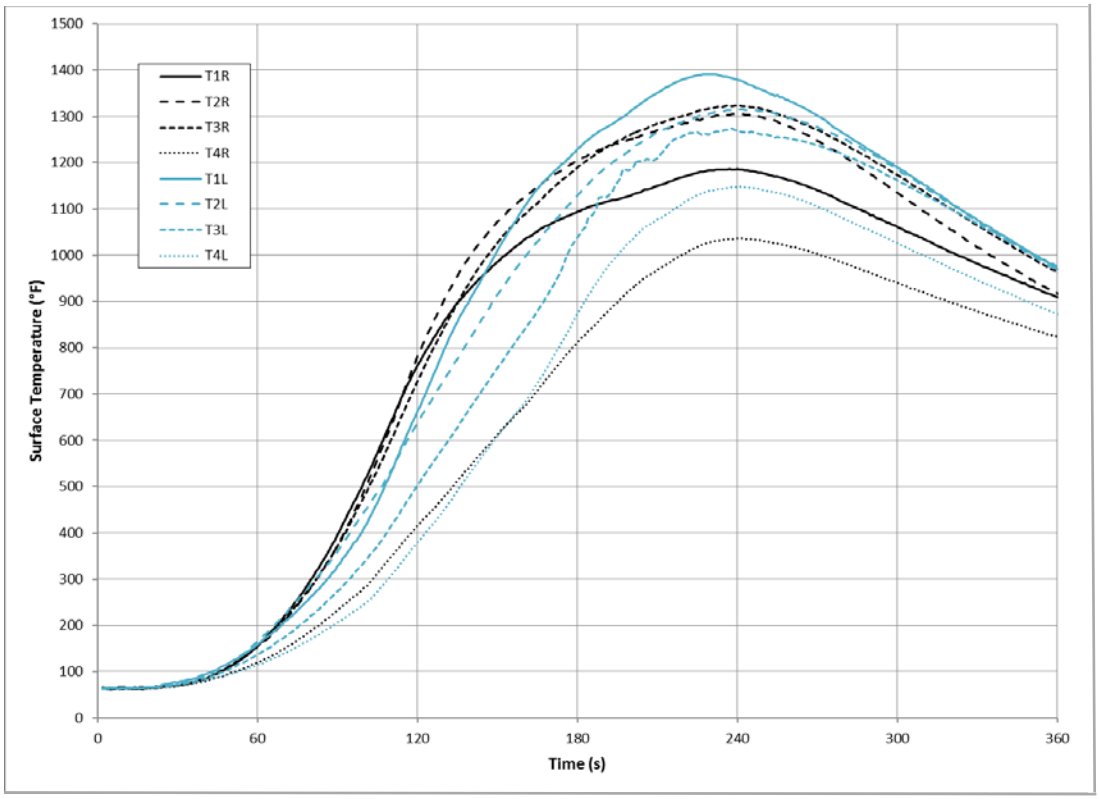

Figure 34. Typical Side Fuselage Temperature—1.4-mph, 90° Crosswinds

Appendix D shows the average and standard deviation data at 15-s intervals for the series of nine trials conducted in the 1.4-mph, 90° crosswind condition. The data for the nine trials were so consistent from trial to trial that time shifting to better align the temperature curves in time, as explained in section 3, was not necessary. Thirty-one separate temperatures and heat fluxes were measured for each trial. The data were compared at 15-s intervals for the first 4 min of each trial for a total of 527 separate RSE values to compare. The percentage of data that fell below the 10% and 30% criteria for each sensor group is summarized in table 7. Sensor groups with at least 80% of their RSE values below 10% were considered a very reliable indicator of repeatability from test to test; those below 30% were considered a good indicator of repeatability.

Table 7. The RSE Values From 1.4-mph, 90° Crosswind Trials

Nine Trials With 1.4-mph, 90° Crosswinds			
Sensor Group	Percent of Data With RSE ≤10%	Percent of Data With RSE ≤30%	Result
Eight perimeter plate-style HFSs	90.4	98.5	Very reliable indicator
Eight perimeter-exposed TCs	100.0	100.0	Very reliable indicator
Three wing underside surface TCs	100.0	100.0	Very reliable indicator
Four fuselage underside surface TCs	100.0	100.0	Very reliable indicator
Four fuselage right-side surface TCs	100.0	100.0	Very reliable indicator
Four fuselage left-side surface TCs	100.0	100.0	Very reliable indicator

The criterion established to determine that the test procedure was repeatable was that at least 80% of the calculated RSE values for the data had to be 30% or less. All sensor groups easily met this requirement. A thorough review of the data indicated that the test procedure was very repeatable and that all results were predictable under the 1.4-mph, 90° crosswind condition.

Statistical analyses were conducted to compare the results from the 1.4-mph, 90° crosswind trials to the trials done in windless conditions. For each individual temperature and HFS, data from the trials at the two different wind conditions were compared by *t*-test at each 15-s interval over a period of 240 s starting when the fires were ignited. Appendix D shows the calculated *p*-value tables for the different sensors. The percentage of data that fell above the 1% (0.01) and 5% (0.05) criteria for each sensor group is summarized in table 8. Data sets with at least 80% of their *p*-values greater than 0.05 were considered to have no probable significant difference between the two. Data sets with at least 80% of their *p*-values greater than 0.01 were considered to have no highly significant difference between them.

Table 8. The *t*-Test Comparison—1.4-mph, 90° Crosswind to Windless Conditions

0- and 1.4-mph, 90° Crosswind *t*-Test		
Sensor Group	Percent of Data With *p*-Values >0.05	Percent of Data With *p*-Values >0.01
Eight perimeter plate-style HFSs	25	28
Eight perimeter-exposed TCs	18	23
Three wing underside surface TCs	0	0
Four fuselage underside surface TCs	10	15
Four fuselage right-side surface TCs	26	38
Four fuselage left-side surface TCs	7	12

Because no sensor groups exceeded the 80% threshold percentage of *p*-values above 0.01 or 0.05, it was concluded that there was a significant difference between the two test conditions. The 1.4-mph, 90° crosswind trials produced different results than those under windless conditions. Difference in wind speed and direction had a significant effect on the results of these trials.

4.2.2.2 Trials With 45° Crosswinds.

The data recorded from a typical 1.4-mph, 45° crosswind test are shown in figures 35 through 39. The data for these graphs are from Trial 4 and are typical for all six trials done in a 1.4-mph, 45° crosswind (see figure 3 for a description of 45° crosswind). The vertical scales of the graphs are the same for all wind conditions for easy comparison among test conditions. The horizontal axis ends at 360 s, with the fire usually dying after 240 s. Time zero is when the JP-8 was ignited with a propane torch.

Figure 35 shows a plot of the perimeter heat flux data measured with the flat-plate heat flux sensors. The sensors were not accurately calibrated because they were intended only to show differences in relative heat flux from trial to trial and not to measure precise heat flux values at each location. There was only a light wind, so the fire leaned over a little in the leeward direction (see figure 3), resulting in higher heat flux values from downwind HT1, HT7, and HT8. The same was evident for the perimeter temperature, as shown in figure 36.

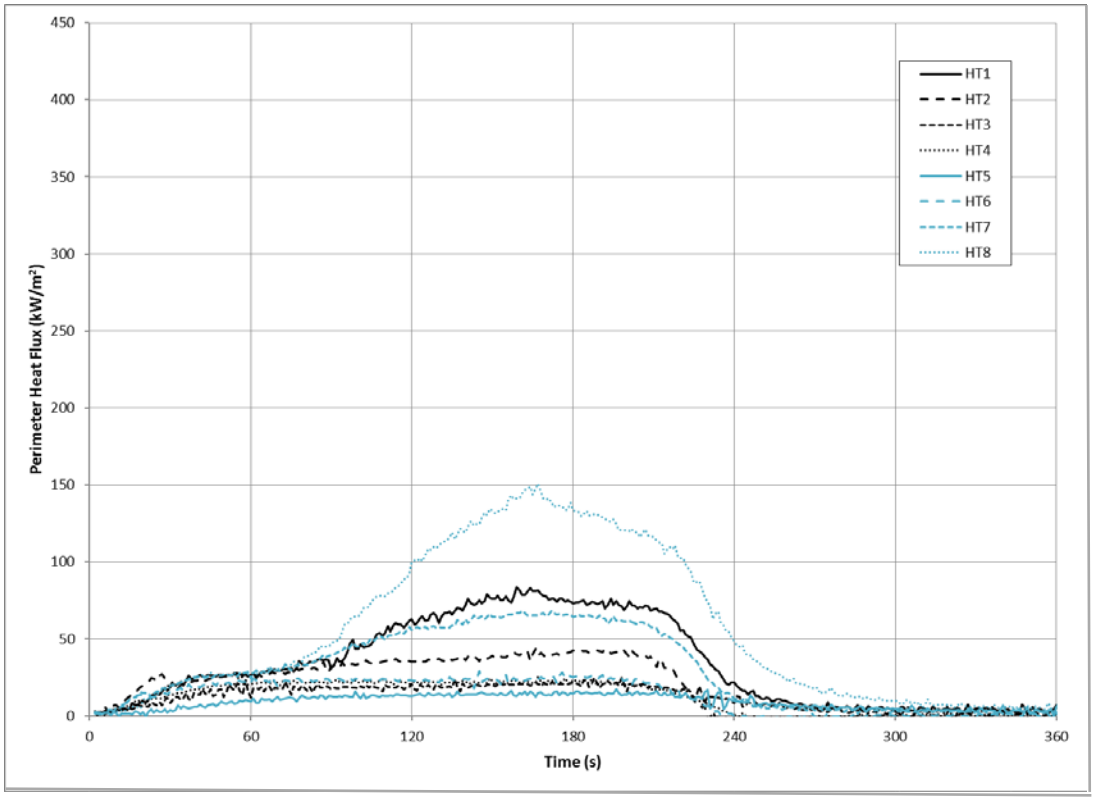

Figure 35. Typical Perimeter Heat Flux—1.4-mph, 45° Crosswinds

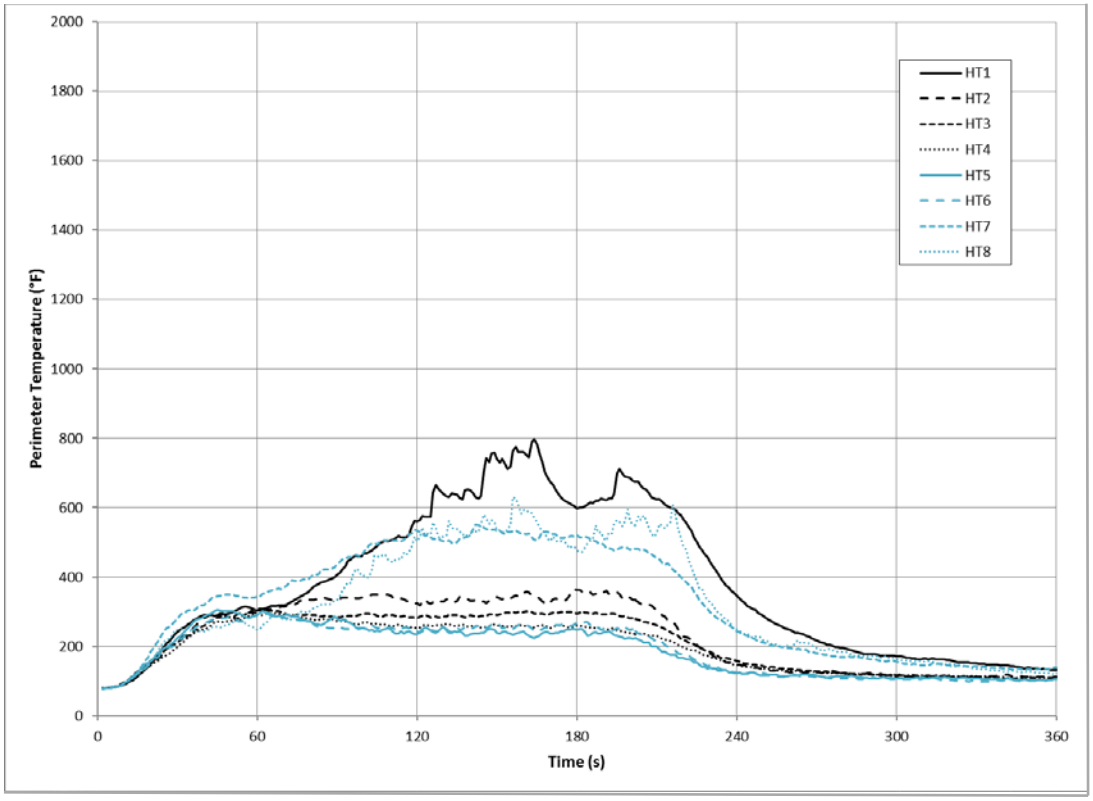

Figure 36. Typical Perimeter Temperature—1.4-mph, 45° Crosswinds

Figure 37 shows a plot of the data from the three wing TCs. The heat capacity of the 0.135-in.-thick steel caused the wing to heat up and cool down slowly, resulting in steady curves. Location T6B reached the highest temperature of the three and showed an increase compared to the windless conditions. The temperature at location T7B also increased compared to the windless tests, while the temperature at T5B decreased slightly.

A graph of the data from the four underside fuselage TCs is shown in figure 38. Similar to the wing TCs, the 1/4-in. steel mass slows the TC's temperature change. Temperatures increased from upwind T1B, in order, to downwind T4B. The temperature range and spread was roughly equivalent to windless conditions.

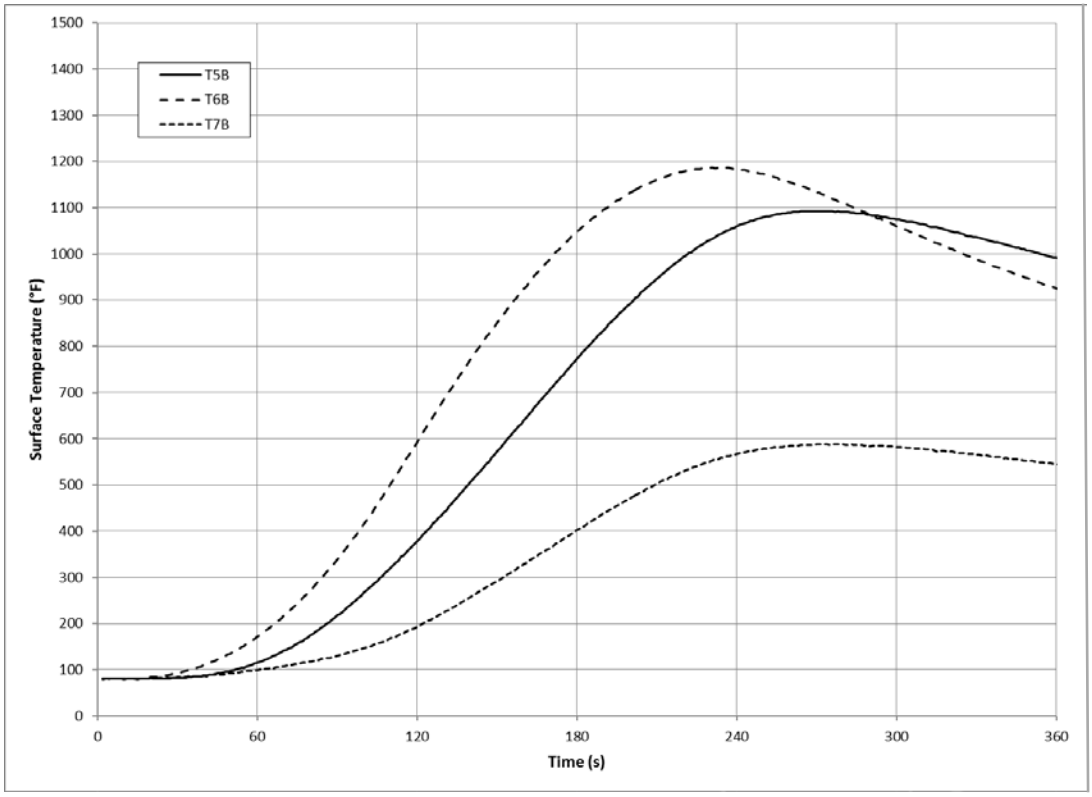

Figure 37. Typical Wing Underside Temperature—1.4-mph, 45° Crosswinds

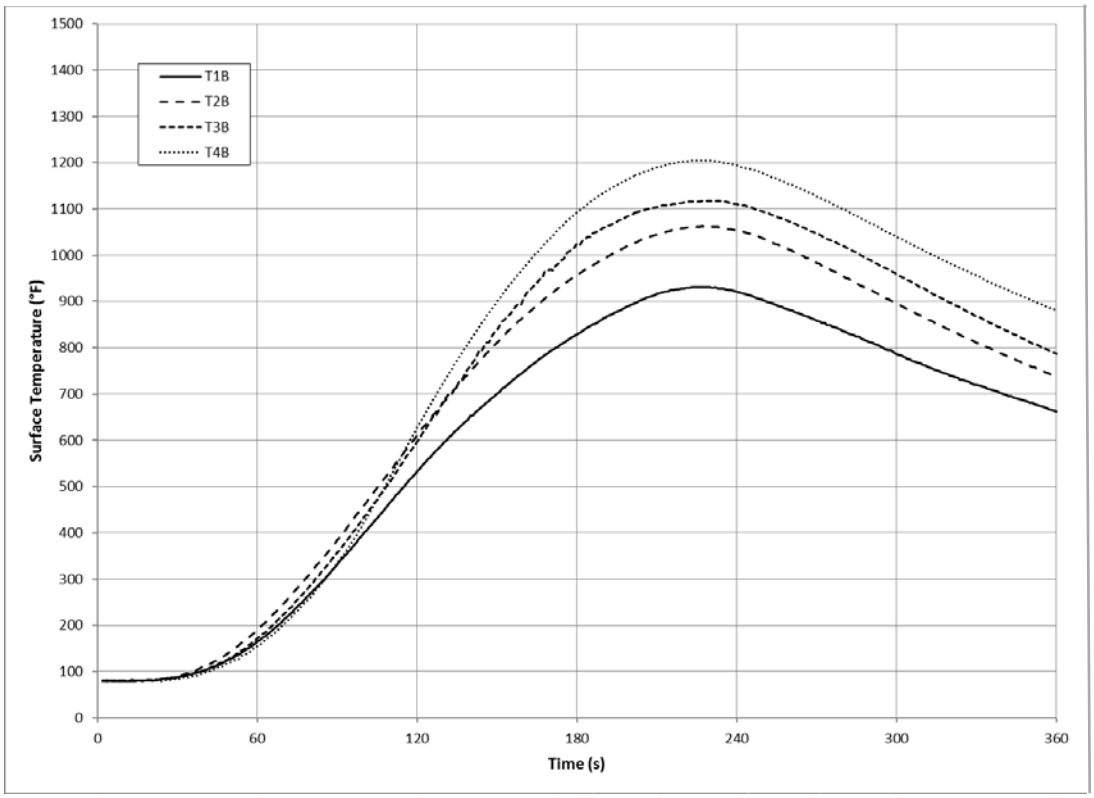

Figure 38. Typical Fuselage Underside Temperature—1.4-mph, 45° Crosswinds

Figure 39 shows the data from the right and left sides of the fuselage. The slightly leaning fire enveloped the fuselage and rose up the left side more, compared to the windless tests. The left and right sides of the fuselage reached similar temperatures. Temperatures increased from upwind T1, in order, to downwind T4 on both the right and left sides.

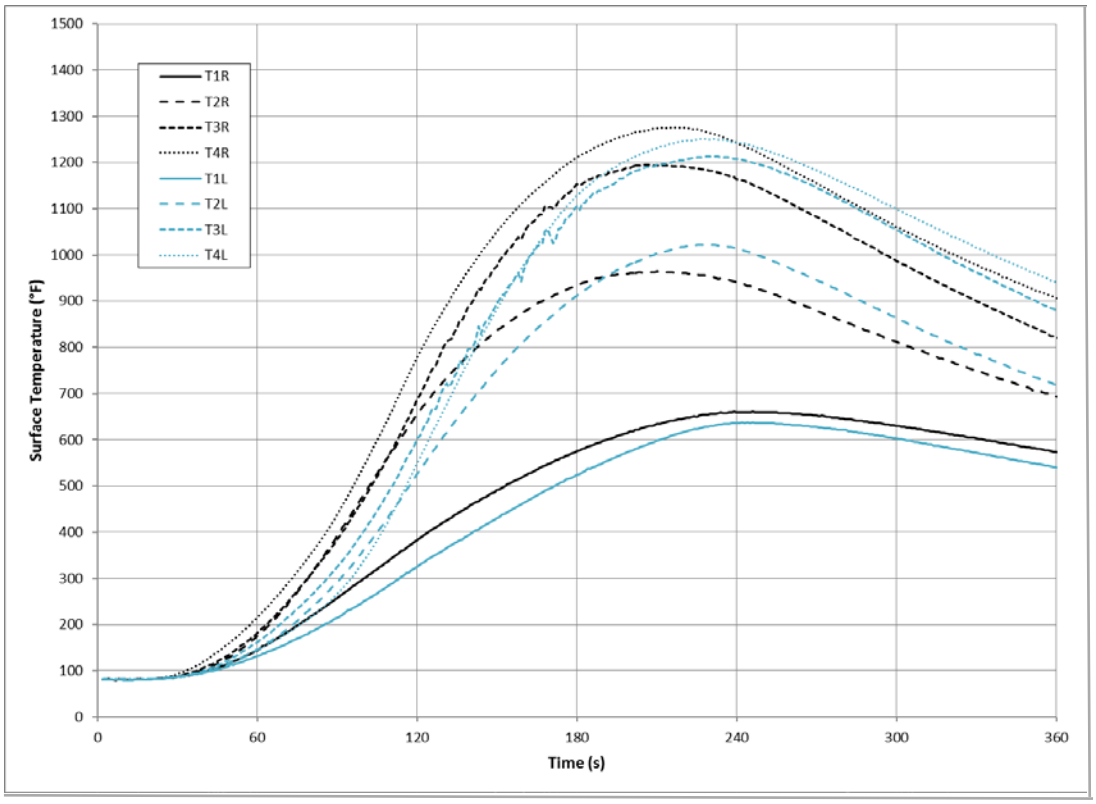

Figure 39. Typical Side Fuselage Temperature—1.4-mph, 45° Crosswinds

Appendix E shows the average and standard deviation data at 15-s intervals for the series of six trials conducted in the 1.4-mph, 45° crosswind condition. The data for the six trials were so consistent from trial to trial that time shifting to better align the temperature curves in time, as explained in section 3, was not necessary. Thirty-one separate temperatures and heat fluxes were measured for each trial. The data were compared at 15-s intervals for the first 4 min of each trial for a total of 527 separate RSE values to compare. The percentage of data that fell below the 10% and 30% criteria for each sensor group is summarized in table 9. Sensor groups with at least 80% of their RSE values below 10% were considered a very reliable indicator of repeatability from test to test; those below 30% were considered a good indicator of repeatability.

Table 9. The RSE Values From the 1.4-mph, 45°-Crosswind Trials

Six Trials With 1.4-mph, 45° Crosswinds			
Sensor Group	Percent of Data With RSE ≤10%	Percent of Data With RSE ≤30%	Result
Eight perimeter plate-style HFSs	86.0	97.1	Very reliable indicator
Eight perimeter-exposed TCs	98.5	100.0	Very reliable indicator
Three wing underside surface TCs	100.0	100.0	Very reliable indicator
Four fuselage underside surface TCs	100.0	100.0	Very reliable indicator
Four fuselage right side surface TCs	100.0	100.0	Very reliable indicator
Four fuselage left side surface TCs	100.0	100.0	Very reliable indicator

The criterion established to determine that the test procedure was repeatable was that at least 80% of the calculated RSE values for the data had to be 30% or less. All sensor groups easily met this requirement. A thorough review of the data indicated that the test procedure is very repeatable and that all results were predictable under the 1.4-mph, 45° crosswind condition.

Statistical analyses were conducted to compare results from the 1.4-mph, 45° crosswind trials and the trials conducted in windless conditions. For each individual temperature and HFS, the data from the trials at the two different wind conditions were compared by *t*-test at each 15-s interval over a period of 240 s starting when the fires were ignited. Appendix E shows the calculated *p*-value tables for the different sensors. The percentage of data that fell above the 1% (0.01) and 5% (0.05) criteria for each sensor group is summarized in table 10. Data sets with at least 80% of their *p*-values greater than 0.05 were considered to have no probable significant difference between the two. Data sets with at least 80% of their *p*-values greater than 0.01 were considered to have no highly significant difference between them.

Table 10. The *t*-Test Comparison—1.4-mph, 45°-Crosswind to Windless Conditions

0- and 1.4-mph, 45° Crosswind *t*-Test		
Sensor Group	Percent of Data With *p*-Values >0.05	Percent of Data With *p*-Values >0.01
Eight perimeter plate-style HFSs	17	26
Eight perimeter-exposed TCs	29	39
Three wing underside surface TCs	2	10
Four fuselage underside surface TCs	37	47
Four fuselage right-side surface TCs	25	31
Four fuselage left-side surface TCs	21	31

Since no sensor groups exceeded the 80% threshold percentage of *p*-values above 0.01 or 0.05, it was concluded that there was a significant difference between the two test conditions. The 1.4-mph, 45° crosswind trials produced different results than those under windless conditions. The difference in wind speed and direction had a significant effect on the results of these trials.

4.2.3 Trials in 5.5-mph Wind Conditions.

To generate 5.5-mph wind speeds inside the hangar, all eight fans, with the original fan blades, were unblocked and used at high rotational speeds. Conducting the 5.5-mph trials in moderate ambient wind conditions allowed a 0.2-mph standard deviation among all trials. Fewer trials were conducted at this crosswind speed because the corresponding full-scale equivalent would be over 17 mph, a speed at which a full-scale test would not be attempted.

4.2.3.1 Trials With 90° Crosswinds.

The data from a typical 5.5-mph, 90° crosswind test are shown in figures 40 through 44. The data for these graphs are from Trial 4, which are typical for all six trials done at 5.5-mph, 90° crosswind (see figure 3 for a description of 90° crosswind). The vertical scales of the graphs are the same for all wind conditions for easy comparison among trial conditions. The horizontal axis ends at 360 s, with the fire usually dying after 240 s. Time zero is when the JP-8 was ignited with a propane torch.

Figure 40 shows a plot of the perimeter heat flux data measured with the flat-plate HFSs. The sensors were not accurately calibrated because they were intended only to show differences in relative heat flux from trial to trial and not to measure precise heat flux values at each location. The high wind speeds during these trials caused the fire to lean significantly, which resulted in significantly higher heat flux values from downwind HT1, HT2, and HT8. The same was evident for the perimeter temperature, as shown in figure 41.

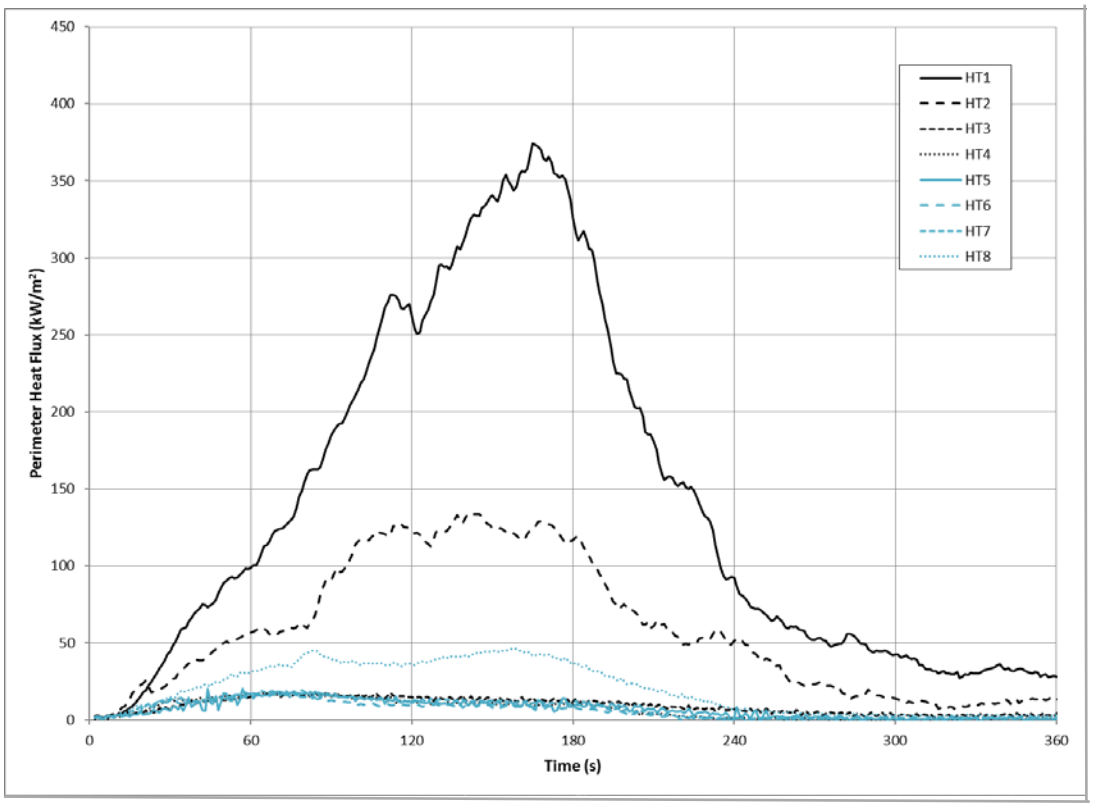

Figure 40. Typical Perimeter Heat Flux—5.5-mph, 90° Crosswinds

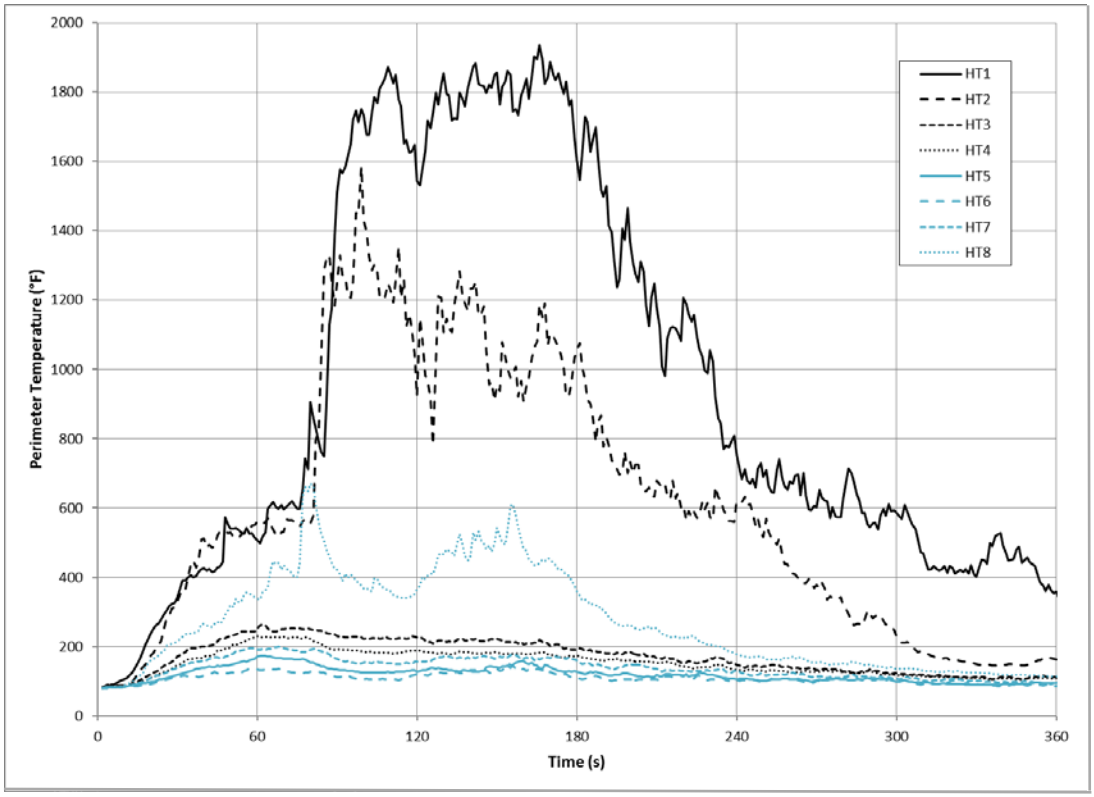

Figure 41. Typical Perimeter Temperature—5.5-mph, 90° Crosswinds

Figure 42 shows a plot of the data from the three wing TCs. The heat capacity of the 0.135-in.-thick steel caused the wing to heat up and cool down slowly, resulting in steady curves. The TCs closer to the center of the fire reached higher temperatures than the TCs near the edge. All temperatures were significantly lower than those recorded during the windless trials.

A graph of the data from the four underside fuselage TCs is shown in figure 43. As observed for the wing TCs, the 1/4-in.-thick steel caused temperatures to change more slowly. As usual, the temperature at the middle was higher than at the ends. The fire plume leaned greatly, turning under the fuselage and out the left side. All temperatures were much lower than those recorded for the windless tests.

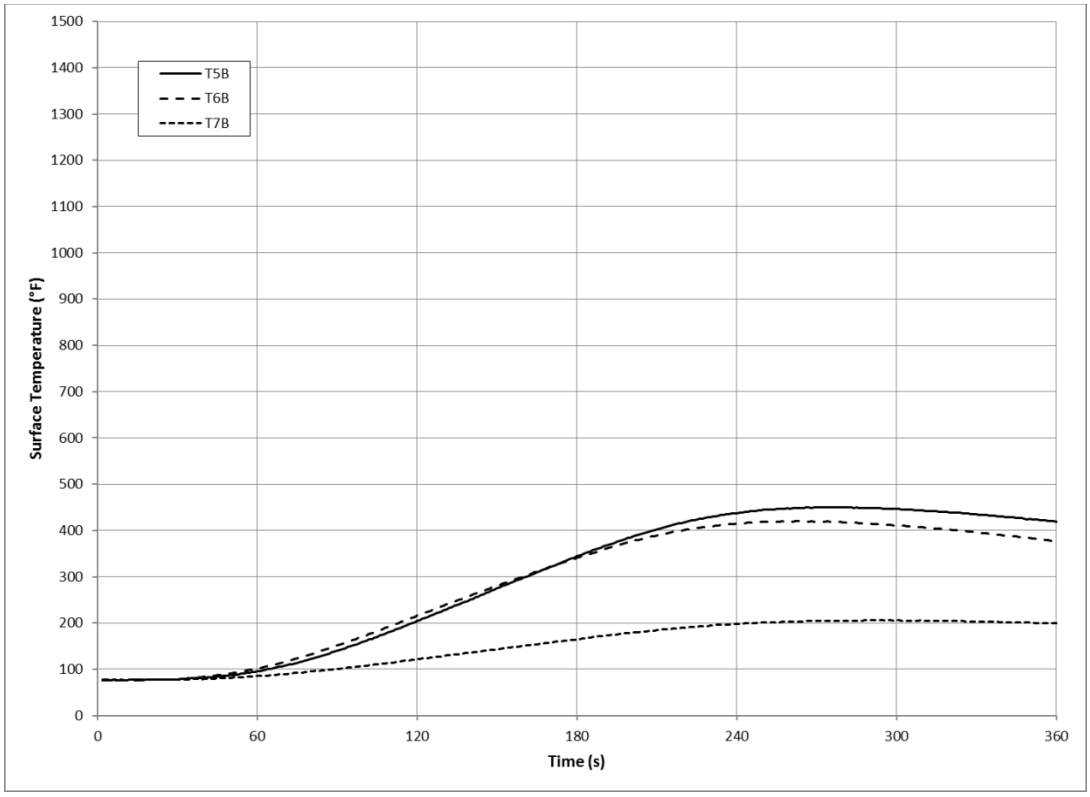

Figure 42. Typical Wing Underside Temperature—5.5-mph, 90° Crosswinds

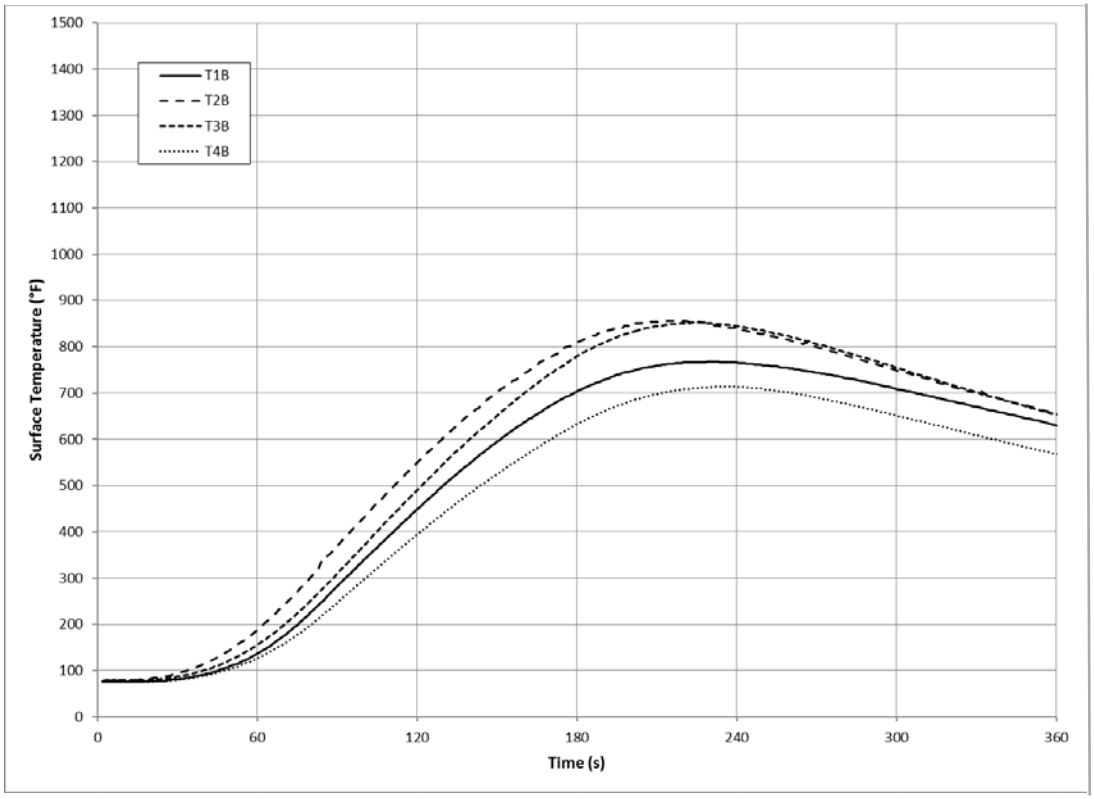

Figure 43. Typical Fuselage Underside Temperature—5.5-mph, 90° Crosswinds

Figure 44 shows a graph of the data from the right and left sides of the fuselage. In this case, the left side of the fuselage became significantly hotter than the right. The right-side temperatures decreased compared to those recorded for the windless tests. Although the left side had roughly the same values as the windless tests, its characteristic shape was much different. Consistent with other controlled wind condition trials, both sides had middle TCs reaching higher temperatures than the TCs near the ends.

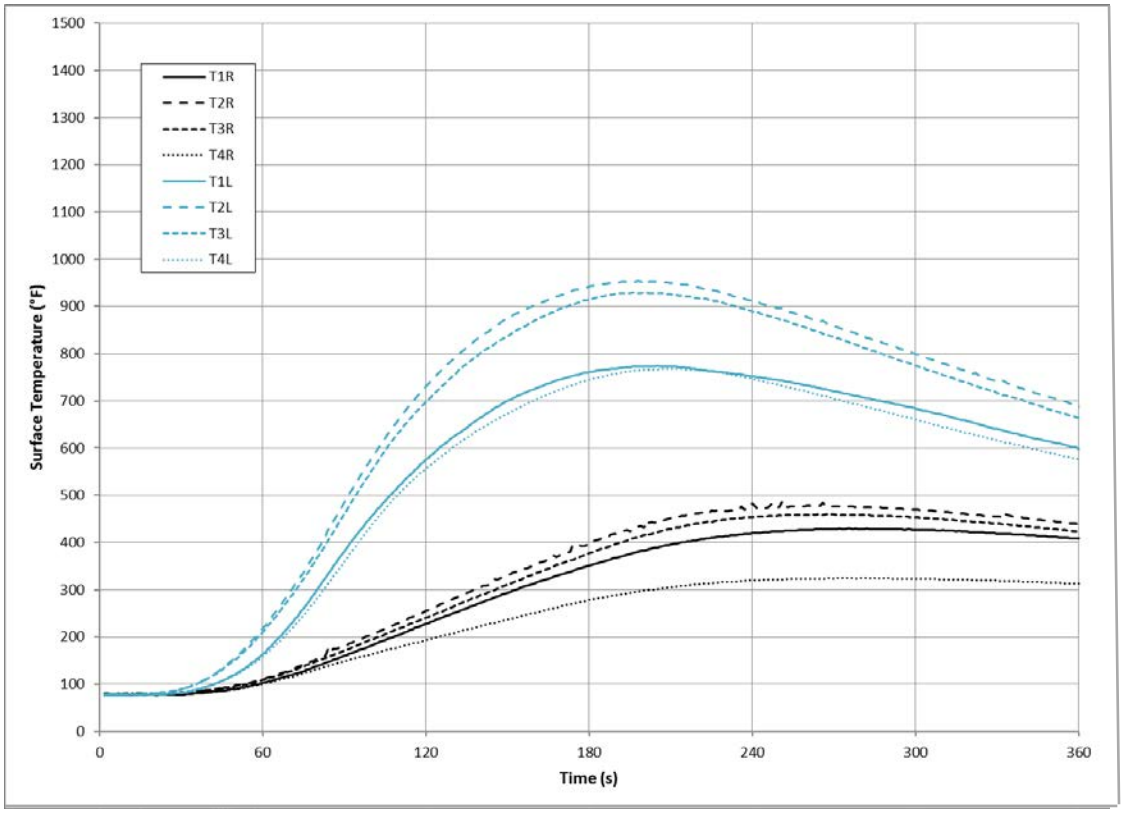

Figure 44. Typical Side Fuselage Temperature—5.5-mph, 90° Crosswinds

Appendix F shows the average and standard deviation data at 15-s intervals for the series of six trials conducted in the 5.5-mph and 90° crosswind condition. The data for the six trials were so consistent from trial to trial that time shifting to better align the temperature curves in time, as explained in section 3, was not necessary. Thirty-one separate temperatures and heat fluxes were measured for each trial. The data were compared at 15-s intervals for the first 4 min of each trial for a total of 527 separate RSE values to compare. The percentage of data that fell below the 10% and 30% criteria for each sensor group is summarized in table 11. Sensor groups with at least 80% of their RSE values below 10% were considered a very reliable indicator of repeatability from test to test; those below 30% were considered a good indicator of repeatability.

Table 11. The RSE Values From the 5.5-mph, 90° Crosswind Trials

Six Trials With 5.5-mph, 90° Crosswinds			
Sensor Group	Percent of Data With RSE ≤10%	Percent of Data With RSE ≤30%	Result
Eight perimeter plate-style HFSs	76.5	93.4	Good indicator
Eight perimeter-exposed TCs	93.4	100.0	Very reliable indicator
Three wing underside surface TCs	100.0	100.0	Very reliable indicator
Four fuselage underside surface TCs	100.0	100.0	Very reliable indicator
Four fuselage right-side surface TCs	95.6	100.0	Very reliable indicator
Four fuselage left-side surface TCs	100.0	100.0	Very reliable indicator

The criterion established to determine that the test procedure was repeatable was that at least 80% of the calculated RSE values for the data had to be 30% or less. All sensor groups easily met this requirement. A thorough review of the data indicated that the test procedure was very repeatable and that all results were predictable under the 5.5-mph, 90° crosswind condition.

Statistical analyses were conducted to compare the results from the 5.5-mph, 90° crosswind trials to the trials conducted in windless conditions. For each individual temperature and HFS, the data from the trials at the two different wind conditions were compared by *t*-test at each 15-s interval over a period of 240 s, starting when the fires were ignited. Appendix F shows the calculated *p*-value tables for the different sensors. The percentage of data that fell above the 1% (0.01) and 5% (0.05) criteria for each sensor group is summarized in table 12. Data sets with at least 80% of their *p*-values greater than 0.05 were considered to have no probable significant difference between the two. Data sets with at least 80% of their *p*-values greater than 0.01 were considered to have no highly significant difference between them.

Table 12. The *t*-Test Comparison—5.5-mph, 90° Crosswind to Windless Conditions

0- and 5.5-mph, 90° Crosswind *t*-Test		
Sensor Group	Percent of Data With *p*-Values >0.05	Percent of Data With *p*-Values >0.01
Eight perimeter plate-style HFSs	17	21
Eight perimeter-exposed TCs	10	14
Three wing underside surface TCs	18	18
Four fuselage underside surface TCs	9	22
Four fuselage right-side surface TCs	10	12
Four fuselage left-side surface TCs	16	24

Because no sensor groups exceeded the 80% threshold percentage of *p*-values above 0.01 or 0.05, it was concluded that there was a significant difference between the two test conditions. The 5.5-mph, 90° crosswind trials produced different results than those under windless conditions. The difference in wind speed and direction had a significant effect on the results of these trials.

4.2.3.2 Trials With 45° Crosswinds.

The data from a typical 5.5-mph, 45° crosswind test are shown in figures 45 through 49. The data for these graphs are from Trial 4, which are typical for all four trials done at 5.5-mph, 45° crosswinds (see figure 3 for a description of 45° crosswinds). The vertical scales of the graphs are the same for all wind conditions for easy comparison among test conditions. The horizontal axis ends at 360 s, with the fire usually dying after 240 s. Time zero is when the JP-8 was ignited with a propane torch.

Figure 45 shows a plot of the perimeter heat flux data measured with the flat-plate HFSs. The sensors were not accurately calibrated because they were intended only to show differences in relative heat flux from trial to trial and not to measure precise heat flux values at each location. Because of the 5.5-mph wind, the fire leaned significantly, resulting in significantly higher heat flux values from downwind HT1, HT7, and HT8. The same was evident with the perimeter temperature, as shown in figure 46.

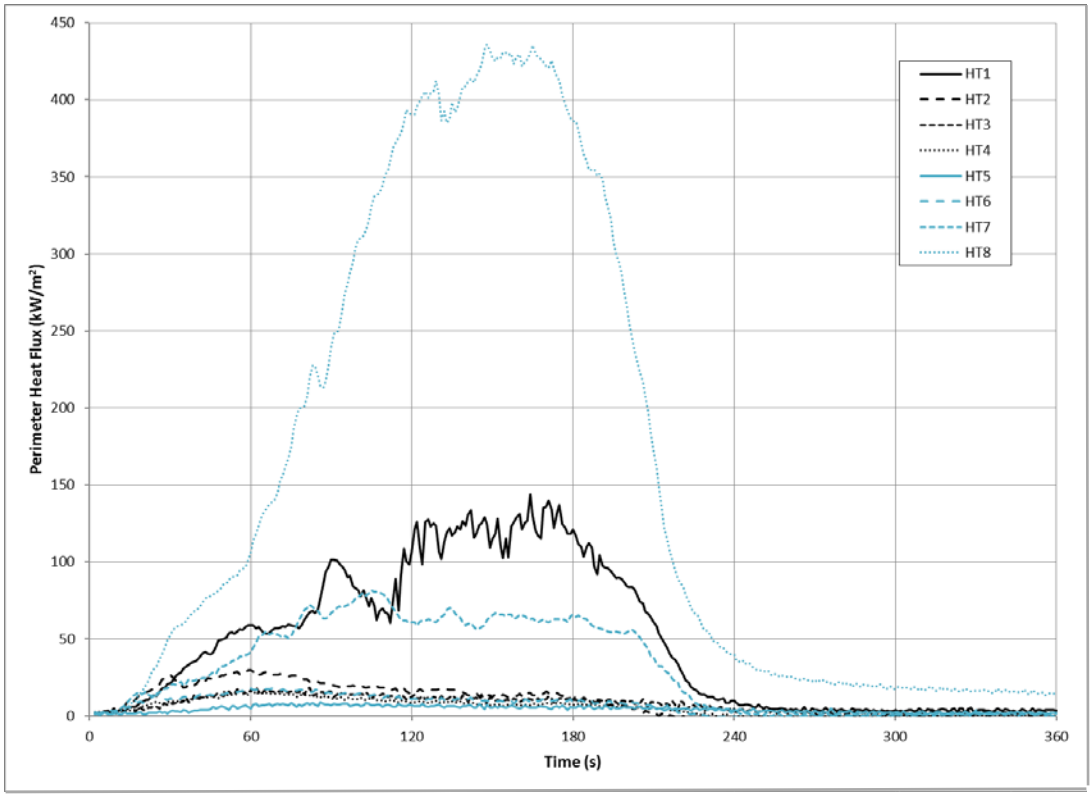

Figure 45. Typical Perimeter Heat Flux—5.5-mph, 45° Crosswinds

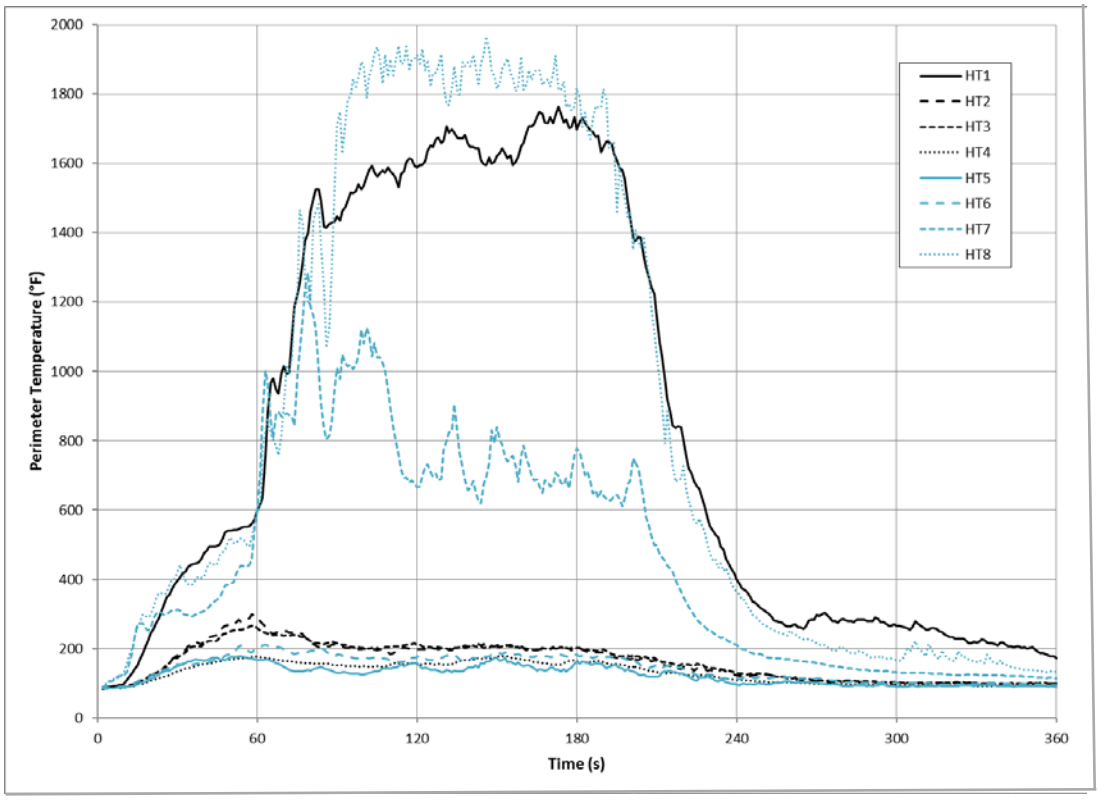

Figure 46. Typical Perimeter Temperature—5.5-mph, 45° Crosswinds

Figure 47 shows a plot of the data from the three wing TCs. The heat capacity of the 0.135-in.-thick steel caused the wing to heat up and cool down slowly, resulting in steady curves. T6B recorded the highest temperatures of the set but decreased from the windless conditions. T5B also decreased, quite dramatically, compared to windless tests; T7B remained roughly the same.

A graph of the data from the four underside fuselage TCs is shown in figure 48. As observed for the wing TCs, the 1/4-in.-thick steel makes them slow to change. Temperatures increased from upwind T1B, in order, to downwind T4B. Overall values are lower than in windless conditions.

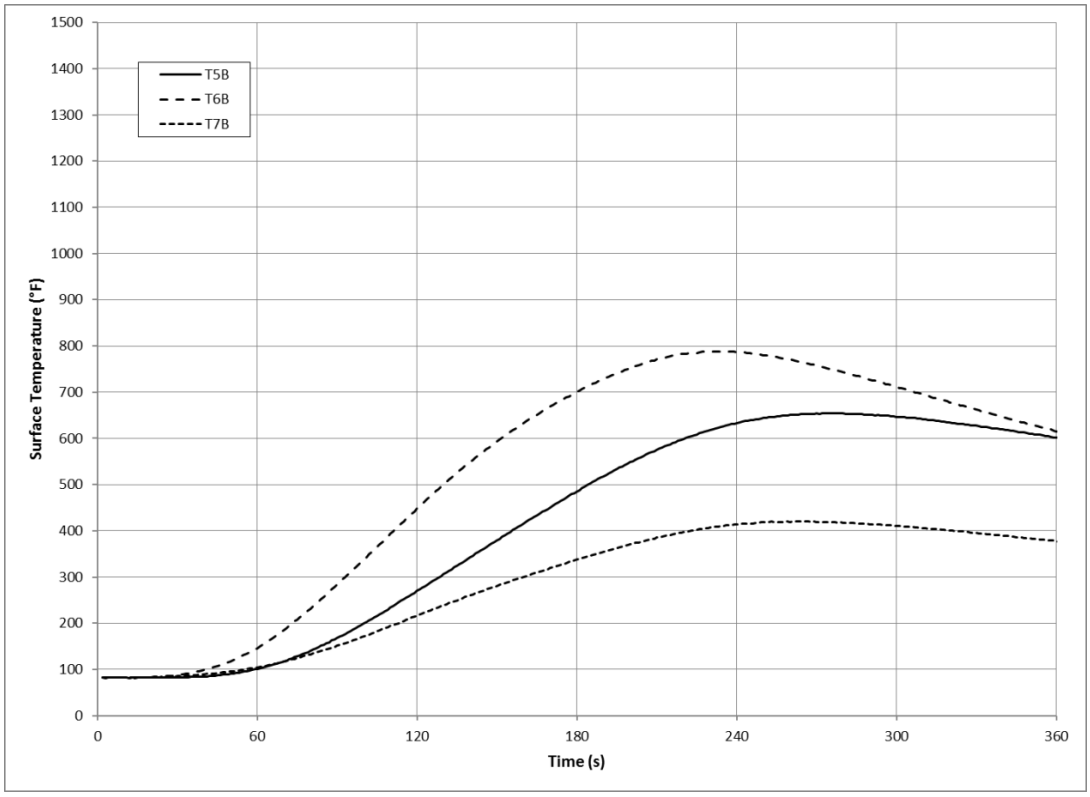

Figure 47. Typical Wing Underside Temperature—5.5-mph, 45° Crosswinds

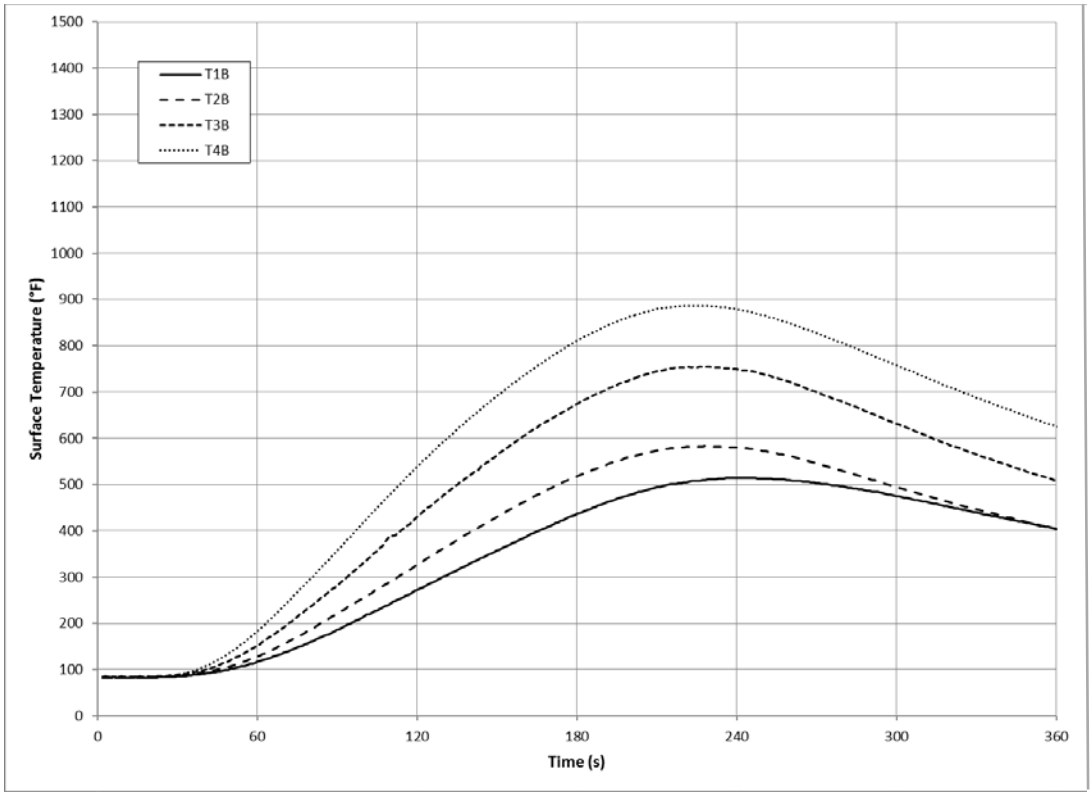

Figure 48. Typical Fuselage Underside Temperature—5.5-mph, 45° Crosswinds

Figure 49 shows a graph of data from the right and left sides of the fuselage. Higher temperatures were recorded on the left side of the fuselage than the right. Temperatures increased from upwind T1, in order, to downwind T4 on both the right and left sides. The right-side temperatures were lower compared to the windless tests. On the left side, T1L, T2L, and T3L temperatures decreased, but T4L increased compared to the windless tests.

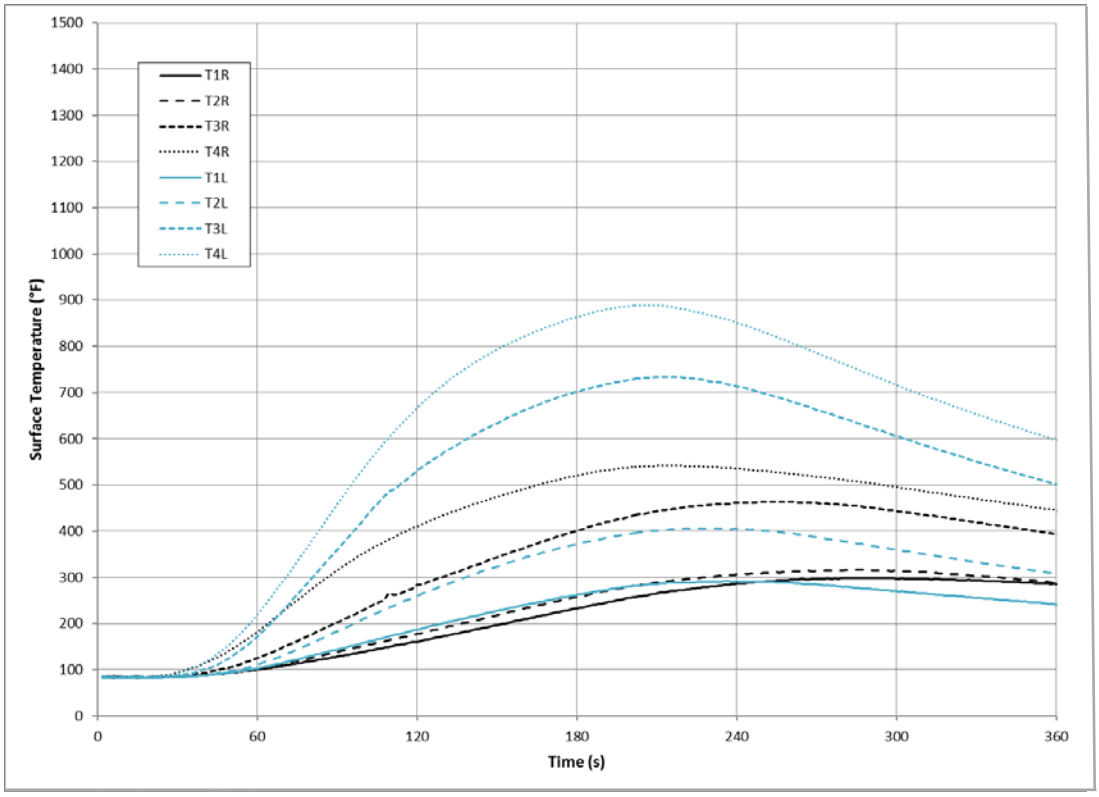

Figure 49. Typical Side Fuselage Temperature—5.5-mph, 45° Crosswinds

Appendix G shows the average and standard deviation data at 15-s intervals for the series of four trials conducted in the 5.5-mph, 45° crosswind condition. The data from the four trials were so consistent from trial to trial that time shifting to better align the temperature curves in time, as explained in section 3, was not necessary. Thirty-one separate temperatures and heat fluxes were measured for each trial. The data were compared at 15-s intervals for the first 4 min of each trial for a total of 527 separate RSE values to compare. The percentage of data that fell below the 10% and 30% criteria for each sensor group is summarized in table 13. Sensor groups with at least 80% of their RSE values below 10% were considered a very reliable indicator of repeatability from test to test; those below 30% were considered a good indicator of repeatability.

Table 13. The RSE Values From the 5.5-mph, 45° Crosswind Trials

Four Trials With 5.5-mph, 45° Crosswinds			
Sensor Group	Percent of Data With RSE ≤10%	Percent of Data With RSE ≤30%	Result
Eight perimeter plate-style HFSs	80.9	94.9	Very reliable indicator
Eight perimeter-exposed TCs	91.9	100.0	Very reliable indicator
Three wing underside surface TCs	100.0	100.0	Very reliable indicator
Four fuselage underside surface TCs	100.0	100.0	Very reliable indicator
Four fuselage right-side surface TCs	100.0	100.0	Very reliable indicator
Four fuselage left-side surface TCs	98.5	100.0	Very reliable indicator

The criterion established to determine that the test procedure was repeatable was that at least 80% of the calculated RSE values for the data had to be 30% or less. All sensor groups easily met this requirement. A thorough review of the data indicated that the test procedure was very repeatable and that all results were predictable under the 5.5-mph, 45° crosswind condition.

Statistical analyses were conducted to compare results from the 5.5-mph, 45° crosswind trials to the trials conducted in windless conditions. For each individual temperature and heat flux sensor, data from trials at the two different wind conditions were compared by *t*-test at each 15-s interval over a period of 240 s starting when the fires were ignited. Tables of the calculated *p*-values for the different sensors are shown in appendix G. The percentage of data that fell above the 1% (0.01) and 5% (0.05) criteria for each sensor group is summarized in table 14. Data sets with at least 80% of their *p*-values greater than 0.05 were considered to have no probable significant difference between the two. Data sets with at least 80% of their *p*-values greater than 0.01 were considered to have no highly significant difference between them.

Table 14. The *t*-Test Comparison—5.5-mph, 45° Crosswind to Windless Conditions

0- and 5.5-mph, 45° Crosswind *t*-Test		
Sensor Group	Percent of Data With *p*-Values >0.05	Percent of Data With *p*-Values >0.01
Eight perimeter plate-style HFSs	12	20
Eight perimeter-exposed TCs	10	25
Three wing underside surface TCs	37	57
Four fuselage underside surface TCs	13	18
Four fuselage right-side surface TCs	21	25
Four fuselage left-side surface TCs	12	18

Since no sensor groups exceeded the 80% threshold of percentage of data above 0.01 or 0.05, it was concluded that there was a significant difference between the two test conditions. The 5.5-mph, 45° crosswind trials produced different results than those recorded under windless conditions. The difference in wind speed and direction had a significant effect on the results of these trials.

4.3 THE 1:10-SCALE NLA MOCKUP PERIMETER HEAT FLUX.

It was observed during 1:10-scale trials that perimeter heat flux sensor data varied with wind speed and direction. The fire plume rose straight up during windless tests, and all the perimeter heat flux sensors measured close to the same low-level radiant heat. During low-wind tests, the fire plume leaned slightly and increased the heat flux on the downwind sensors. The fire plume leaned to a much higher extent during high-wind tests, greatly increasing heat flux on the downwind sensors. Since there were eight sensors around the fire, this effect should have been measurable regardless of wind direction. As the fire plume leaned, the increase in heat flux on the downwind sensors was much greater than the decrease in heat flux to the upwind sensors. Moreover, integrating and summing each of the eight perimeter heat flux values generated a partial measure of the total heat released from the fire. This method provided a way to compare the results across different wind speed conditions. The aforementioned approach does not apply to temperature, because temperature is an intrinsic physical property that is a measure of hot and cold; temperature is not additive. The summation of heat flux over time, however, is energy, and an extrinsic property that is additive.

Figure 50 shows a plot of cumulative integrated perimeter heat flux as a function of during-test wind speed for all 1:10-scale NLA mockup trials. The blue diamonds represent 90° crosswind tests, and the red squares indicate 45° crosswind tests. Both data sets make up the linear interpolation line, which indicates a linear correlation among all data. Heat flux was not integrated over a specific period of time. Instead, a minimum threshold value of 10 kW/m^2 was used for each sensor (anything less was considered noise), and all eight perimeter heat flux measurements exceeding 10 kW/m^2 were integrated over time and then summed to calculate the integrated perimeter heat flux. As stated in section 4.2, average during-test wind speeds were taken directly from the north–south component velocity data recorded at 1-s intervals from the time the fire was ignited until 240 s later.

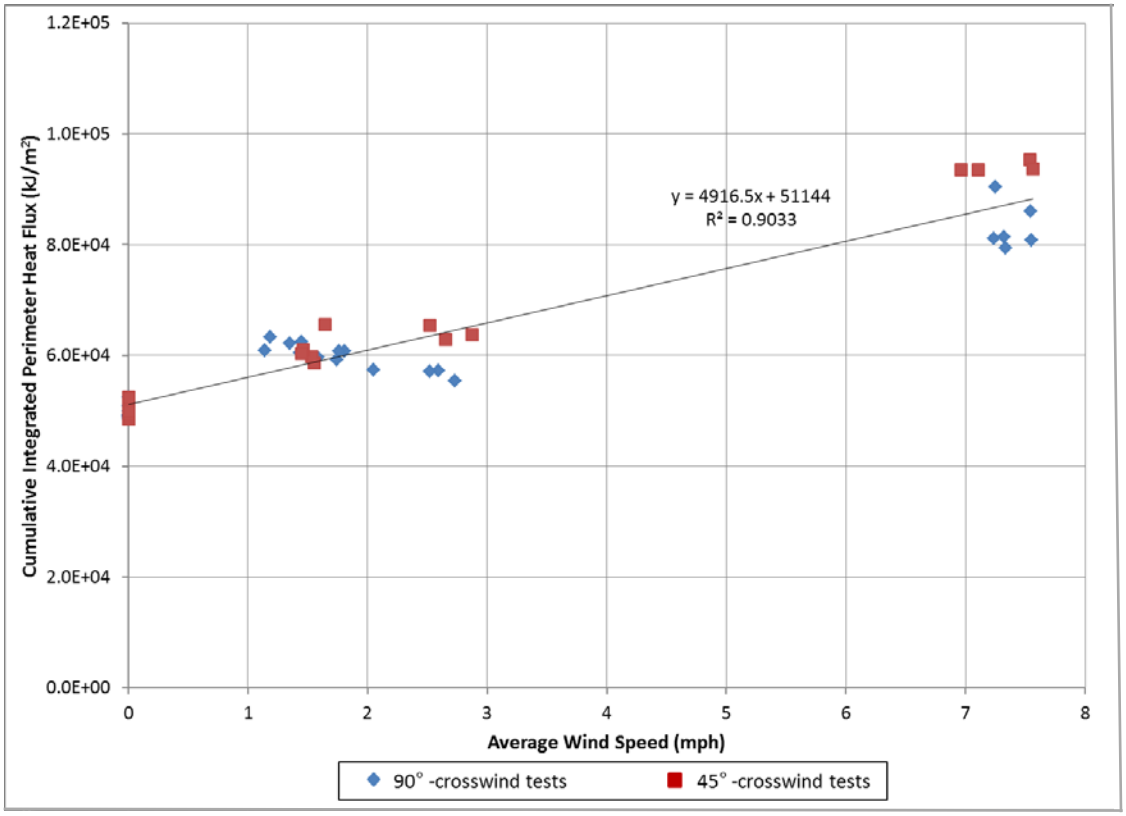

Figure 50. Cumulative Integrated Perimeter Heat Flux vs During-Test Wind Speed

Figure 50 demonstrates that a quantifiable linear relationship exists between the integrated perimeter heat flux and the wind speed from any direction for the 1:10-scale NLA mockup pool fires. Because these data represent unsuppressed, fully-involved fire conditions, the quantitative effect of scaled firefighting application techniques, equipment, and tactics, or a combination thereof can be determined when compared to these baseline reference conditions.

4.4 THE 1:10-SCALE NLA MOCKUP FUEL COVERAGE TRIALS.

JP-8 was added to the pan incrementally such that the total fuel in the fire pan increased in volume accordingly: 1, 2, 3, 5, 7.5, and 10 gal. After each addition of fuel, the fan power was set to 0, 40, 60, 80, and 100 percent output, which corresponded to measured wind speeds of 0, 1.8, 2.6, 3.7, and 4.3 mph, respectively. In this configuration, all fans were unblocked; and five fans had low-pitch blades installed. After each change in wind speed, the fuel was given several minutes to react to the new wind speed before the total fuel coverage was estimated. After the 100% fan speed measurement was made, the fans were turned off before more fuel was added.

Estimation of the fuel coverage was complicated by several factors. At low fuel volumes, the fuel tended to accumulate around the edge of the fire pan, which left oval-shaped regions of exposed water towards the center of the fire pan. As the wind speed was increased, the wind introduced a clockwise rotation (as observed from above the fire pan) of fuel around the fire pan. This made coverage estimates even more difficult. Fuel tended to accumulate only on the downwind side of the fire pan for the higher wind speeds, forming a crescent-like shape.

Therefore, in most cases, coverage estimates were reported for only the 3.7- and 4.3-mph wind conditions.

Figure 51 presents a plot of estimated fuel coverage as a function of measured wind speed. Fuel coverage was noted to fall into three general categories. With 1, 2, or 3 gal of fuel, there was an insufficient volume of fuel to cover the entire fire pan even under windless conditions. With 5 and 7.5 gal of fuel, the fire pan was completely covered under zero- or low-wind speed conditions. However, water became exposed under higher-wind conditions. With 10 gal of fuel added, the fire pan was always covered by a layer of fuel even under the highest wind conditions tested. Therefore, the minimum quantity of fuel required to completely cover the fire pan under high-wind conditions (up to 4.3 mph) was between 7.5 and 10 gal. Scaled up to the full-scale NLA mockup fire pit, it would require between 750 and 1000 gal of fuel to provide complete coverage for wind speeds up to 4.3 mph. The wind speed for the fuel coverage trials should remain similar from 1:10 to full scale.

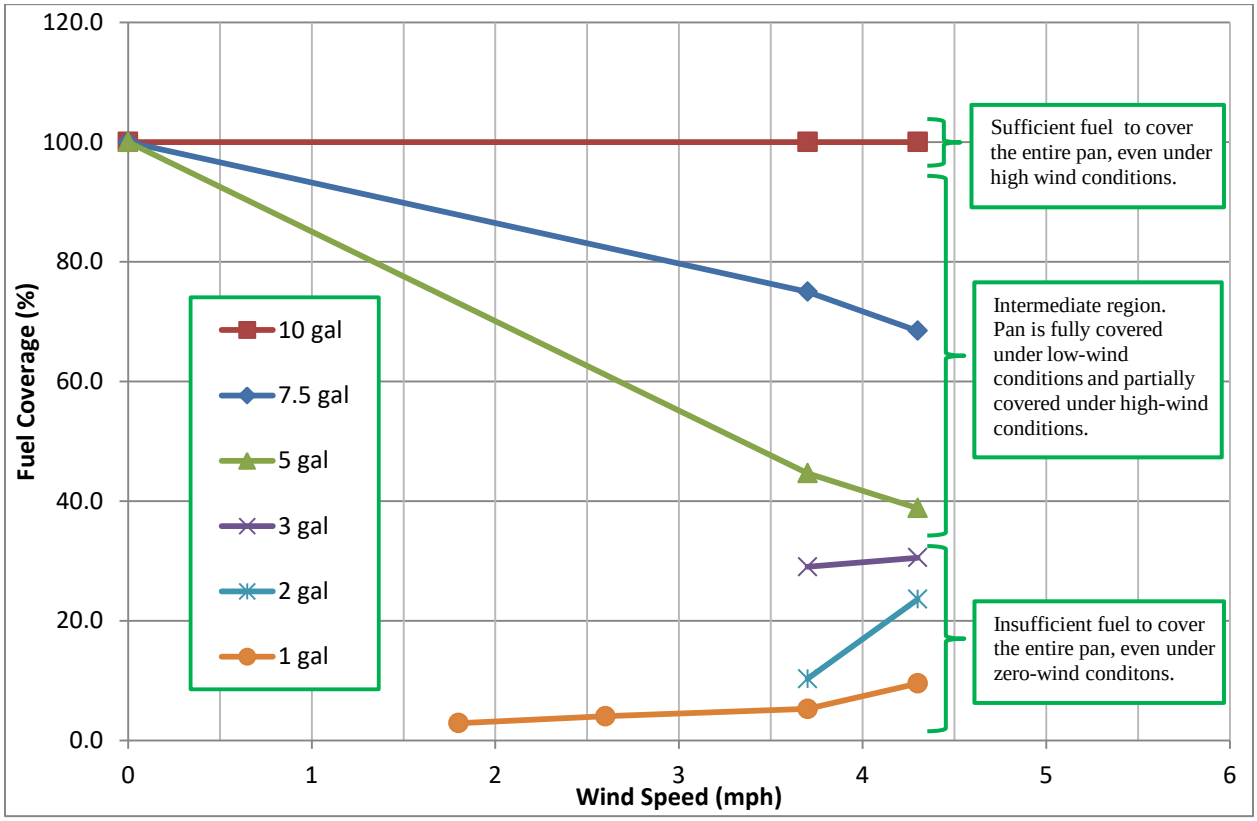

Figure 51. Wind Speed vs Observed Fuel Coverage

Figure 52 presents four photographs taken during this test series. Note that the photographs were software-enhanced to increase the red/blue contrast.

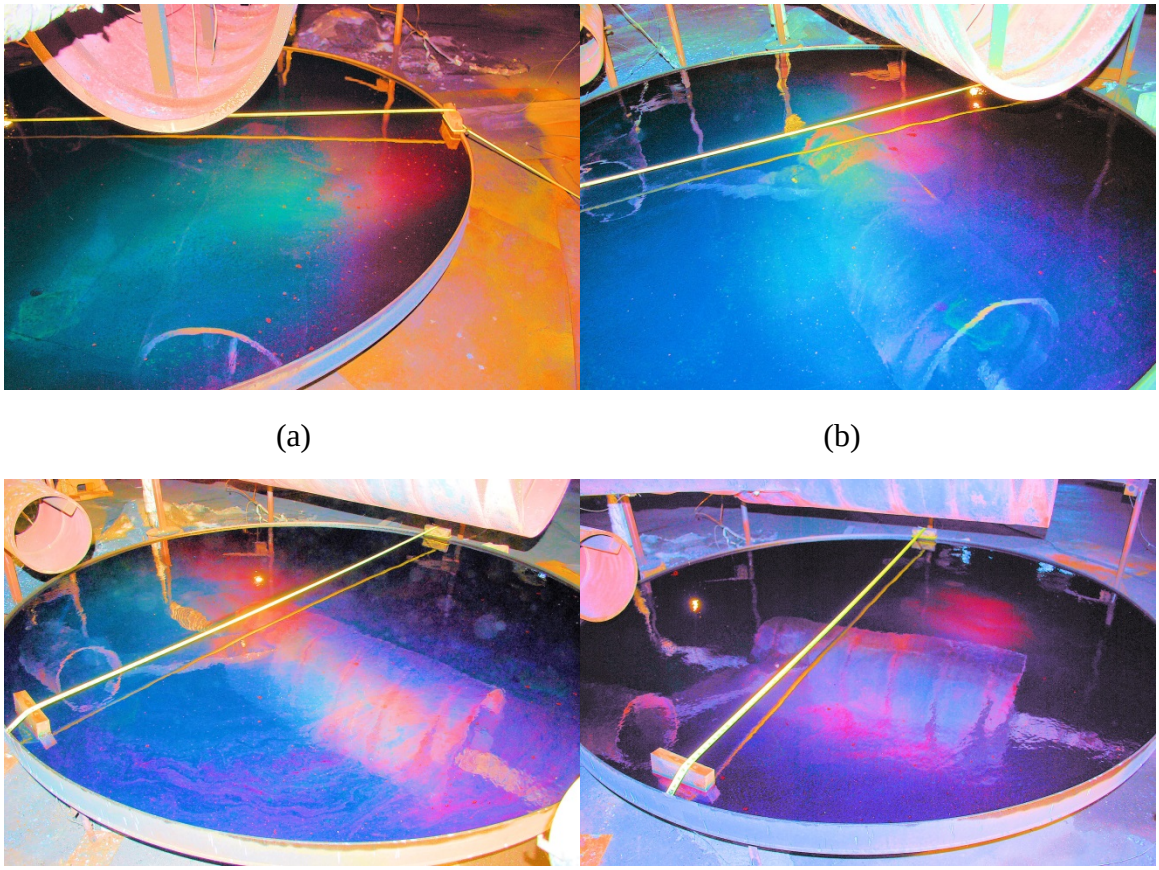

(a) (b)

(c) (d)

Figure 52. Trends Observed During Fuel Spread Estimations for (a) 1 gal Under 3.2-mph Wind Conditions, (b) 5 gal Under 3.7-mph Wind Conditions, (c) 7.5 gal Under 4.3-mph Wind Conditions, and (d) 10 gal Under 4.3-mph Wind Conditions
(Note: Photographs were software-enhanced to increase the red/blue contrast.)

4.5 FULL-SCALE NLA MOCKUP TRIALS.

Trials were conducted on the full-scale NLA mockup to see if the linear relationship between cumulative integrated perimeter heat flux and wind speed remained true at full scale similar to the 1:10-scale environment. A total of eight tests were conducted under various ambient wind conditions. There was significant variability in the tested ambient wind conditions ranging from 1.2 to 8.3 mph (as shown in figure 53), with winds out of the north by northwest, west by northwest, west, southwest, south by southwest, southeast, and east by southeast. Two anemometers were used to record wind speed, one at an elevation of 25 ft and one at an elevation of 8.5 ft, as discussed in section 3.1.4. Average during-test wind speeds were taken from the north–south and east–west component velocity data recorded at 1-s intervals from the time the fire was ignited until 240 s later. Each north–south and east–west velocity component was averaged over the 240-s interval. The resultant of these components was calculated to obtain the during-test wind speeds. All perimeter heat flux measurements exceeding 1.5 kW/m^2 (anything less was considered noise) were integrated over time and then summed to calculate cumulative integrated perimeter heat flux. Figure 53 shows a plot of cumulative integrated perimeter heat

flux as a function of during-test wind speeds measured at a height of 25 ft for all full-scale NLA mockup trials. For the anemometer located 8.5 ft off the ground, there was a high degree of scatter in the data and no consistent relationship between the integrated perimeter heat flux and wind speed. It may be plausible that, due to atmospheric boundary layer interaction effects, the anemometer mounted 8.5 ft high was too low to the ground to measure a true representation of wind speeds that influenced the fire.

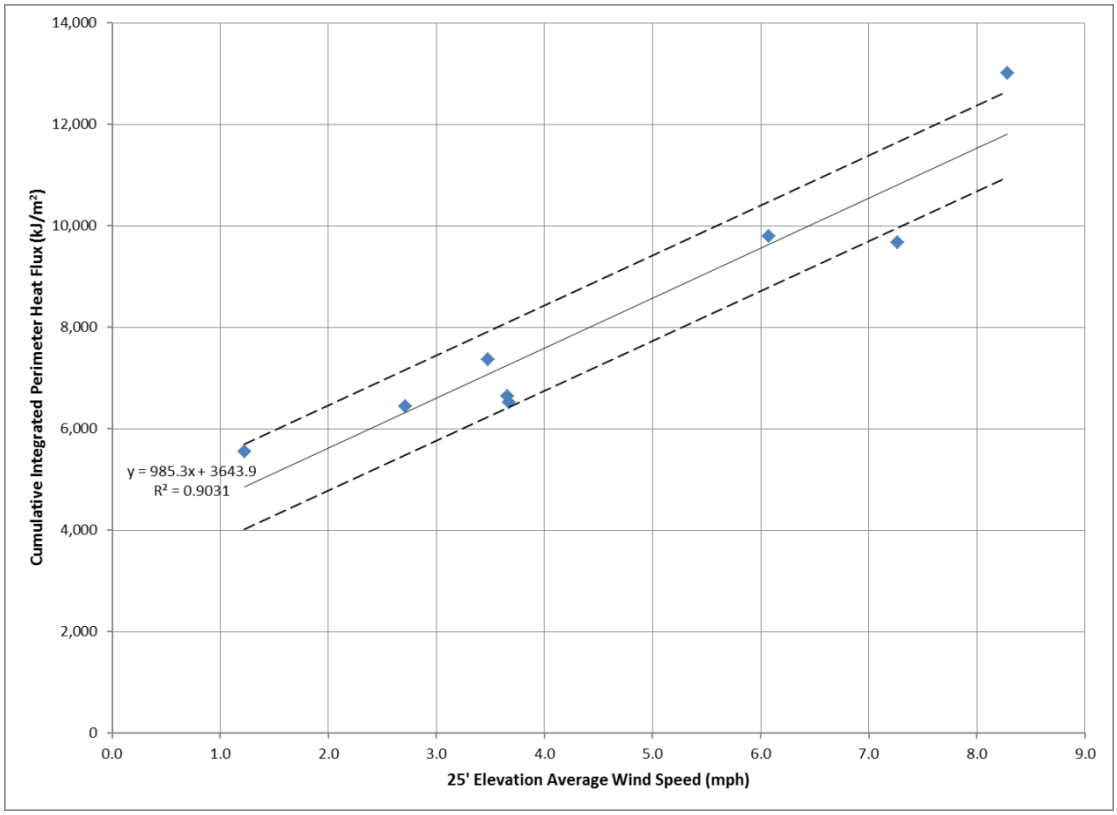

Figure 53. The NLA Cumulative Integrated Perimeter Heat Flux vs During-Test Wind Speed

A standard error of 841 kJ/m^2 was calculated from the measured data points and the indicated regression line. The dashed lines above and below the regression line have a vertical offset equal to the standard error. For data normally distributed about the regression line, 68% of data points would fall between the dashed lines [7]. The standard error of 841 kJ/m^2 represents a 17% error at low (1.2 mph) wind speeds and a 7% error at high (8.3 mph) wind speeds.

The data indicated that the linear relationship between integrated perimeter heat flux and wind speed still held true at full scale. It should be noted that in the open air of the full-scale environment, there was no clear differentiation between pretest and during-test wind speeds as there was with 1:10-scale NLA mockup trials (see figure 19). Wind speeds measured by the two anemometers during full-scale NLA mockup tests did not change significantly at any point during each fire trials.

5. CONCLUSIONS.

The 1:10-scale New Large Aircraft (NLA) mockup pool fire tests revealed that the proposed test protocol produced very repeatable results for temperature and heat flux when wind speed and

direction were held constant. However, for different initial conditions of wind speed or direction, temperature and heat flux were statistically different, even for small changes in wind speed or direction. Therefore, there was no wind speed and direction envelope for which the temperature or heat flux data could be compared directly. The test results could be compared only for tests with identical initial wind conditions.

However, both 1:10- and full-scale NLA mockup trials demonstrated a deterministic, quantifiable relationship between the measured perimeter heat flux and wind speed, independent of wind direction. This relationship may meet the objective to devise a general test protocol to determine the effect wind, firefighting agents, delivery apparatus, and firefighting techniques have on the NLA mockup pool fire environment. At a quasi-constant wind speed, the cumulative integrated perimeter heat flux for an unsuppressed, fully involved fire can be predicted. In potential future efforts, any measurable total heat release less than the expected baseline conditions measured in the present study must be due to firefighting agents, delivery apparatuses, and firefighting techniques, or some combination thereof.

A linear relationship between cumulative integrated perimeter heat flux and wind speed was evident across scales. This correlation was independent of wind direction. Parameters such as anemometer height and distance from the mockup, as well as perimeter heat flux sensor height and distance from the mockup may need to be optimized as a key logistical problem is addressed: how to accurately measure perimeter heat flux without hindering apparatus movement around the fire pit during fire suppression efforts. It was shown that heat release can be predicted over a range of wind conditions with an error of no more than 17% at low wind speeds and 7%at high wind speeds. If the practical problems posed in the approach can be resolved, the proposed test procedure offers a way to compare the effects of firefighting agents, delivery apparatus, and firefighting techniques on large-scale fires.

Limited trials were conducted on the 1:10-scale NLA mockup to establish a relationship between the amount of fuel needed for full pool coverage and wind speed. If the fuel coverage results are scaled up to the NLA fire pit, tests indicate that it would require between 750 and 1000 gallons of fuel to provide complete fire pit surface coverage for wind speeds up to 4.3 mph.

6. REFERENCES.

1. Blanchat, T., Humphries, L., and Gill, W., “Sandia Heat Flux Gauge Thermal Response and Uncertainty Models,” American Society for Testing and Materials (ASTM) STP 1427, January 2003.

2. Munson, B.R., Young, D.F., Okiishi, T.H., and Huebsch, W.W., *Fundamentals of Fluid Mechanics*, 6th ed., John Wiley & Sons, Ltd., Hoboken, New Jersey, 2009.

3. Hamins, A., Kashiwagi, T., and Burch, R.R., “Characteristics of Pool Fire Burning,” *Fire Resistance of Industrial Fluids*, Indianapolis, Indiana, June 20, 1995.

4. Lautkaski, R., “Validation of Flame Drag Correlations with Data from Large Pool Fires,” *Journal of Loss Prevention in the Process Industries*, Vol. 5, No. 3, 1992.

5. Department of the Treasury, Internal Revenue Service, ” IRS Publication 510 (Revised July 2013) Excise Taxes,” Available: http://www.irs.gov/file_source/pub/irs-pdf/p510.pdf (date last visited 04/13/2016).

6. Gritzo, L.A. and Suo-Anttila, J.M., “Thermal Measurements From a Series of Tests with a Large Cylindrical Calorimeter on the Leeward Edge of a JP-8 Pool Fire in Cross-Flow,” Sandia Report, SAND 2001-1986, Albuquerque, New Mexico, July 2001.

7. Spiegel, M., *Schaum’s Outline of Theory and Problems of Probability and Statistics*, McGraw-Hill, New York, New York, 1975.

APPENDIX A—WINDLESS DATA

In this appendix and in all the appendices that follow, the numbering convention used in the data tables for sensors on the 1:10-scale New Large Aircraft mockup and around the fire pan can be found in figure 3 of the main document.

Figures A-1 through A-4 show the statistics compiled using data from nine trials. Data with $0.1 \leq$ relative standard error (equation 1 in the main document) < 0.3 are highlighted in gray. The small number of gray-shaded cells in the tables in this appendix, and in the corresponding tables in the other appendices, is a good visual indication of how repeatable results were for tests with the same initial conditions.

Windless Conditions																
	Perimeter Heat Flux (Kw/m^2)															
	HT1		HT2		HT3		HT4		HT5		HT6		HT7		HT8	
Time (s)	avg.	std. dev.	avg.	std. dev.	avg.	std. dev.	avg.	std. dev.	avg.	std. dev.	avg.	std. dev.	avg.	std. dev.	avg.	std. dev.
0	2	0	2	0	2	0	1	0	1	0	2	0	2	0	2	0
15	10	1	20	2	4	0	5	1	2	0	5	1	7	1	11	1
30	18	1	20	1	11	1	15	1	6	1	17	3	15	1	16	1
45	21	1	24	1	18	1	23	1	13	0	22	1	22	1	20	1
60	22	1	25	1	20	2	26	2	17	1	25	2	24	1	22	1
75	22	1	25	1	20	1	26	2	19	2	24	3	24	1	22	1
90	22	1	25	2	21	2	26	2	19	1	24	1	25	1	22	1
105	23	1	26	1	23	2	29	2	21	2	26	2	27	1	23	1
120	23	0	27	1	24	2	32	3	23	2	29	3	28	1	24	1
135	24	1	27	1	25	2	35	2	25	2	30	2	29	1	24	1
150	24	1	28	1	26	2	38	2	28	2	32	2	30	1	24	1
165	25	1	29	1	28	2	40	3	30	2	33	1	31	1	25	1
180	26	1	31	1	29	2	41	2	32	2	33	3	32	2	26	1
195	28	1	32	1	29	1	39	2	31	1	33	2	34	1	29	1
210	30	2	34	2	30	1	39	2	32	1	34	1	37	1	31	1
225	28	2	31	3	30	1	37	2	32	1	33	1	36	2	30	2
240	21	4	21	6	25	2	30	2	29	1	25	2	28	4	24	3

Figure A-1. Perimeter Heat Flux Statistics for Windless Condition Trials

Windless Conditions																
	Perimeter Air Temperature (°F)															
	HT1		HT2		HT3		HT4		HT5		HT6		HT7		HT8	
Time (s)	avg.	std. dev.	avg.	std. dev.	avg.	std. dev.	avg.	std. dev.	avg.	std. dev.	avg.	std. dev.	avg.	std. dev.	avg.	std. dev.
0	81	5	80	5	80	5	80	5	80	5	80	5	80	5	80	5
15	155	10	154	13	124	12	111	11	107	13	99	9	123	14	146	13
30	233	5	251	17	246	25	245	25	216	25	203	14	255	12	242	17
45	272	16	296	16	314	26	326	19	261	25	252	20	316	16	280	20
60	287	17	312	16	337	24	353	32	277	43	276	33	344	18	297	20
75	295	17	317	10	346	33	343	26	275	36	281	31	353	18	301	13
90	294	16	320	13	345	37	352	27	267	34	282	19	336	17	307	18
105	303	15	338	14	367	36	375	28	285	47	298	17	360	15	316	16
120	305	15	344	9	354	43	383	23	298	53	318	15	387	25	321	18
135	307	19	337	24	346	38	377	20	318	41	326	15	395	25	327	21
150	307	21	332	23	358	35	390	22	336	36	325	24	404	13	324	13
165	310	18	337	14	365	43	366	17	341	30	320	22	381	23	329	17
180	321	15	345	5	372	40	363	26	336	26	304	30	390	23	334	15
195	337	22	357	16	369	47	346	33	343	27	317	26	377	31	357	24
210	343	24	366	17	382	47	351	31	332	39	323	12	364	33	374	21
225	319	20	343	23	368	47	323	37	317	28	314	14	332	21	355	20
240	270	22	286	16	312	41	275	32	274	37	261	28	279	35	304	24

Figure A-2. Perimeter Air Statistics for Windless Condition Trials

Windless Conditions																
	Fuselage Side Surface Temperature (°F)															
	T1R		T2R		T3R		T4R		T1L		T2L		T3L		T4L	
Time (s)	avg.	std. dev.	avg.	std. dev.	avg.	std. dev.	avg.	std. dev.	avg.	std. dev.	avg.	std. dev.	avg.	std. dev.	avg.	std. dev.
0	78	5	80	5	80	5	77	5	77	5	80	5	78	5	76	5
15	79	5	81	5	81	5	77	5	78	5	81	5	80	5	77	5
30	87	5	102	9	99	8	87	6	86	4	99	3	99	4	89	4
45	112	8	163	14	154	13	110	9	104	4	127	5	127	6	109	4
60	159	14	265	18	247	18	148	13	128	6	165	8	165	8	135	5
75	225	20	398	19	368	21	195	17	159	9	214	11	214	11	167	7
90	307	27	547	19	504	21	249	19	195	11	273	14	270	14	203	10
105	402	36	693	19	642	20	308	22	237	14	337	17	332	18	243	13
120	510	42	826	20	770	19	370	23	284	16	405	19	396	21	286	14
135	623	47	942	19	882	16	434	24	334	17	474	21	458	23	328	16
150	734	49	1034	18	975	13	499	23	384	19	538	22	516	24	370	16
165	839	48	1105	19	1047	11	560	23	432	20	597	23	568	24	409	17
180	935	44	1161	23	1103	13	619	24	479	21	651	23	615	25	444	18
195	1023	38	1201	29	1149	18	681	25	525	23	703	24	660	26	481	20
210	1095	32	1220	40	1182	25	748	28	571	25	749	14	706	27	522	21
225	1150	27	1227	52	1200	36	811	32	618	28	801	14	754	29	565	23
240	1187	26	1255	22	1212	34	861	39	659	32	846	16	797	34	604	26

Figure A-3. Fuselage Side Surface Temperature Statistics for Windless Condition Trials

Windless Conditions														
	Fuselage and Wing Underside Surface Temperature (°F)													
	T1B		T2B		T3B		T4B		T5B		T6B		T7B	
Time (s)	avg.	std. dev.	avg.	std. dev.	avg.	std. dev.	avg.	std. dev.	avg.	std. dev.	avg.	std. dev.	avg.	std. dev.
0	77	5	79	5	79	5	75	5	76	5	76	5	76	5
15	78	5	86	5	82	5	76	5	76	5	76	5	76	5
30	91	4	124	7	104	6	87	6	86	7	81	6	77	5
45	122	6	194	10	157	9	113	8	115	10	101	8	82	5
60	175	10	289	13	239	12	158	12	162	16	136	11	91	6
75	250	15	404	14	345	14	221	16	227	22	184	15	104	6
90	341	19	531	14	465	16	297	18	306	28	243	19	119	7
105	442	21	655	13	589	17	379	20	394	33	311	23	137	8
120	545	21	768	12	705	18	464	22	486	37	385	28	156	10
135	642	21	865	12	808	19	546	23	579	38	464	32	178	11
150	733	21	946	11	895	18	621	24	670	38	544	32	202	13
165	814	20	1011	12	966	18	691	23	756	37	621	32	227	13
180	885	18	1063	13	1024	16	754	22	838	35	694	32	254	14
195	949	17	1109	12	1074	15	816	22	913	33	763	34	282	14
210	1009	16	1149	12	1119	15	879	21	981	31	826	36	310	15
225	1062	17	1181	12	1156	17	940	20	1041	29	882	38	337	18
240	1102	18	1203	10	1181	20	991	22	1091	27	927	37	362	20

Figure A-4. Fuselage and Wing Underside Surface Temperature Statistics for Windless Condition Trials

APPENDIX B—DATA FROM THE 0.7-mph, 90° CROSSWIND TRIALS

Figures B-1 through B-4 show statistics compiled using data from six trials on the 1:10-scale New Large Aircraft (NLA) mockup under 0.7-mph, 90° crosswind conditions. Data with 0.1 ≤ relative standard error (RSE) < 0.3 are highlighted in light gray, and data with 0.3 ≤ RSE are highlighted in dark gray.

0.7mph 90° crosswinds																
	Perimeter Heat Flux (Kw/m^2)															
	HT1		HT2		HT3		HT4		HT5		HT6		HT7		HT8	
Time (s)	avg.	std. dev.	avg.	std. dev.	avg.	std. dev.	avg.	std. dev.	avg.	std. dev.	avg.	std. dev.	avg.	std. dev.	avg.	std. dev.
0	2	1	2	0	2	1	1	1	1	0	2	0	1	0	2	0
15	4	1	9	2	4	1	8	2	2	2	9	2	7	2	4	1
30	14	3	19	2	10	1	33	2	3	1	15	2	15	2	13	2
45	24	2	26	1	16	1	40	4	6	1	20	1	23	1	22	1
60	27	1	27	1	18	1	39	3	8	1	21	1	25	1	25	1
75	27	1	27	1	18	2	37	2	9	0	20	1	25	1	25	1
90	27	1	28	1	19	1	35	1	10	0	20	1	26	1	27	1
105	36	3	38	2	21	2	38	1	10	0	20	1	27	2	32	3
120	49	6	50	4	26	2	39	3	11	0	20	1	27	2	37	3
135	56	5	56	3	26	1	39	1	12	0	20	0	29	2	42	5
150	64	3	61	1	28	1	38	2	12	1	20	1	29	2	46	6
165	70	4	65	3	29	1	37	1	12	1	20	1	29	2	52	8
180	76	2	70	2	30	0	37	2	12	0	20	0	30	2	55	6
195	73	2	67	2	30	1	38	1	13	1	22	1	33	1	59	9
210	71	2	66	2	32	1	42	3	13	1	23	2	36	2	61	7
225	67	3	64	3	31	2	37	4	14	1	22	2	35	3	60	5
240	60	5	55	3	27	2	24	4	13	1	16	3	28	3	53	5

Figure B-1. Perimeter Heat Flux Statistics for the 0.7-mph, 90° Crosswind Condition

0.7mph 90° crosswinds																
	Perimeter Air Temperature (°F)															
	HT1		HT2		HT3		HT4		HT5		HT6		HT7		HT8	
Time (s)	avg.	std. dev.	avg.	std. dev.	avg.	std. dev.	avg.	std. dev.	avg.	std. dev.	avg.	std. dev.	avg.	std. dev.	avg.	std. dev.
0	64	5	63	5	64	6	66	5	67	6	69	8	68	8	64	5
15	84	8	85	8	97	12	106	11	106	19	110	21	98	13	90	9
30	169	24	184	17	196	18	216	10	193	13	194	19	217	22	194	27
45	239	24	256	8	237	33	273	10	230	11	224	9	286	15	271	13
60	269	26	278	3	250	27	298	14	244	8	240	14	311	20	302	14
75	287	24	288	13	236	30	307	10	249	9	258	16	320	8	306	11
90	285	23	297	14	230	23	303	8	256	9	264	15	310	14	303	12
105	340	46	330	22	272	36	311	8	241	11	240	30	274	15	319	32
120	393	52	351	25	317	45	319	10	236	12	238	25	272	25	378	28
135	394	58	377	24	298	42	310	11	231	11	232	24	269	31	414	25
150	390	33	404	20	308	40	303	6	228	8	227	21	273	27	441	37
165	406	33	411	20	312	29	306	13	230	11	215	27	271	23	466	39
180	420	31	443	21	322	28	305	14	229	11	218	22	268	21	473	29
195	418	47	399	25	303	32	299	9	236	16	229	25	287	32	488	36
210	418	37	405	18	305	30	314	19	249	16	242	23	303	25	489	26
225	415	26	395	35	295	43	300	19	233	22	224	29	284	28	478	18
240	375	28	345	29	256	45	264	15	205	14	194	30	249	28	424	29

Figure B-2. Perimeter Air Temperature Statistics for the 0.7-mph, 90° Crosswind Condition

0.7mph 90° crosswinds																
	Fuselage Side Surface Temperature (°F)															
	T1R		T2R		T3R		T4R		T1L		T2L		T3L		T4L	
Time (s)	avg.	std. dev.	avg.	std. dev.	avg.	std. dev.	avg.	std. dev.	avg.	std. dev.	avg.	std. dev.	avg.	std. dev.	avg.	std. dev.
0	62	6	65	6	65	5	62	6	63	6	64	6	65	6	63	6
15	63	6	65	6	65	5	63	6	63	7	64	6	65	6	63	6
30	71	8	71	7	71	7	69	7	68	7	67	7	68	8	67	8
45	104	11	100	11	102	11	90	9	87	9	82	9	84	10	83	11
60	165	12	165	18	164	14	129	12	121	11	118	13	119	14	113	15
75	252	15	270	23	258	20	183	15	170	13	177	17	165	15	152	19
90	355	17	406	28	385	26	247	17	225	20	252	21	218	15	201	22
105	486	22	571	36	541	26	333	21	315	29	344	28	291	18	269	28
120	670	25	795	42	731	29	447	29	512	36	489	35	398	24	373	42
135	858	19	998	34	908	29	562	45	757	30	662	43	529	29	493	62
150	1019	17	1155	28	1050	29	667	62	996	25	836	53	662	37	606	75
165	1136	23	1266	26	1157	27	761	73	1174	28	983	58	786	44	717	79
180	1217	26	1348	22	1240	21	849	81	1303	27	1100	56	903	52	828	80
195	1278	26	1410	22	1304	21	927	84	1391	20	1192	49	1005	57	934	83
210	1330	22	1463	18	1360	21	1006	80	1445	23	1269	46	1097	51	1035	80
225	1358	22	1487	15	1397	19	1071	72	1463	19	1315	39	1171	46	1113	73
240	1358	24	1481	12	1410	18	1109	61	1440	14	1331	30	1215	38	1155	65

Figure B-3. Fuselage Side Surface Temperature Statistics for the 0.7-mph, 90° Crosswind Condition

0.7mph 90° crosswinds														
	Fuselage and Wing Underside Surface Temperature (°F)													
	T1B		T2B		T3B		T4B		T5B		T6B		T7B	
Time (s)	avg.	std. dev.	avg.	std. dev.	avg.	std. dev.	avg.	std. dev.	avg.	std. dev.	avg.	std. dev.	avg.	std. dev.
0	62	6	64	6	65	5	62	6	62	6	62	6	62	6
15	63	6	64	6	65	5	62	6	62	6	62	6	62	6
30	70	8	70	6	70	7	66	7	64	7	68	8	64	7
45	99	14	94	12	93	15	83	12	71	8	86	10	69	7
60	156	23	150	23	148	25	124	19	91	9	120	11	79	7
75	244	31	239	32	219	29	191	27	127	12	168	12	91	7
90	355	38	353	39	321	37	284	33	182	14	227	12	106	7
105	496	44	488	44	456	47	403	39	255	17	295	11	122	7
120	683	47	659	48	620	52	549	45	343	19	365	11	140	7
135	868	46	820	49	771	56	696	49	444	22	433	13	157	6
150	1025	43	953	56	896	61	824	48	552	24	497	16	176	7
165	1145	37	1058	59	1003	64	938	43	661	26	555	19	194	6
180	1236	30	1149	58	1097	61	1037	39	764	26	607	22	212	7
195	1308	27	1222	58	1176	63	1118	38	858	24	653	23	229	7
210	1365	24	1285	55	1244	61	1187	39	942	22	695	24	247	7
225	1396	21	1325	49	1291	54	1240	38	1013	19	733	25	264	7
240	1398	12	1342	40	1314	43	1271	32	1070	16	767	24	281	7

Figure B-4. Fuselage and Wing Underside Surface Temperature Statistics for the 0.7-mph, 90° Crosswind Condition

In this appendix, statistical analyses by *t*-test were conducted to compare the results from wind-driven trials, 0.7-mph, 90° crosswind in this particular appendix, to the trials done in windless conditions. The *t*-test function built into Microsoft® Excel® was used to do the analysis, assuming a two-tailed test with unequal variance. For each individual sensor at each of the 15-second intervals, Microsoft® Excel® generated a *p*-value (probability value). *p*-values less than 5% (0.05) indicated a statistically significant difference in the data, meaning the change in wind condition did have a significant effect on the results of the individual sensor. *p*-values greater than 5% indicated no statistically significant difference in the data and implied that the change in wind condition had NLA mockup under 0.7-mph, 90° crosswind conditions.

Cells with 0.01 <*p*-value ≤0.05 are highlighted in light gray. Cells with *p*-value ≤0.01 are highlighted in dark gray. The amount of gray in the tables below, and in the corresponding tables in the other appendices, presents a good visual indication of how dissimilar results were between tests with two different initial test conditions.

	Underside Surface Temperature t-test p-values						
Time (s)	T1B	T2B	T3B	T4B	T5B	T6B	T7B
0	0.00	0.00	0.00	0.00	0.00	0.00	0.00
15	0.00	0.00	0.00	0.00	0.00	0.00	0.00
30	0.00	0.00	0.00	0.00	0.00	0.01	0.00
45	0.01	0.00	0.00	0.00	0.00	0.01	0.00
60	0.10	0.00	0.00	0.00	0.00	0.02	0.00
75	0.68	0.00	0.00	0.04	0.00	0.03	0.00
90	0.46	0.00	0.00	0.41	0.00	0.06	0.01
105	0.03	0.00	0.00	0.21	0.00	0.11	0.00
120	0.00	0.00	0.01	0.00	0.00	0.07	0.00
135	0.00	0.08	0.18	0.00	0.00	0.02	0.00
150	0.00	0.76	0.97	0.00	0.00	0.00	0.00
165	0.00	0.10	0.23	0.00	0.00	0.00	0.00
180	0.00	0.01	0.03	0.00	0.00	0.00	0.00
195	0.00	0.00	0.01	0.00	0.00	0.00	0.00
210	0.00	0.00	0.00	0.00	0.01	0.00	0.00
225	0.00	0.00	0.00	0.00	0.04	0.00	0.00
240	0.00	0.00	0.00	0.00	0.07	0.00	0.00

	Perimeter Temperature t-test p-values							
Time (s)	HT1	HT2	HT3	HT4	HT5	HT6	HT7	HT8
0	0.00	0.00	0.00	0.00	0.00	0.02	0.01	0.00
15	0.00	0.00	0.00	0.36	0.93	0.27	0.00	0.00
30	0.00	0.00	0.00	0.01	0.04	0.34	0.01	0.01
45	0.02	0.00	0.00	0.00	0.01	0.00	0.00	0.26
60	0.16	0.00	0.00	0.00	0.06	0.01	0.01	0.62
75	0.48	0.00	0.00	0.00	0.06	0.08	0.00	0.44
90	0.45	0.01	0.00	0.00	0.37	0.06	0.01	0.63
105	0.10	0.45	0.00	0.00	0.03	0.00	0.00	0.88
120	0.01	0.54	0.14	0.00	0.01	0.00	0.00	0.00
135	0.01	0.01	0.05	0.00	0.00	0.00	0.00	0.00
150	0.00	0.00	0.03	0.00	0.00	0.00	0.00	0.00
165	0.00	0.00	0.01	0.00	0.00	0.00	0.00	0.00
180	0.00	0.00	0.01	0.00	0.00	0.00	0.00	0.00
195	0.01	0.01	0.01	0.00	0.00	0.00	0.00	0.00
210	0.00	0.00	0.00	0.01	0.00	0.00	0.00	0.00
225	0.00	0.01	0.01	0.15	0.00	0.00	0.01	0.00
240	0.00	0.00	0.03	0.37	0.00	0.00	0.08	0.00

	Fuselage Side Surface Temperature t-test p-values							
Time (s)	T1R	T2R	T3R	T4R	T1L	T2L	T3L	T4L
0	0.00	0.00	0.00	0.00	0.00	0.00	0.00	0.00
15	0.00	0.00	0.00	0.00	0.00	0.00	0.00	0.00
30	0.00	0.00	0.00	0.00	0.00	0.00	0.00	0.00
45	0.12	0.00	0.00	0.00	0.00	0.00	0.00	0.00
60	0.39	0.00	0.00	0.02	0.19	0.00	0.00	0.01
75	0.01	0.00	0.00	0.16	0.13	0.00	0.00	0.13
90	0.00	0.00	0.00	0.87	0.01	0.07	0.00	0.80
105	0.00	0.00	0.00	0.04	0.00	0.60	0.00	0.08
120	0.00	0.13	0.02	0.00	0.00	0.00	0.85	0.00
135	0.00	0.01	0.09	0.00	0.00	0.00	0.00	0.00
150	0.00	0.00	0.00	0.00	0.00	0.00	0.00	0.00
165	0.00	0.00	0.00	0.00	0.00	0.00	0.00	0.00
180	0.00	0.00	0.00	0.00	0.00	0.00	0.00	0.00
195	0.00	0.00	0.00	0.00	0.00	0.00	0.00	0.00
210	0.00	0.00	0.00	0.00	0.00	0.00	0.00	0.00
225	0.00	0.00	0.00	0.00	0.00	0.00	0.00	0.00
240	0.00	0.00	0.00	0.00	0.00	0.00	0.00	0.00

	Perimeter Heat Flux t-test p-values							
Time (s)	HT1	HT2	HT3	HT4	HT5	HT6	HT7	HT8
0	0.43	0.04	0.37	0.79	0.06	0.56	0.22	0.05
15	0.00	0.00	0.22	0.01	0.81	0.01	0.67	0.00
30	0.03	0.38	0.12	0.00	0.00	0.16	0.93	0.01
45	0.04	0.01	0.00	0.00	0.00	0.00	0.10	0.06
60	0.00	0.01	0.01	0.00	0.00	0.00	0.21	0.00
75	0.00	0.00	0.01	0.00	0.00	0.01	0.09	0.00
90	0.00	0.00	0.02	0.00	0.00	0.00	0.06	0.00
105	0.00	0.00	0.29	0.00	0.00	0.00	0.66	0.00
120	0.00	0.00	0.10	0.00	0.00	0.00	0.22	0.00
135	0.00	0.00	0.05	0.00	0.00	0.00	0.59	0.00
150	0.00	0.00	0.04	0.68	0.00	0.00	0.16	0.00
165	0.00	0.00	0.17	0.02	0.00	0.00	0.11	0.00
180	0.00	0.00	0.14	0.00	0.00	0.00	0.11	0.00
195	0.00	0.00	0.03	0.58	0.00	0.00	0.18	0.00
210	0.00	0.00	0.03	0.04	0.00	0.00	0.43	0.00
225	0.00	0.00	0.06	0.87	0.00	0.00	0.78	0.00
240	0.00	0.00	0.07	0.02	0.00	0.00	0.81	0.00

Figure B-5. The *t*-Test Data for 0.7-mph, 90° Crosswind Trials

APPENDIX C—DATA FROM THE 0.7-mph, 45° CROSSWIND TRIALS

Figures C-1 through C-4 show statistics compiled using data from six trials of the 1:10-scale New Large Aircraft mockup under 0.7-mph, 45° crosswind conditions. Data with 0.1 ≤relative standard error < 0.3 are highlighted in gray.

0.7mph 45° crosswinds																
	Perimeter Heat Flux (Kw/m^2)															
	HT1		HT2		HT3		HT4		HT5		HT6		HT7		HT8	
Time (s)	avg.	std. dev.	avg.	std. dev.	avg.	std. dev.	avg.	std. dev.	avg.	std. dev.	avg.	std. dev.	avg.	std. dev.	avg.	std. dev.
0	2	0	2	0	2	1	1	0	1	0	2	1	1	1	2	0
15	4	2	9	1	5	1	7	1	2	0	10	2	9	2	5	1
30	15	2	24	3	10	1	13	1	2	0	16	1	16	2	14	2
45	23	3	23	1	16	1	19	0	6	1	21	1	24	1	24	1
60	27	2	25	2	19	2	21	0	9	1	22	0	26	1	26	1
75	26	2	24	2	18	1	22	0	9	1	22	1	25	1	25	2
90	31	4	28	2	20	2	22	1	10	1	21	1	28	1	29	3
105	41	3	33	1	19	1	23	1	14	5	23	1	34	1	41	3
120	50	3	35	1	19	1	23	1	13	3	23	0	39	2	51	3
135	56	3	37	1	19	2	24	0	17	9	24	1	46	1	64	4
150	61	3	37	1	20	1	23	1	13	1	25	2	52	4	77	8
165	68	2	39	1	20	1	24	1	14	2	26	1	59	4	91	6
180	67	4	38	2	20	1	25	0	14	1	27	1	62	3	93	8
195	62	4	38	2	22	2	26	1	14	1	28	1	62	2	86	5
210	64	3	41	2	22	1	27	2	14	2	29	2	61	2	82	4
225	59	2	37	2	21	2	24	2	13	4	27	3	58	3	78	3
240	47	3	25	4	18	1	19	3	15	2	20	3	52	3	68	4

Figure C-1. Perimeter Heat Flux Statistics for the 0.7-mph, 45° Crosswind Condition

0.7mph 45° crosswinds																
	Perimeter Air Temperature (°F)															
	HT1		HT2		HT3		HT4		HT5		HT6		HT7		HT8	
Time (s)	avg.	std. dev.	avg.	std. dev.	avg.	std. dev.	avg.	std. dev.	avg.	std. dev.	avg.	std. dev.	avg.	std. dev.	avg.	std. dev.
0	75	3	74	2	77	2	81	4	78	4	80	4	84	12	79	5
15	101	9	99	6	117	8	121	10	134	11	123	10	115	16	116	12
30	193	18	196	9	213	16	220	19	256	19	234	23	227	13	234	17
45	264	4	271	14	267	11	274	13	290	10	273	10	302	11	289	6
60	279	11	293	19	294	7	301	17	316	12	268	12	337	10	310	18
75	278	12	271	26	301	10	307	17	322	14	272	17	338	15	323	11
90	305	18	279	10	303	13	303	14	319	15	261	24	327	22	342	19
105	361	10	331	8	294	12	298	17	311	26	266	18	331	14	402	29
120	399	10	345	12	287	7	293	17	286	13	254	14	370	12	427	28
135	425	17	340	18	279	13	289	17	280	21	267	25	408	14	428	33
150	448	26	340	25	277	10	287	16	283	21	271	14	430	24	447	35
165	480	24	348	19	279	6	289	13	278	19	276	23	455	27	477	37
180	479	22	331	20	276	7	289	15	282	23	283	16	467	18	473	27
195	484	24	338	12	281	10	304	20	290	30	280	18	439	15	482	18
210	493	53	351	22	293	12	306	20	287	20	286	25	437	22	467	20
225	460	33	319	20	274	19	282	25	260	21	269	24	421	23	450	25
240	404	19	255	15	227	8	247	19	211	21	216	24	364	11	398	33

Figure C-2. Perimeter Air Temperature Statistics for the 0.7-mph, 45° Crosswind Condition

0.7mph 45° crosswinds																
	Fuselage Side Surface Temperature (°F)															
	T1R		T2R		T3R		T4R		T1L		T2L		T3L		T4L	
Time (s)	avg.	std. dev.	avg.	std. dev.	avg.	std. dev.	avg.	std. dev.	avg.	std. dev.	avg.	std. dev.	avg.	std. dev.	avg.	std. dev.
0	74	3	75	2	74	2	73	2	74	2	75	2	76	4	74	2
15	74	2	75	2	74	2	73	3	74	2	75	2	76	4	74	2
30	80	3	81	2	80	3	79	5	78	3	77	3	79	4	76	4
45	101	5	106	6	106	9	103	10	90	3	88	4	91	6	89	7
60	143	7	164	13	162	15	148	15	114	3	116	6	129	13	115	8
75	203	10	259	19	249	20	208	17	149	4	162	10	174	17	149	9
90	274	15	383	23	362	23	279	17	193	6	224	17	229	27	191	11
105	348	22	522	26	494	23	363	17	245	9	300	27	296	36	243	13
120	419	27	658	28	625	21	478	23	303	13	393	39	384	52	317	15
135	487	31	786	28	752	21	629	29	363	16	502	51	500	65	431	18
150	550	33	897	26	885	22	804	37	423	17	623	61	649	77	596	26
165	609	34	988	27	1020	22	979	38	482	17	747	64	826	90	789	34
180	659	33	1055	26	1131	17	1112	28	538	15	858	64	972	71	964	34
195	700	33	1099	27	1193	16	1193	23	585	15	946	54	1067	60	1087	36
210	736	32	1129	26	1241	13	1244	17	627	13	1010	46	1158	60	1165	30
225	771	31	1155	25	1276	13	1286	14	665	10	1060	38	1217	60	1222	24
240	794	31	1163	26	1285	11	1301	12	693	7	1086	32	1223	51	1252	21

Figure C-3. Fuselage Side Surface Temperature Statistics for the 0.7-mph, 45° Crosswind Condition

0.7mph 45° crosswinds														
	Fuselage and Wing Underside Surface Temperature (°F)													
	T1B		T2B		T3B		T4B		T5B		T6B		T7B	
Time (s)	avg.	std. dev.	avg.	std. dev.	avg.	std. dev.	avg.	std. dev.	avg.	std. dev.	avg.	std. dev.	avg.	std. dev.
0	73	3	74	2	73	2	72	2	73	2	72	2	74	2
15	74	2	74	3	74	2	72	3	73	3	73	3	74	2
30	80	3	81	3	79	3	75	5	74	4	79	7	76	4
45	103	7	109	6	105	13	92	11	82	7	101	13	82	6
60	150	12	167	7	161	18	129	17	101	12	142	20	94	7
75	226	16	254	9	235	29	188	20	138	17	199	28	108	8
90	327	21	360	13	337	34	270	20	192	23	270	33	123	8
105	439	25	477	17	457	33	367	18	264	27	357	38	142	9
120	550	29	588	19	581	30	480	18	351	30	465	44	166	11
135	655	32	693	19	693	24	610	15	447	31	587	50	194	13
150	748	32	790	17	798	21	754	15	544	30	715	53	227	16
165	829	32	879	16	898	16	896	16	637	28	837	53	266	21
180	893	31	954	14	984	11	1012	15	722	26	949	49	312	24
195	944	31	1016	14	1032	9	1092	18	798	25	1046	42	361	27
210	991	28	1064	12	1076	4	1145	16	865	23	1127	35	415	31
225	1032	24	1102	11	1111	4	1188	12	921	22	1190	29	469	32
240	1051	23	1123	11	1124	5	1211	10	967	21	1235	22	520	29

Figure C-4. Fuselage and Wing Underside Surface Temperature Statistics for the 0.7-mph, 45° Crosswind Condition

In this appendix, statistical analyses by *t*-test were conducted to compare the results from wind-driven trials, 0.7-mph, 45° crosswind in this particular appendix, to the trials done in windless conditions. The *t*-test function built into Microsoft® Excel® was used to do the analysis assuming a two-tailed test with unequal variance. For each individual sensor at each of the 15-second intervals, Microsoft® Excel® generated a *p*-value (probability value). Results are shown in figure C-5. Cells with $0.01 < p\text{-value} \leq 0.05$ are highlighted in light gray. Cells with *p*-value ≤ 0.01 are highlighted in dark gray.

	Underside Surface Temperature t-test p-values						
Time (s)	T1B	T2B	T3B	T4B	T5B	T6B	T7B
0	0.07	0.01	0.04	0.16	0.20	0.13	0.22
15	0.04	0.00	0.00	0.10	0.11	0.17	0.22
30	0.00	0.00	0.00	0.00	0.00	0.53	0.48
45	0.00	0.00	0.00	0.00	0.00	0.98	0.95
60	0.00	0.00	0.00	0.01	0.00	0.54	0.55
75	0.02	0.00	0.00	0.01	0.00	0.28	0.37
90	0.19	0.00	0.00	0.03	0.00	0.12	0.32
105	0.79	0.00	0.00	0.26	0.00	0.03	0.24
120	0.68	0.00	0.00	0.16	0.00	0.00	0.12
135	0.42	0.00	0.00	0.00	0.00	0.00	0.04
150	0.33	0.00	0.00	0.00	0.00	0.00	0.01
165	0.33	0.00	0.00	0.00	0.00	0.00	0.00
180	0.56	0.00	0.00	0.00	0.00	0.00	0.00
195	0.73	0.00	0.00	0.00	0.00	0.00	0.00
210	0.20	0.00	0.00	0.00	0.00	0.00	0.00
225	0.03	0.00	0.00	0.00	0.00	0.00	0.00
240	0.00	0.00	0.00	0.00	0.00	0.00	0.00

	Perimeter Temperature t-test p-values							
Time (s)	HT1	HT2	HT3	HT4	HT5	HT6	HT7	HT8
0	0.01	0.00	0.06	0.79	0.52	0.97	0.46	0.60
15	0.00	0.00	0.21	0.10	0.00	0.00	0.36	0.00
30	0.00	0.00	0.01	0.04	0.00	0.02	0.00	0.39
45	0.17	0.01	0.00	0.00	0.01	0.02	0.08	0.27
60	0.24	0.07	0.00	0.00	0.03	0.54	0.31	0.23
75	0.04	0.01	0.00	0.01	0.00	0.52	0.10	0.00
90	0.24	0.00	0.01	0.00	0.00	0.10	0.44	0.00
105	0.00	0.23	0.00	0.00	0.18	0.01	0.00	0.00
120	0.00	0.81	0.00	0.00	0.54	0.00	0.10	0.00
135	0.00	0.78	0.00	0.00	0.04	0.00	0.19	0.00
150	0.00	0.56	0.00	0.00	0.00	0.00	0.05	0.00
165	0.00	0.27	0.00	0.00	0.00	0.00	0.00	0.00
180	0.00	0.18	0.00	0.00	0.00	0.10	0.00	0.00
195	0.00	0.03	0.00	0.01	0.01	0.01	0.00	0.00
210	0.00	0.20	0.00	0.00	0.01	0.01	0.00	0.00
225	0.00	0.06	0.00	0.03	0.00	0.00	0.00	0.00
240	0.00	0.00	0.00	0.06	0.00	0.01	0.00	0.00

	Fuselage Side Surface Temperature t-test p-values							
Time (s)	T1R	T2R	T3R	T4R	T1L	T2L	T3L	T4L
0	0.04	0.03	0.02	0.08	0.10	0.02	0.25	0.37
15	0.03	0.01	0.01	0.05	0.08	0.01	0.08	0.22
30	0.01	0.00	0.00	0.01	0.00	0.00	0.00	0.00
45	0.01	0.00	0.00	0.24	0.00	0.00	0.00	0.00
60	0.01	0.00	0.00	0.93	0.00	0.00	0.00	0.00
75	0.01	0.00	0.00	0.19	0.01	0.00	0.00	0.00
90	0.01	0.00	0.00	0.01	0.64	0.00	0.01	0.05
105	0.00	0.00	0.00	0.00	0.16	0.02	0.06	0.99
120	0.00	0.00	0.00	0.00	0.02	0.48	0.62	0.00
135	0.00	0.00	0.00	0.00	0.01	0.25	0.18	0.00
150	0.00	0.00	0.00	0.00	0.00	0.02	0.01	0.00
165	0.00	0.00	0.03	0.00	0.00	0.00	0.00	0.00
180	0.00	0.00	0.01	0.00	0.00	0.00	0.00	0.00
195	0.00	0.00	0.00	0.00	0.00	0.00	0.00	0.00
210	0.00	0.00	0.00	0.00	0.00	0.00	0.00	0.00
225	0.00	0.00	0.00	0.00	0.00	0.00	0.00	0.00
240	0.00	0.00	0.00	0.00	0.01	0.00	0.00	0.00

	Perimeter Heat Flux t-test p-values							
Time (s)	HT1	HT2	HT3	HT4	HT5	HT6	HT7	HT8
0	0.25	0.01	0.21	0.38	0.94	0.40	0.28	0.01
15	0.00	0.00	0.63	0.00	0.36	0.00	0.07	0.00
30	0.00	0.01	0.17	0.03	0.00	0.45	0.49	0.10
45	0.31	0.15	0.00	0.00	0.00	0.01	0.00	0.00
60	0.00	0.42	0.35	0.00	0.00	0.01	0.01	0.00
75	0.01	0.63	0.00	0.00	0.00	0.04	0.18	0.00
90	0.00	0.01	0.46	0.00	0.00	0.00	0.00	0.00
105	0.00	0.00	0.00	0.00	0.02	0.00	0.00	0.00
120	0.00	0.00	0.00	0.00	0.00	0.00	0.00	0.00
135	0.00	0.00	0.00	0.00	0.07	0.00	0.00	0.00
150	0.00	0.00	0.00	0.00	0.00	0.00	0.00	0.00
165	0.00	0.00	0.00	0.00	0.00	0.00	0.00	0.00
180	0.00	0.00	0.00	0.00	0.00	0.00	0.00	0.00
195	0.00	0.00	0.00	0.00	0.00	0.00	0.00	0.00
210	0.00	0.00	0.00	0.00	0.00	0.00	0.00	0.00
225	0.00	0.00	0.00	0.00	0.00	0.00	0.00	0.00
240	0.00	0.12	0.00	0.00	0.00	0.01	0.00	0.00

Figure C-5. The *t*-Test Data for 0.7-mph, 45° Crosswind Trials

APPENDIX D—DATA FROM THE 1.4-mph, 90° CROSSWIND TRIALS

Figure D-1 through D-4 show statistics compiled using data from nine trials of the 1:10-scale New Large Aircraft mockup under 1.4-mph, 90° crosswind conditions. Data with 0.1 ≤ relative standard error (RSE) < 0.3 are highlighted in light gray, and data with 0.3 ≤ RSE are highlighted in dark gray.

1.4mph 90° crosswinds																
	Perimeter Heat Flux (Kw/m^2)															
	HT1		HT2		HT3		HT4		HT5		HT6		HT7		HT8	
Time (s)	avg.	std. dev.	avg.	std. dev.	avg.	std. dev.	avg.	std. dev.	avg.	std. dev.	avg.	std. dev.	avg.	std. dev.	avg.	std. dev.
0	1	1	1	1	3	1	1	1	1	2	1	1	1	0	2	1
15	7	1	15	2	4	2	5	1	3	1	6	1	7	1	8	1
30	20	1	21	1	11	3	14	1	11	1	13	1	13	1	15	1
45	28	1	28	2	17	1	21	1	18	0	18	1	20	1	21	1
60	28	1	30	1	20	4	25	1	23	1	21	1	23	0	22	1
75	31	2	32	1	22	1	25	1	24	1	20	1	23	1	23	2
90	41	6	40	4	22	2	26	2	25	1	20	1	23	1	28	3
105	53	6	50	5	24	2	27	2	25	1	20	1	24	3	35	5
120	63	7	59	4	25	3	27	2	25	2	20	2	23	1	39	5
135	72	8	65	6	26	3	27	2	26	2	20	1	24	1	42	3
150	83	9	75	4	28	2	27	2	25	1	20	2	24	1	44	4
165	91	10	79	3	27	2	28	2	25	2	20	2	25	2	47	3
180	93	9	78	4	28	4	28	2	26	3	19	2	26	3	50	4
195	85	10	76	2	29	3	28	4	26	3	21	1	27	3	52	2
210	77	8	72	4	28	3	27	4	26	4	19	2	26	4	50	4
225	69	7	56	10	23	5	20	6	22	4	14	3	21	5	44	7
240	45	9	24	17	16	4	8	5	15	3	6	4	10	5	29	7

Figure D-1. Perimeter Heat Flux Statistics for the 1.4-mph, 90° Crosswind Condition

1.4mph 90° crosswinds																
	Perimeter Air Temperature (°F)															
	HT1		HT2		HT3		HT4		HT5		HT6		HT7		HT8	
Time (s)	avg.	std. dev.	avg.	std. dev.	avg.	std. dev.	avg.	std. dev.	avg.	std. dev.	avg.	std. dev.	avg.	std. dev.	avg.	std. dev.
0	70	2	69	2	69	2	70	2	71	3	70	2	69	2	70	2
15	106	4	117	9	103	6	98	6	94	3	85	2	100	6	124	6
30	208	12	268	18	229	10	213	10	224	11	156	10	196	11	270	13
45	230	8	323	17	319	9	295	9	302	7	225	5	274	17	335	10
60	246	7	345	13	324	15	329	13	332	12	255	8	291	22	343	12
75	278	26	354	15	337	26	332	16	324	17	242	20	283	22	337	8
90	324	20	416	23	346	28	335	19	310	21	210	23	274	24	358	13
105	348	22	465	34	356	28	334	19	301	23	199	22	262	11	406	42
120	390	29	516	33	370	39	329	21	285	25	193	17	264	18	425	43
135	402	33	539	43	376	35	330	23	276	28	200	18	272	26	428	14
150	427	22	577	27	373	31	321	19	271	26	198	19	262	13	434	10
165	439	31	578	41	383	29	314	18	257	28	189	9	268	21	447	21
180	427	23	568	22	386	25	318	18	261	30	198	16	270	16	451	18
195	403	22	528	35	380	31	316	27	268	42	206	31	288	38	453	28
210	447	74	502	35	358	37	307	38	252	42	201	34	271	44	429	28
225	378	49	415	66	283	50	252	46	209	44	168	32	223	43	367	57
240	268	37	281	54	196	37	189	30	155	26	137	20	165	31	250	47

Figure D-2. Perimeter Air Temperature Statistics for the 1.4-mph, 90° Crosswind Condition

1.4mph 90° crosswinds																
	Fuselage Side Surface Temperature (°F)															
	T1R		T2R		T3R		T4R		T1L		T2L		T3L		T4L	
Time (s)	avg.	std. dev.	avg.	std. dev.	avg.	std. dev.	avg.	std. dev.	avg.	std. dev.	avg.	std. dev.	avg.	std. dev.	avg.	std. dev.
0	67	2	70	2	69	3	67	3	67	2	69	2	68	4	68	2
15	68	3	70	3	70	3	68	3	69	3	70	3	68	5	69	3
30	77	3	82	8	81	9	77	4	82	4	81	7	80	7	79	4
45	109	7	122	21	120	23	99	7	117	5	115	16	114	15	103	8
60	171	14	196	40	193	42	136	10	174	10	172	25	170	23	141	14
75	270	16	307	61	303	61	189	16	253	13	254	34	249	32	195	22
90	412	17	468	80	450	79	269	23	376	31	367	41	353	42	280	40
105	594	16	680	89	630	85	373	33	565	68	523	49	484	55	399	65
120	770	23	882	80	810	80	488	47	780	93	697	56	634	64	541	87
135	910	43	1037	62	957	59	596	63	965	102	862	57	779	71	687	105
150	1011	60	1131	49	1065	37	691	81	1105	86	995	44	912	72	826	121
165	1079	77	1203	61	1140	40	741	41	1212	68	1110	38	1026	69	947	125
180	1123	91	1235	73	1190	52	806	31	1289	61	1200	35	1125	47	1053	105
195	1165	105	1272	92	1221	69	866	32	1362	60	1268	28	1201	24	1141	79
210	1199	121	1300	111	1251	86	917	46	1411	62	1324	35	1256	20	1199	57
225	1207	125	1303	120	1266	100	976	106	1412	52	1348	37	1287	22	1226	41
240	1189	122	1280	121	1249	107	979	106	1373	38	1337	32	1291	25	1223	37

Figure D-3. Fuselage Side Surface Temperature Statistics for the 1.4-mph, 90° Crosswind Condition

1.4mph 90° crosswinds														
	Fuselage and Wing Underside Surface Temperature (°F)													
	T1B		T2B		T3B		T4B		T5B		T6B		T7B	
Time (s)	avg.	std. dev.	avg.	std. dev.	avg.	std. dev.	avg.	std. dev.	avg.	std. dev.	avg.	std. dev.	avg.	std. dev.
0	67	2	68	3	69	3	67	2	67	3	67	3	67	3
15	68	3	70	4	70	3	67	3	67	3	67	3	67	3
30	81	5	86	17	83	9	77	5	69	4	73	3	69	2
45	120	9	130	34	122	17	106	8	80	8	89	3	73	2
60	195	14	203	52	189	29	159	12	104	15	120	5	80	3
75	306	19	307	69	286	43	243	19	146	25	163	7	90	3
90	458	23	444	79	411	55	360	28	205	36	215	9	101	3
105	643	26	615	78	563	55	504	38	281	47	273	10	115	3
120	828	27	790	70	725	52	658	43	370	57	330	13	130	3
135	984	24	941	57	876	49	804	44	465	63	386	18	144	4
150	1103	19	1061	43	1005	43	931	44	563	66	441	26	160	4
165	1189	21	1154	34	1106	37	1036	39	658	65	491	36	176	5
180	1252	30	1224	25	1183	27	1118	29	744	63	537	45	192	6
195	1310	42	1281	20	1244	17	1183	18	821	61	578	53	208	8
210	1353	52	1328	31	1291	27	1233	15	887	61	597	32	224	9
225	1363	52	1348	37	1312	36	1262	20	942	63	626	35	239	11
240	1338	52	1336	37	1306	40	1261	31	982	68	647	38	253	12

Figure D-4. Fuselage and Wing Underside Surface Temperature Statistics for the 1.4-mph, 90° Crosswind Condition

In this appendix, statistical analyses by *t*-test were conducted to compare the results from wind-driven trials, 1.4-mph, 90° crosswind in this particular appendix, to the trials done in windless conditions. The *t*-test function built into Microsoft® Excel® was used to do the analysis assuming a two-tailed test with unequal variance. For each individual sensor at each of the 15-second intervals, Microsoft® Excel® generated a *p*-value (probability value). The results are shown in figure D-5. Cells with 0.01 <*p*-value ≤0.05 are highlighted in light gray. Cells with *p*-value ≤0.01 are highlighted in dark gray.

	Underside Surface Temperature t-test p-values						
Time (s)	T1B	T2B	T3B	T4B	T5B	T6B	T7B
0	0.00	0.00	0.00	0.00	0.00	0.00	0.00
15	0.00	0.00	0.00	0.00	0.00	0.00	0.00
30	0.00	0.00	0.00	0.00	0.00	0.00	0.00
45	0.67	0.00	0.00	0.08	0.00	0.00	0.00
60	0.00	0.00	0.00	0.89	0.00	0.00	0.00
75	0.00	0.00	0.00	0.02	0.00	0.00	0.00
90	0.00	0.01	0.02	0.00	0.00	0.00	0.00
105	0.00	0.16	0.22	0.00	0.00	0.00	0.00
120	0.00	0.38	0.31	0.00	0.00	0.00	0.00
135	0.00	0.00	0.00	0.00	0.00	0.00	0.00
150	0.00	0.00	0.00	0.00	0.00	0.00	0.00
165	0.00	0.00	0.00	0.00	0.00	0.00	0.00
180	0.00	0.00	0.00	0.00	0.00	0.00	0.00
195	0.00	0.00	0.00	0.00	0.00	0.00	0.00
210	0.00	0.00	0.00	0.00	0.00	0.00	0.00
225	0.00	0.00	0.00	0.00	0.00	0.00	0.00
240	0.00	0.00	0.00	0.00	0.00	0.00	0.00

	Perimeter Temperature t-test p-values							
Time (s)	HT1	HT2	HT3	HT4	HT5	HT6	HT7	HT8
0	0.00	0.00	0.00	0.00	0.00	0.00	0.00	0.00
15	0.00	0.00	0.00	0.01	0.01	0.00	0.00	0.00
30	0.00	0.06	0.08	0.00	0.39	0.00	0.00	0.00
45	0.00	0.00	0.60	0.00	0.00	0.00	0.00	0.00
60	0.00	0.00	0.19	0.06	0.00	0.11	0.00	0.00
75	0.12	0.00	0.56	0.28	0.00	0.01	0.00	0.00
90	0.00	0.00	0.96	0.14	0.01	0.00	0.00	0.00
105	0.00	0.00	0.47	0.00	0.38	0.00	0.00	0.00
120	0.00	0.00	0.43	0.00	0.52	0.00	0.00	0.00
135	0.00	0.00	0.10	0.00	0.03	0.00	0.00	0.00
150	0.00	0.00	0.35	0.00	0.00	0.00	0.00	0.00
165	0.00	0.00	0.31	0.00	0.00	0.00	0.00	0.00
180	0.00	0.00	0.38	0.00	0.00	0.00	0.00	0.00
195	0.00	0.00	0.55	0.05	0.00	0.00	0.00	0.00
210	0.00	0.00	0.25	0.02	0.00	0.00	0.00	0.00
225	0.01	0.01	0.00	0.00	0.00	0.00	0.00	0.58
240	0.87	0.80	0.00	0.00	0.00	0.00	0.00	0.01

	Fuselage Side Surface Temperature t-test p-values							
Time (s)	T1R	T2R	T3R	T4R	T1L	T2L	T3L	T4L
0	0.00	0.00	0.00	0.00	0.00	0.00	0.00	0.00
15	0.00	0.00	0.00	0.00	0.00	0.00	0.00	0.00
30	0.00	0.00	0.00	0.00	0.03	0.00	0.00	0.00
45	0.33	0.00	0.00	0.01	0.00	0.05	0.03	0.06
60	0.07	0.00	0.00	0.05	0.00	0.40	0.57	0.29
75	0.00	0.00	0.01	0.46	0.00	0.01	0.01	0.00
90	0.00	0.02	0.07	0.06	0.00	0.00	0.00	0.00
105	0.00	0.69	0.71	0.00	0.00	0.00	0.00	0.00
120	0.00	0.07	0.18	0.00	0.00	0.00	0.00	0.00
135	0.00	0.00	0.00	0.00	0.00	0.00	0.00	0.00
150	0.00	0.00	0.00	0.00	0.00	0.00	0.00	0.00
165	0.00	0.00	0.00	0.00	0.00	0.00	0.00	0.00
180	0.00	0.04	0.00	0.00	0.00	0.00	0.00	0.00
195	0.00	0.09	0.02	0.00	0.00	0.00	0.00	0.00
210	0.03	0.11	0.06	0.00	0.00	0.00	0.00	0.00
225	0.22	0.16	0.11	0.00	0.00	0.00	0.00	0.00
240	0.96	0.61	0.38	0.01	0.00	0.00	0.00	0.00

	Perimeter Heat Flux t-test p-values							
Time (s)	HT1	HT2	HT3	HT4	HT5	HT6	HT7	HT8
0	0.03	0.00	0.81	0.95	0.80	0.55	0.43	0.32
15	0.00	0.00	0.72	0.36	0.00	0.29	0.55	0.00
30	0.00	0.00	0.60	0.13	0.00	0.00	0.01	0.00
45	0.00	0.00	0.06	0.00	0.00	0.00	0.00	0.05
60	0.00	0.00	0.74	0.23	0.00	0.00	0.00	0.25
75	0.00	0.00	0.05	0.70	0.00	0.00	0.09	0.15
90	0.00	0.00	0.07	0.79	0.00	0.00	0.00	0.00
105	0.00	0.00	0.09	0.01	0.00	0.00	0.06	0.00
120	0.00	0.00	0.20	0.00	0.06	0.00	0.00	0.00
135	0.00	0.00	0.17	0.00	0.51	0.00	0.00	0.00
150	0.00	0.00	0.17	0.00	0.00	0.00	0.00	0.00
165	0.00	0.00	0.53	0.00	0.00	0.00	0.00	0.00
180	0.00	0.00	0.39	0.00	0.00	0.00	0.00	0.00
195	0.00	0.00	0.84	0.00	0.00	0.00	0.00	0.00
210	0.00	0.00	0.07	0.00	0.00	0.00	0.00	0.00
225	0.00	0.00	0.01	0.00	0.00	0.00	0.00	0.00
240	0.00	0.66	0.00	0.00	0.00	0.00	0.00	0.13

Figure D-5. The *t*-Test Data for 1.4-mph, 90° Crosswind Trials

APPENDIX E—DATA FROM THE 1.4-mph, 45° CROSSWIND TRIALS

Figures E-1 through E-4 show statistics compiled using data from six trials of the 1:10-scale New Large Aircraft mockup under 1.4-mph, 45° crosswind conditions. Data with 0.1 ≤ relative standard error (RSE) < 0.3 are highlighted in light gray, and data with 0.3 ≤ RSE are highlighted in dark gray.

1.4mph 45° crosswinds																
	Perimeter Heat Flux (Kw/m^2)															
	HT1		HT2		HT3		HT4		HT5		HT6		HT7		HT8	
Time (s)	avg.	std. dev.	avg.	std. dev.	avg.	std. dev.	avg.	std. dev.	avg.	std. dev.	avg.	std. dev.	avg.	std. dev.	avg.	std. dev.
0	2	1	2	2	2	1	2	1	1	1	2	0	2	0	2	1
15	7	2	13	2	4	1	7	2	2	1	10	1	12	1	6	1
30	19	2	21	3	10	2	14	1	4	1	15	1	19	1	18	2
45	27	1	24	1	15	3	19	1	7	1	20	1	25	2	26	2
60	26	3	26	1	18	1	22	1	9	1	22	1	27	2	27	1
75	30	2	28	2	18	2	21	0	11	1	23	1	30	2	32	2
90	39	3	31	2	19	2	22	1	13	0	24	2	38	5	45	7
105	50	3	34	1	19	1	23	1	13	2	23	1	47	4	67	8
120	59	2	36	2	18	1	22	1	14	0	24	1	54	6	87	11
135	67	3	37	2	19	1	22	2	15	1	24	2	58	5	107	15
150	74	5	37	3	20	2	23	1	13	1	24	1	62	5	122	14
165	76	4	39	2	20	1	22	2	14	1	24	2	64	6	139	23
180	74	4	38	2	19	1	22	2	15	1	24	2	65	3	135	12
195	72	1	39	3	20	2	22	4	15	1	24	2	64	2	121	14
210	68	5	37	6	20	3	19	5	14	1	22	3	58	4	114	14
225	56	9	24	12	18	2	15	6	12	2	16	6	48	10	98	10
240	32	11	4	9	12	3	6	6	10	3	6	6	24	12	64	12

Figure E-1. Perimeter Heat Flux Statistics for the 1.4-mph, 45° Crosswind Condition

1.4mph 45° crosswinds																
	Perimeter Air Temperature (°F)															
	HT1		HT2		HT3		HT4		HT5		HT6		HT7		HT8	
Time (s)	avg.	std. dev.	avg.	std. dev.	avg.	std. dev.	avg.	std. dev.	avg.	std. dev.	avg.	std. dev.	avg.	std. dev.	avg.	std. dev.
0	82	3	82	2	84	2	84	3	82	3	82	3	84	6	82	2
15	122	5	118	14	127	11	121	7	131	6	125	5	142	8	129	7
30	241	8	227	18	220	15	190	43	212	53	214	15	276	16	231	16
45	284	12	291	11	289	7	265	6	289	15	278	6	322	16	253	18
60	297	13	292	15	306	14	282	22	286	25	268	13	338	17	274	15
75	332	16	312	15	299	7	285	9	284	21	270	13	360	21	311	18
90	395	27	325	21	292	14	263	41	257	52	274	20	428	40	370	19
105	464	27	344	9	292	8	272	11	261	10	266	12	483	22	424	48
120	518	36	343	26	292	6	262	21	250	28	266	19	502	36	471	51
135	573	49	346	23	292	8	254	39	230	44	269	20	514	18	519	43
150	637	72	353	31	297	11	250	34	228	42	266	15	521	13	520	28
165	700	151	342	28	293	12	257	22	224	23	266	14	536	28	609	152
180	607	38	348	28	297	10	262	22	259	27	277	20	521	18	494	14
195	601	61	344	38	293	20	259	29	231	25	276	23	508	13	508	48
210	587	36	326	48	280	30	246	35	222	36	256	41	485	25	514	42
225	526	31	265	59	240	37	218	41	187	42	206	48	419	57	441	39
240	392	46	191	43	188	31	179	34	150	25	157	27	312	54	308	48

Figure E-2. Perimeter Air Temperature Statistics for the 1.4-mph, 45° Crosswind Condition

1.4mph 45° crosswinds																
	Fuselage Side Surface Temperature (°F)															
	T1R		T2R		T3R		T4R		T1L		T2L		T3L		T4L	
Time (s)	avg.	std. dev.	avg.	std. dev.	avg.	std. dev.	avg.	std. dev.	avg.	std. dev.	avg.	std. dev.	avg.	std. dev.	avg.	std. dev.
0	82	2	83	1	84	3	81	1	84	2	83	1	83	1	84	3
15	83	2	83	1	85	4	82	1	84	3	83	2	83	2	84	3
30	88	4	88	3	93	4	95	3	89	5	87	4	89	2	91	2
45	108	8	114	10	125	3	137	15	105	10	107	9	115	4	114	2
60	150	13	172	19	189	8	201	30	136	17	147	15	164	8	150	4
75	207	18	267	27	282	15	286	42	178	20	210	22	230	14	197	8
90	273	21	390	31	399	19	403	58	227	21	292	25	311	21	262	14
105	341	23	524	30	534	27	558	75	282	22	393	26	415	37	364	30
120	406	23	653	25	688	36	730	77	339	22	513	26	546	49	514	48
135	467	28	760	27	841	26	887	67	394	24	633	25	694	51	686	58
150	521	34	843	38	973	25	1016	59	447	26	744	28	835	57	855	65
165	567	40	901	54	1073	37	1115	58	495	30	837	34	957	54	1001	68
180	606	46	941	68	1140	56	1185	62	538	33	911	43	1049	49	1113	64
195	638	51	965	80	1178	72	1236	72	577	38	968	52	1118	42	1192	59
210	665	57	980	94	1203	94	1267	83	612	44	1009	61	1171	42	1241	55
225	686	64	984	106	1209	107	1276	92	639	51	1032	69	1197	39	1267	51
240	697	69	975	113	1194	112	1262	101	654	56	1033	76	1202	36	1271	50

Figure E-3. Fuselage Side Surface Temperature Statistics for the 1.4-mph, 45° Crosswind Condition

1.4mph 45° crosswinds														
	Fuselage and Wing Underside Surface Temperature (°F)													
	T1B		T2B		T3B		T4B		T5B		T6B		T7B	
Time (s)	avg.	std. dev.	avg.	std. dev.	avg.	std. dev.	avg.	std. dev.	avg.	std. dev.	avg.	std. dev.	avg.	std. dev.
0	82	2	81	2	82	1	80	1	82	2	80	2	82	2
15	83	3	82	2	82	2	81	1	82	2	82	2	82	1
30	90	5	90	5	91	2	88	2	84	2	94	4	85	2
45	114	12	123	12	123	4	117	7	96	2	122	9	91	2
60	165	20	184	20	183	7	169	12	121	4	167	16	101	2
75	243	29	272	28	269	11	246	17	165	7	231	24	114	2
90	340	34	376	33	377	15	347	22	227	10	319	31	131	3
105	447	33	488	35	496	21	476	29	304	12	428	38	156	7
120	554	29	602	33	621	28	622	32	391	13	558	39	191	13
135	654	28	711	29	742	27	765	33	485	14	689	36	234	21
150	742	30	809	23	855	24	894	28	582	16	812	32	280	27
165	815	36	891	20	951	14	1000	22	678	19	920	32	330	32
180	870	42	956	23	1025	10	1085	17	770	22	1011	34	380	39
195	914	50	1007	31	1077	10	1148	14	855	24	1084	37	428	44
210	950	63	1044	41	1113	22	1189	16	929	26	1138	41	473	47
225	970	78	1066	51	1131	28	1213	19	992	26	1173	47	513	47
240	967	87	1067	61	1129	33	1213	27	1040	25	1185	56	543	46

Figure E-4. Fuselage and Wing Underside Surface Temperature Statistics for the 1.4-mph, 45° Crosswind Condition

In this appendix, statistical analyses by *t*-test were conducted to compare the results from wind-driven trials, 1.4-mph, 45° crosswind in this particular appendix, to the trials done in windless conditions. The *t*-test function built into Microsoft® Excel® was used to do the analysis assuming a two-tailed test with unequal variance. For each individual sensor at each of the 15-second intervals, Microsoft® Excel® generated a *p*-value (probability value). The results are shown in figure D-5. Cells with $0.01 < p\text{-value} \leq 0.05$ are highlighted in light gray. Cells with $p\text{-value} \leq 0.01$ are highlighted in dark gray.

	Underside Surface Temperature t-test p-values						
Time (s)	T1B	T2B	T3B	T4B	T5B	T6B	T7B
0	0.01	0.29	0.13	0.01	0.01	0.03	0.01
15	0.03	0.06	0.85	0.02	0.01	0.01	0.01
30	0.78	0.00	0.00	0.41	0.45	0.00	0.00
45	0.16	0.00	0.00	0.41	0.00	0.00	0.00
60	0.29	0.00	0.00	0.11	0.00	0.00	0.00
75	0.60	0.00	0.00	0.01	0.00	0.00	0.00
90	0.93	0.00	0.00	0.00	0.00	0.00	0.00
105	0.78	0.00	0.00	0.00	0.00	0.00	0.00
120	0.52	0.00	0.00	0.00	0.00	0.00	0.00
135	0.41	0.00	0.00	0.00	0.00	0.00	0.00
150	0.54	0.00	0.01	0.00	0.00	0.00	0.00
165	0.96	0.00	0.10	0.00	0.00	0.00	0.00
180	0.45	0.00	0.91	0.00	0.00	0.00	0.00
195	0.14	0.00	0.67	0.00	0.00	0.00	0.00
210	0.07	0.00	0.59	0.00	0.00	0.00	0.00
225	0.03	0.00	0.09	0.00	0.01	0.00	0.00
240	0.01	0.00	0.01	0.00	0.00	0.00	0.00

	Perimeter Temperature t-test p-values							
Time (s)	HT1	HT2	HT3	HT4	HT5	HT6	HT7	HT8
0	0.73	0.49	0.05	0.09	0.22	0.30	0.24	0.31
15	0.00	0.00	0.74	0.05	0.00	0.00	0.01	0.01
30	0.04	0.03	0.02	0.02	0.86	0.19	0.02	0.24
45	0.13	0.50	0.02	0.00	0.02	0.00	0.46	0.02
60	0.23	0.03	0.01	0.00	0.62	0.55	0.48	0.02
75	0.00	0.47	0.00	0.00	0.55	0.41	0.54	0.25
90	0.00	0.59	0.00	0.00	0.69	0.44	0.00	0.00
105	0.00	0.39	0.00	0.00	0.17	0.00	0.00	0.00
120	0.00	0.93	0.00	0.00	0.04	0.00	0.00	0.00
135	0.00	0.46	0.00	0.00	0.00	0.00	0.00	0.00
150	0.00	0.18	0.00	0.00	0.00	0.00	0.00	0.00
165	0.00	0.71	0.00	0.00	0.00	0.00	0.00	0.01
180	0.00	0.75	0.00	0.00	0.00	0.06	0.00	0.00
195	0.00	0.46	0.00	0.00	0.00	0.01	0.00	0.00
210	0.00	0.10	0.00	0.00	0.00	0.01	0.00	0.00
225	0.00	0.02	0.00	0.00	0.00	0.00	0.01	0.00
240	0.00	0.00	0.00	0.00	0.00	0.00	0.22	0.85

	Fuselage Side Surface Temperature t-test p-values							
Time (s)	T1R	T2R	T3R	T4R	T1L	T2L	T3L	T4L
0	0.05	0.14	0.05	0.03	0.01	0.10	0.03	0.00
15	0.07	0.26	0.12	0.03	0.01	0.42	0.19	0.00
30	0.59	0.00	0.08	0.01	0.28	0.00	0.00	0.21
45	0.32	0.00	0.00	0.00	0.76	0.00	0.00	0.01
60	0.23	0.00	0.00	0.01	0.30	0.04	0.71	0.00
75	0.10	0.00	0.00	0.00	0.07	0.70	0.04	0.00
90	0.02	0.00	0.00	0.00	0.01	0.13	0.00	0.00
105	0.00	0.00	0.00	0.00	0.00	0.00	0.00	0.00
120	0.00	0.00	0.00	0.00	0.00	0.00	0.00	0.00
135	0.00	0.00	0.01	0.00	0.00	0.00	0.00	0.00
150	0.00	0.00	0.89	0.00	0.00	0.00	0.00	0.00
165	0.00	0.00	0.15	0.00	0.00	0.00	0.00	0.00
180	0.00	0.00	0.17	0.00	0.01	0.00	0.00	0.00
195	0.00	0.00	0.38	0.00	0.02	0.00	0.00	0.00
210	0.00	0.00	0.61	0.00	0.08	0.00	0.00	0.00
225	0.00	0.00	0.85	0.00	0.39	0.00	0.00	0.00
240	0.00	0.00	0.71	0.00	0.86	0.00	0.00	0.00

	Perimeter Heat Flux t-test p-values							
Time (s)	HT1	HT2	HT3	HT4	HT5	HT6	HT7	HT8
0	0.45	0.97	0.29	0.27	0.99	0.06	0.60	0.48
15	0.02	0.00	0.52	0.02	0.17	0.00	0.00	0.00
30	0.08	0.24	0.33	0.07	0.00	0.20	0.00	0.03
45	0.00	0.29	0.02	0.00	0.00	0.00	0.02	0.00
60	0.02	0.11	0.01	0.00	0.00	0.01	0.01	0.00
75	0.00	0.02	0.02	0.00	0.00	0.26	0.00	0.00
90	0.00	0.00	0.05	0.00	0.00	0.74	0.00	0.00
105	0.00	0.00	0.00	0.00	0.00	0.00	0.00	0.00
120	0.00	0.00	0.00	0.00	0.00	0.00	0.00	0.00
135	0.00	0.00	0.00	0.00	0.00	0.00	0.00	0.00
150	0.00	0.00	0.00	0.00	0.00	0.00	0.00	0.00
165	0.00	0.00	0.00	0.00	0.00	0.00	0.00	0.00
180	0.00	0.00	0.00	0.00	0.00	0.00	0.00	0.00
195	0.00	0.00	0.00	0.00	0.00	0.00	0.00	0.00
210	0.00	0.16	0.00	0.00	0.00	0.00	0.00	0.00
225	0.00	0.22	0.00	0.00	0.00	0.00	0.04	0.00
240	0.06	0.00	0.00	0.00	0.00	0.00	0.56	0.00

Figure E-5. The *t*-Test Data for 1.4-mph, 45° Crosswind Trials

APPENDIX F—DATA FROM THE 5.5-mph, 90° CROSSWIND TRIALS

Figures F-1 through F-4 show statistics compiled using data from six trials of the 1:10-scale New Large Aircraft mockup under 5.5-mph, 90° crosswind conditions. Data with 0.1 ≤ relative standard error (RSE) < 0.3 are highlighted in light gray, and data with 0.3 ≤ RSE are highlighted in dark gray.

5.5mph 90° crosswinds																
	Perimeter Heat Flux (Kw/m^2)															
	HT1		HT2		HT3		HT4		HT5		HT6		HT7		HT8	
Time (s)	avg.	std. dev.	avg.	std. dev.	avg.	std. dev.	avg.	std. dev.	avg.	std. dev.	avg.	std. dev.	avg.	std. dev.	avg.	std. dev.
0	2	0	2	1	2	1	1	0	1	0	1	0	1	0	2	0
15	11	1	17	3	4	1	4	1	3	1	5	1	6	1	9	0
30	48	7	28	4	9	1	13	2	6	4	13	1	12	1	17	4
45	74	12	42	3	13	1	18	5	9	7	13	1	15	1	26	4
60	97	18	63	7	17	2	21	7	13	4	16	1	18	1	35	4
75	136	24	71	12	17	1	19	4	15	2	14	1	17	1	37	5
90	184	20	99	11	16	1	16	1	13	3	12	1	15	1	35	3
105	221	31	104	16	15	1	13	1	12	2	10	1	14	0	36	2
120	261	17	119	10	14	1	12	1	11	2	9	0	12	0	36	2
135	293	23	124	9	13	1	12	1	11	3	10	1	12	0	39	2
150	323	36	136	10	14	1	11	1	10	3	9	1	11	1	40	4
165	359	29	136	12	13	1	10	1	10	2	8	0	11	1	39	3
180	322	31	117	24	13	2	9	1	9	2	8	0	11	0	37	2
195	263	44	82	23	11	1	7	1	9	1	6	1	7	1	28	2
210	174	42	50	18	8	1	3	1	6	1	3	1	3	1	19	2
225	105	49	32	20	6	1	0	2	5	1	1	1	1	2	10	6
240	52	22	21	17	4	2	-1	2	2	2	0	1	0	1	5	4

Figure F-1. Perimeter Heat Flux Statistics for the 5.5-mph, 90° Crosswind Condition

5.5mph 90° crosswinds																
	Perimeter Air Temperature (°F)															
	HT1		HT2		HT3		HT4		HT5		HT6		HT7		HT8	
Time (s)	avg.	std. dev.	avg.	std. dev.	avg.	std. dev.	avg.	std. dev.	avg.	std. dev.	avg.	std. dev.	avg.	std. dev.	avg.	std. dev.
0	80	6	80	9	74	6	77	7	76	7	75	7	74	7	75	5
15	185	14	134	20	103	11	95	10	87	10	84	9	95	10	124	13
30	405	38	362	90	185	17	153	15	124	14	109	9	150	15	292	74
45	482	29	445	45	236	14	205	14	153	15	124	9	180	12	329	29
60	582	60	651	113	293	30	236	12	165	13	134	9	204	8	440	142
75	931	229	874	270	269	15	223	5	147	12	117	9	179	11	472	81
90	1544	115	1335	88	249	15	193	9	130	8	108	8	166	10	403	22
105	1692	138	1155	133	232	18	183	13	125	10	109	11	157	9	407	25
120	1770	105	1182	126	224	16	180	12	129	9	115	9	157	13	395	35
135	1787	58	1112	125	220	16	181	13	135	8	126	9	170	7	454	46
150	1774	136	1213	140	224	16	180	11	139	9	125	11	167	11	434	53
165	1854	153	1128	190	215	20	177	14	132	14	124	12	163	13	438	48
180	1670	135	930	182	199	24	167	14	123	15	112	13	156	17	380	45
195	1522	175	720	117	176	17	154	13	119	13	113	11	145	11	314	38
210	1134	254	573	122	155	11	143	9	111	5	106	8	134	6	251	17
225	831	279	431	190	136	14	127	11	105	11	103	10	121	8	200	25
240	513	170	324	169	128	10	121	9	98	8	96	6	113	7	169	21

Figure F-2. Perimeter Air Temperature Statistics for the 5.5-mph, 90° Crosswind Condition

5.5mph 90° crosswinds																
	Fuselage Side Surface Temperature (°F)															
	T1R		T2R		T3R		T4R		T1L		T2L		T3L		T4L	
Time (s)	avg.	std. dev.	avg.	std. dev.	avg.	std. dev.	avg.	std. dev.	avg.	std. dev.	avg.	std. dev.	avg.	std. dev.	avg.	std. dev.
0	72	6	74	6	74	6	72	6	71	6	74	6	74	6	71	6
15	72	6	75	6	75	6	72	6	72	6	74	6	75	6	72	6
30	74	7	78	6	78	6	75	6	78	8	86	8	87	7	80	7
45	83	7	91	9	90	9	84	8	108	11	133	19	131	13	110	12
60	104	11	118	22	114	18	104	13	176	19	220	36	215	27	173	27
75	134	22	156	41	146	32	129	20	281	39	343	54	331	43	268	44
90	166	31	192	51	179	41	152	24	392	53	482	73	463	58	375	56
105	198	38	226	58	211	47	174	27	489	59	608	84	584	67	472	63
120	230	42	261	64	244	52	196	29	567	60	711	88	684	67	551	64
135	262	46	297	68	279	56	218	30	633	59	793	87	764	63	613	63
150	293	49	332	71	313	59	240	30	685	58	855	85	826	57	662	58
165	323	50	367	72	345	60	261	30	729	52	902	79	872	52	698	54
180	350	51	398	73	377	61	281	30	756	45	932	70	905	44	727	49
195	374	49	426	70	405	60	297	29	772	38	947	58	923	34	746	42
210	393	48	449	67	427	57	309	28	776	33	948	47	926	24	754	35
225	407	46	462	64	443	53	318	27	770	29	936	39	915	18	750	30
240	415	44	470	60	452	50	323	26	757	24	914	33	894	15	736	26

Figure F-3. Fuselage Side Surface Temperature Statistics for the 5.5-mph, 90° Crosswind Condition

5.5mph 90° crosswinds														
	Fuselage and Wing Underside Surface Temperature (°F)													
	T1B		T2B		T3B		T4B		T5B		T6B		T7B	
Time (s)	avg.	std. dev.	avg.	std. dev.	avg.	std. dev.	avg.	std. dev.	avg.	std. dev.	avg.	std. dev.	avg.	std. dev.
0	71	6	73	6	74	6	71	6	71	6	71	6	71	6
15	71	6	75	6	74	6	71	6	71	6	71	6	71	6
30	77	7	89	8	82	7	76	6	73	6	74	6	72	6
45	99	9	127	17	108	9	95	8	79	6	83	6	75	6
60	143	17	192	35	156	18	131	14	91	7	100	7	81	6
75	212	34	277	56	227	32	187	25	111	10	124	8	88	7
90	292	49	369	74	310	46	255	35	138	14	152	10	97	6
105	374	60	458	86	397	59	328	42	169	19	184	13	107	6
120	452	67	541	94	483	67	400	46	203	24	217	15	118	7
135	527	71	619	98	565	74	469	47	239	28	250	16	129	6
150	593	73	687	100	641	77	531	46	275	30	282	17	140	6
165	653	70	748	98	708	78	586	44	310	33	313	18	151	6
180	700	66	795	91	767	76	635	42	344	35	342	18	161	6
195	734	59	827	81	809	70	673	38	375	35	369	18	171	6
210	753	52	842	70	834	63	699	34	402	35	390	18	181	6
225	758	47	841	59	841	55	710	31	423	34	406	17	188	6
240	753	42	827	50	833	49	710	28	437	33	415	17	194	6

Figure F-4. Fuselage and Wing Underside Surface Temperature Statistics for the 5.5-mph, 90° Crosswind Condition

In this appendix, statistical analyses by *t*-test were conducted to compare the results from wind-driven trials, 5.5-mph, 90° crosswind in this particular appendix, to the trials done in windless conditions. The *t*-test function built into Microsoft® Excel® was used to do the analysis assuming a two-tailed test with unequal variance. For each individual sensor at each of the 15-second intervals, Microsoft® Excel® generated a *p*-value (probability value). The results are shown in figure F-5. Cells with $0.01 < p\text{-value} \leq 0.05$ are highlighted in light gray. Cells with $p\text{-value} \leq 0.01$ are highlighted in dark gray.

	Underside Surface Temperature t-test p-values						
Time (s)	T1B	T2B	T3B	T4B	T5B	T6B	T7B
0	0.07	0.06	0.14	0.16	0.16	0.13	0.16
15	0.04	0.01	0.04	0.16	0.12	0.16	0.15
30	0.00	0.00	0.00	0.01	0.00	0.06	0.14
45	0.00	0.00	0.00	0.00	0.00	0.00	0.06
60	0.00	0.00	0.00	0.00	0.00	0.00	0.01
75	0.04	0.00	0.00	0.02	0.00	0.00	0.00
90	0.06	0.00	0.00	0.03	0.00	0.00	0.00
105	0.04	0.00	0.00	0.03	0.00	0.00	0.00
120	0.02	0.00	0.00	0.02	0.00	0.00	0.00
135	0.01	0.00	0.00	0.01	0.00	0.00	0.00
150	0.00	0.00	0.00	0.00	0.00	0.00	0.00
165	0.00	0.00	0.00	0.00	0.00	0.00	0.00
180	0.00	0.00	0.00	0.00	0.00	0.00	0.00
195	0.00	0.00	0.00	0.00	0.00	0.00	0.00
210	0.00	0.00	0.00	0.00	0.00	0.00	0.00
225	0.00	0.00	0.00	0.00	0.00	0.00	0.00
240	0.00	0.00	0.00	0.00	0.00	0.00	0.00

	Perimeter Temperature t-test p-values							
Time (s)	HT1	HT2	HT3	HT4	HT5	HT6	HT7	HT8
0	0.62	0.84	0.08	0.38	0.27	0.13	0.11	0.13
15	0.00	0.06	0.00	0.01	0.01	0.01	0.00	0.01
30	0.00	0.03	0.00	0.00	0.00	0.00	0.00	0.16
45	0.00	0.00	0.00	0.00	0.00	0.00	0.00	0.01
60	0.00	0.00	0.01	0.00	0.00	0.00	0.00	0.06
75	0.00	0.00	0.00	0.00	0.00	0.00	0.00	0.00
90	0.00	0.00	0.00	0.00	0.00	0.00	0.00	0.00
105	0.00	0.00	0.00	0.00	0.00	0.00	0.00	0.00
120	0.00	0.00	0.00	0.00	0.00	0.00	0.00	0.00
135	0.00	0.00	0.00	0.00	0.00	0.00	0.00	0.00
150	0.00	0.00	0.00	0.00	0.00	0.00	0.00	0.00
165	0.00	0.00	0.00	0.00	0.00	0.00	0.00	0.00
180	0.00	0.00	0.00	0.00	0.00	0.00	0.00	0.05
195	0.00	0.00	0.00	0.00	0.00	0.00	0.00	0.04
210	0.00	0.01	0.00	0.00	0.00	0.00	0.00	0.00
225	0.01	0.31	0.00	0.00	0.00	0.00	0.00	0.00
240	0.02	0.61	0.00	0.00	0.00	0.00	0.00	0.00

	Fuselage Side Surface Temperature t-test p-values							
Time (s)	T1R	T2R	T3R	T4R	T1L	T2L	T3L	T4L
0	0.07	0.10	0.12	0.12	0.08	0.06	0.18	0.17
15	0.04	0.08	0.10	0.11	0.07	0.04	0.12	0.20
30	0.00	0.00	0.00	0.00	0.05	0.01	0.00	0.03
45	0.00	0.00	0.00	0.00	0.37	0.45	0.52	0.91
60	0.00	0.00	0.00	0.00	0.00	0.01	0.01	0.02
75	0.00	0.00	0.00	0.00	0.00	0.00	0.00	0.00
90	0.00	0.00	0.00	0.00	0.00	0.00	0.00	0.00
105	0.00	0.00	0.00	0.00	0.00	0.00	0.00	0.00
120	0.00	0.00	0.00	0.00	0.00	0.00	0.00	0.00
135	0.00	0.00	0.00	0.00	0.00	0.00	0.00	0.00
150	0.00	0.00	0.00	0.00	0.00	0.00	0.00	0.00
165	0.00	0.00	0.00	0.00	0.00	0.00	0.00	0.00
180	0.00	0.00	0.00	0.00	0.00	0.00	0.00	0.00
195	0.00	0.00	0.00	0.00	0.00	0.00	0.00	0.00
210	0.00	0.00	0.00	0.00	0.00	0.00	0.00	0.00
225	0.00	0.00	0.00	0.00	0.00	0.00	0.00	0.00
240	0.00	0.00	0.00	0.00	0.00	0.00	0.00	0.00

	Perimeter Heat Flux t-test p-values							
Time (s)	HT1	HT2	HT3	HT4	HT5	HT6	HT7	HT8
0	0.11	0.47	0.28	0.14	0.72	0.37	0.35	0.65
15	0.07	0.05	0.86	0.22	0.15	0.75	0.06	0.00
30	0.00	0.01	0.00	0.01	0.82	0.00	0.00	0.70
45	0.00	0.00	0.00	0.04	0.22	0.00	0.00	0.02
60	0.00	0.00	0.01	0.16	0.03	0.00	0.00	0.00
75	0.00	0.00	0.00	0.00	0.00	0.00	0.00	0.00
90	0.00	0.00	0.00	0.00	0.00	0.00	0.00	0.00
105	0.00	0.00	0.00	0.00	0.00	0.00	0.00	0.00
120	0.00	0.00	0.00	0.00	0.00	0.00	0.00	0.00
135	0.00	0.00	0.00	0.00	0.00	0.00	0.00	0.00
150	0.00	0.00	0.00	0.00	0.00	0.00	0.00	0.00
165	0.00	0.00	0.00	0.00	0.00	0.00	0.00	0.00
180	0.00	0.00	0.00	0.00	0.00	0.00	0.00	0.00
195	0.00	0.00	0.00	0.00	0.00	0.00	0.00	0.47
210	0.00	0.08	0.00	0.00	0.00	0.00	0.00	0.00
225	0.01	0.94	0.00	0.00	0.00	0.00	0.00	0.00
240	0.02	1.00	0.00	0.00	0.00	0.00	0.00	0.00

Figure F-5. The *t*-Test Data for 5.5-mph, 90° Crosswind Trials

APPENDIX G—DATA FROM THE 5.5-mph, 45° CROSSWIND TRIALS

Figures G-1 through G-4 show statistics compiled using data from four trials of the 1:10-scale New Large Aircraft mockup under 5.5-mph, 45° crosswind conditions. Data with 0.1 ≤ relative standard error (RSE) < 0.3 are highlighted in light gray, and data with 0.3 ≤ RSE are highlighted in dark gray.

5.5mph 45° crosswinds																
	Perimeter Heat Flux (Kw/m^2)															
	HT1		HT2		HT3		HT4		HT5		HT6		HT7		HT8	
Time (s)	avg.	std. dev.	avg.	std. dev.	avg.	std. dev.	avg.	std. dev.	avg.	std. dev.	avg.	std. dev.	avg.	std. dev.	avg.	std. dev.
0	2	1	2	1	3	0	1	0	2	0	2	0	1	0	2	0
15	8	1	12	1	4	1	5	0	1	0	8	1	12	1	10	1
30	29	2	21	2	9	1	9	0	3	0	11	1	22	2	57	9
45	42	2	23	1	12	1	13	0	6	1	15	1	29	3	88	13
60	53	4	28	2	16	2	15	0	7	1	17	1	61	15	128	18
75	69	11	24	2	15	1	13	0	7	0	16	1	53	6	201	21
90	84	12	21	1	15	2	11	0	7	0	15	1	63	9	281	39
105	87	23	20	0	14	1	10	0	7	1	11	1	58	15	344	32
120	104	15	17	1	12	1	8	1	7	0	11	0	49	7	402	24
135	125	4	17	1	12	1	9	0	6	0	10	1	49	11	425	22
150	147	38	15	2	11	1	8	1	6	0	9	0	52	10	437	31
165	138	18	15	2	11	1	8	1	5	1	9	0	50	8	430	31
180	127	14	12	1	11	1	7	1	6	1	9	1	48	12	372	12
195	84	10	6	2	10	2	7	0	5	1	8	1	41	9	266	24
210	38	12	-1	2	9	1	4	0	5	0	5	0	28	4	140	25
225	14	4	-3	2	6	1	1	1	4	1	1	2	10	6	65	12
240	8	2	-2	1	3	1	-1	0	4	1	-1	1	3	3	38	2

Figure G-1. Perimeter Heat Flux Statistics for the 5.5-mph, 45° Crosswind Condition

5.5mph 45° crosswinds																
	Perimeter Air Temperature (°F)															
	HT1		HT2		HT3		HT4		HT5		HT6		HT7		HT8	
Time (s)	avg.	std. dev.	avg.	std. dev.	avg.	std. dev.	avg.	std. dev.	avg.	std. dev.	avg.	std. dev.	avg.	std. dev.	avg.	std. dev.
0	88	9	83	2	88	4	83	2	82	2	83	3	95	7	90	2
15	172	24	111	4	117	6	100	2	98	3	108	4	204	52	280	15
30	373	74	188	13	187	3	138	2	131	17	147	6	386	62	484	62
45	455	92	251	21	235	6	164	2	141	19	163	12	444	147	550	69
60	604	50	260	28	240	12	172	2	144	16	188	14	1084	327	991	379
75	1296	271	215	27	230	9	159	4	130	8	165	16	842	227	1532	238
90	1480	125	202	17	216	9	151	3	123	8	161	14	911	124	1797	125
105	1580	47	194	9	203	6	147	3	129	10	159	14	730	199	1872	47
120	1582	52	194	12	205	2	155	1	142	7	167	9	575	106	1901	50
135	1651	23	202	6	205	4	159	7	140	13	165	6	583	113	1894	56
150	1617	71	202	8	205	6	162	11	157	12	177	7	618	118	1875	32
165	1732	38	201	5	203	3	162	5	143	6	173	5	557	77	1816	58
180	1700	41	190	5	193	8	157	6	147	12	166	11	556	125	1722	61
195	1532	75	162	10	174	7	143	8	132	9	161	10	482	87	1466	64
210	929	95	143	11	157	4	127	5	120	12	142	3	399	50	979	203
225	521	81	129	12	139	12	119	5	119	3	131	4	286	54	565	129
240	336	25	121	8	126	5	109	4	103	6	120	5	200	20	371	35

Figure G-2. Perimeter Air Temperature Statistics for the 5.5-mph, 45° Crosswind Condition

5.5mph 45° crosswinds																
	Fuselage Side Surface Temperature (°F)															
	T1R		T2R		T3R		T4R		T1L		T2L		T3L		T4L	
Time (s)	avg.	std. dev.	avg.	std. dev.	avg.	std. dev.	avg.	std. dev.	avg.	std. dev.	avg.	std. dev.	avg.	std. dev.	avg.	std. dev.
0	81	2	83	2	83	2	80	2	81	2	83	2	83	2	81	2
15	81	2	83	2	83	2	81	2	81	2	83	2	83	2	81	2
30	83	2	84	2	86	2	94	2	83	2	85	2	88	2	95	2
45	89	2	90	2	99	3	127	5	91	2	93	2	120	5	143	3
60	100	2	102	3	128	11	171	14	107	3	117	4	215	64	229	3
75	114	3	120	3	156	10	227	23	129	4	155	7	282	12	342	6
90	129	3	140	4	191	14	279	31	152	5	202	10	383	13	461	9
105	145	3	160	5	225	18	324	35	175	5	247	14	475	5	570	12
120	163	4	181	6	259	20	364	36	197	5	289	17	552	10	662	11
135	180	4	203	7	293	19	400	35	219	7	327	21	616	16	739	7
150	199	4	226	8	326	18	433	32	239	7	359	23	667	20	799	6
165	217	4	247	8	357	17	463	30	257	7	386	23	706	21	843	8
180	235	4	267	7	387	16	485	28	273	6	407	23	733	21	873	9
195	253	4	284	7	412	16	502	26	286	5	422	22	750	19	889	9
210	268	3	298	9	430	15	509	25	293	4	430	20	754	16	889	7
225	279	3	309	9	442	15	510	24	295	4	431	18	745	13	872	6
240	288	3	316	9	449	14	507	22	295	3	427	16	725	11	848	6

Figure G-3. Fuselage Side Surface Temperature Statistics for the 5.5-mph, 45° Crosswind Condition

5.5mph 45° crosswinds														
	Fuselage and Wing Underside Surface Temperature (°F)													
	T1B		T2B		T3B		T4B		T5B		T6B		T7B	
Time (s)	ave.	std. dev.	ave.	std. dev.	ave.	std. dev.	ave.	std. dev.	ave.	std. dev.	ave.	std. dev.	ave.	std. dev.
0	81	2	82	2	82	2	80	2	80	2	80	2	80	2
15	81	2	82	2	83	2	80	2	80	2	80	2	80	2
30	84	2	86	2	89	2	89	2	81	2	87	2	83	2
45	97	2	102	2	112	3	122	4	86	2	109	3	90	3
60	123	4	135	3	159	5	183	8	99	3	146	6	102	4
75	159	6	183	6	220	5	263	13	124	7	198	13	120	6
90	204	10	237	9	288	8	349	18	159	11	262	22	143	8
105	250	12	292	10	358	10	436	22	202	16	329	31	169	12
120	296	13	346	11	428	12	521	24	250	21	398	41	197	16
135	341	15	400	11	496	11	603	23	300	24	464	48	225	20
150	383	16	449	11	560	10	680	22	352	26	526	51	251	23
165	423	15	494	10	619	10	751	25	404	27	582	51	277	24
180	458	13	531	8	670	10	805	21	455	28	631	50	301	27
195	487	11	559	5	709	10	841	15	502	28	671	50	324	28
210	507	9	574	3	731	11	865	14	544	28	700	49	344	30
225	516	7	578	4	739	11	872	13	576	27	716	48	359	30
240	517	5	572	5	731	11	863	13	601	27	720	45	370	30

Figure G-4. Fuselage and Underside Surface Temperature Statistics for the 5.5-mph, 45° Crosswind Condition

In this appendix, statistical analyses by *t*-test were conducted to compare the results from wind-driven trials, 5.5-mph, 45° crosswind in this particular appendix, to the trials done in windless conditions. The *t*-test function built into Microsoft® Excel® was used to do the analysis assuming a two-tailed test with unequal variance. For each individual sensor at each of the 15-second intervals, Microsoft® Excel® generated a *p*-value (probability value). The results are shown in figure G-5. Cells with $0.01 < p\text{-value} \leq 0.05$ are highlighted in light gray. Cells with $p\text{-value} \leq 0.01$ are highlighted in dark gray.

	Underside Surface Temperature t-test p-values						
Time (s)	T1B	T2B	T3B	T4B	T5B	T6B	T7B
0	0.08	0.13	0.12	0.04	0.06	0.09	0.08
15	0.16	0.14	0.69	0.05	0.14	0.07	0.07
30	0.00	0.00	0.00	0.23	0.05	0.02	0.03
45	0.00	0.00	0.00	0.02	0.00	0.03	0.01
60	0.00	0.00	0.00	0.00	0.00	0.07	0.00
75	0.00	0.00	0.00	0.00	0.00	0.13	0.00
90	0.00	0.00	0.00	0.00	0.00	0.22	0.00
105	0.00	0.00	0.00	0.01	0.00	0.36	0.01
120	0.00	0.00	0.00	0.01	0.00	0.61	0.01
135	0.00	0.00	0.00	0.01	0.00	0.99	0.01
150	0.00	0.00	0.00	0.00	0.00	0.54	0.02
165	0.00	0.00	0.00	0.01	0.00	0.23	0.02
180	0.00	0.00	0.00	0.01	0.00	0.08	0.03
195	0.00	0.00	0.00	0.04	0.00	0.03	0.05
210	0.00	0.00	0.00	0.19	0.00	0.01	0.10
225	0.00	0.00	0.00	0.00	0.00	0.00	0.24
240	0.00	0.00	0.00	0.00	0.00	0.00	0.67

	Perimeter Temperature t-test p-values							
Time (s)	HT1	HT2	HT3	HT4	HT5	HT6	HT7	HT8
0	0.22	0.15	0.02	0.14	0.26	0.10	0.02	0.00
15	0.25	0.00	0.18	0.02	0.08	0.03	0.05	0.00
30	0.03	0.00	0.00	0.00	0.00	0.00	0.02	0.00
45	0.03	0.02	0.00	0.00	0.00	0.00	0.18	0.00
60	0.00	0.03	0.00	0.00	0.00	0.00	0.02	0.04
75	0.01	0.00	0.00	0.00	0.00	0.00	0.02	0.00
90	0.00	0.00	0.00	0.00	0.00	0.00	0.00	0.00
105	0.00	0.00	0.00	0.00	0.00	0.00	0.03	0.00
120	0.00	0.00	0.00	0.00	0.00	0.00	0.04	0.00
135	0.00	0.00	0.00	0.00	0.00	0.00	0.04	0.00
150	0.00	0.00	0.00	0.00	0.00	0.00	0.04	0.00
165	0.00	0.00	0.00	0.00	0.00	0.00	0.02	0.00
180	0.00	0.00	0.00	0.00	0.00	0.00	0.08	0.00
195	0.00	0.00	0.00	0.00	0.00	0.00	0.09	0.00
210	0.00	0.00	0.00	0.00	0.00	0.00	0.27	0.01
225	0.01	0.00	0.00	0.00	0.00	0.00	0.18	0.05
240	0.01	0.00	0.00	0.00	0.00	0.00	0.00	0.02

	Fuselage Side Surface Temperature t-test p-values							
Time (s)	T1R	T2R	T3R	T4R	T1L	T2L	T3L	T4L
0	0.24	0.19	0.16	0.10	0.08	0.12	0.03	0.02
15	0.34	0.39	0.37	0.10	0.11	0.40	0.21	0.03
30	0.07	0.00	0.00	0.01	0.06	0.00	0.00	0.00
45	0.00	0.00	0.00	0.00	0.00	0.00	0.05	0.00
60	0.00	0.00	0.00	0.03	0.00	0.00	0.21	0.00
75	0.00	0.00	0.00	0.06	0.00	0.00	0.00	0.00
90	0.00	0.00	0.00	0.15	0.00	0.00	0.00	0.00
105	0.00	0.00	0.00	0.43	0.00	0.00	0.00	0.00
120	0.00	0.00	0.00	0.76	0.00	0.00	0.00	0.00
135	0.00	0.00	0.00	0.14	0.00	0.00	0.00	0.00
150	0.00	0.00	0.00	0.02	0.00	0.00	0.00	0.00
165	0.00	0.00	0.00	0.00	0.00	0.00	0.00	0.00
180	0.00	0.00	0.00	0.00	0.00	0.00	0.00	0.00
195	0.00	0.00	0.00	0.00	0.00	0.00	0.00	0.00
210	0.00	0.00	0.00	0.00	0.00	0.00	0.00	0.00
225	0.00	0.00	0.00	0.00	0.00	0.00	0.45	0.00
240	0.00	0.00	0.00	0.00	0.00	0.00	0.00	0.00

	Perimeter Heat Flux t-test p-values							
Time (s)	HT1	HT2	HT3	HT4	HT5	HT6	HT7	HT8
0	0.51	0.78	0.29	0.50	0.03	0.59	0.54	0.05
15	0.03	0.00	0.68	0.35	0.00	0.00	0.00	0.24
30	0.00	0.38	0.00	0.00	0.00	0.00	0.00	0.00
45	0.00	0.45	0.00	0.00	0.00	0.00	0.02	0.00
60	0.00	0.03	0.00	0.00	0.00	0.00	0.02	0.00
75	0.00	0.45	0.00	0.00	0.00	0.00	0.00	0.00
90	0.00	0.00	0.00	0.00	0.00	0.00	0.00	0.00
105	0.01	0.00	0.00	0.00	0.00	0.00	0.03	0.00
120	0.00	0.00	0.00	0.00	0.00	0.00	0.01	0.00
135	0.00	0.00	0.00	0.00	0.00	0.00	0.04	0.00
150	0.01	0.00	0.00	0.00	0.00	0.00	0.02	0.00
165	0.00	0.00	0.00	0.00	0.00	0.00	0.02	0.00
180	0.00	0.00	0.00	0.00	0.00	0.00	0.07	0.00
195	0.00	0.00	0.00	0.00	0.00	0.00	0.20	0.00
210	0.25	0.00	0.00	0.00	0.00	0.00	0.02	0.00
225	0.00	0.00	0.00	0.00	0.00	0.00	0.00	0.01
240	0.00	0.00	0.00	0.00	0.00	0.00	0.00	0.00

Figure G-5. The *t*-Test Data for 5.5-mph, 45° Crosswind Trials